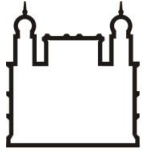


**INSTITUTO CARLOS CHAGAS
DOCTORATE IN BIOSCIENCE AND BIOTECHNOLOGY**

JULIANA BERNARDI AGGIO

**NEUTROPHIL RESPONSE AND CELLULAR MIGRATION TO DRAINING LYMPH
NODES IN ZIKA VIRUS INFECTION**

**CURITIBA
2021**



Ministério da Saúde

FIOCRUZ

Fundação Oswaldo Cruz

**INSTITUTO CARLOS CHAGAS
GRADUATE PROGRAM OF BIOSCIENCE AND BIOTECHNOLOGY**

JULIANA BERNARDI AGGIO

**NEUTROPHIL RESPONSE AND CELLULAR MIGRATION TO DRAINING LYMPH
NODES IN ZIKA VIRUS INFECTION**

Thesis submitted to Instituto Carlos Chagas as part of the requirements for obtaining the title of Doctor of Biosciences and Biotechnology.

Supervisor: Priscilla Fanini Wowk

Co-supervisor: Ana Luiza Pamplona Mosimann

CURITIBA

2021

ii

Aggio, Juliana Bernardi.

Neutrophil response and cellular migration to draining lymph nodes in Zika virus infection / Juliana Bernardi Aggio. - Curitiba, 2021.
viii, 115f f.; il.

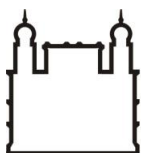
(Doutorado) - Instituto Carlos Chagas, Pós-Graduação em Biociências e Biotecnologia, 2021.

Orientadora: Priscilla Fanini Wowk.

Co-orientadora: Ana Luiza Pamplona Mosimann.

Bibliografia: Inclui Bibliografias.

1. dendritic cells. 2. migration. 3. neutrophil. 4. vaccinia virus. 5. Zika virus. I. Título.



Ministério da Saúde

FIOCRUZ

Fundação Oswaldo Cruz

Minutes of the public session of the dissertation examination to obtain the degree of Doctor in Biosciences and Biotechnology:



Ministério da Saúde

FIOCRUZ - PARANÁ
Instituto Carlos Chagas

Ata da Sessão Pública de exame de tese para obtenção do grau de Doutora em
Biociências e Biotecnologia.

Aos **15 dias do mês de junho de dois mil e vinte um, às 9:00 horas**, através de teleconferência <https://us02web.zoom.us/j/4239063043>, reuniu-se a Banca Examinadora designada pelo Colegiado do Programa de Pós-Graduação em Biociências e Biotecnologia, composta pelos Professores: **Dr^a. Letusa Albrecht, Dr^a. Karina Alves de Toledo e Dr. Daniel Santos Mansur**, com a finalidade de julgar a tese da candidata **Juliana Bernardi Aggio**, intitulada: “**NEUTROPHIL RESPONSE AND CELLULAR MIGRATION TO DRAINING LYMPH NODES IN ZIKA VIRUS INFECTION**”, sob a orientação de orientação de Dr^a. Priscilla Fanini Wowk e Coorientação de Dr^a. Ana Luiza Pamplona Mosimann, para obtenção do grau de **Doutora** em Biociências e Biotecnologia. A candidata teve até 45 (quarenta e cinco) minutos para a apresentação, e cada examinador teve um tempo máximo de arguição de 30 (trinta) minutos, seguido de 30 (trinta) minutos para resposta do (a) candidato(a) ou de 60 (sessenta) minutos quando houve diálogo na arguição. O desenvolvimento dos trabalhos seguiu o roteiro de sessão de defesa, estabelecido pela Coordenação do Programa, com abertura, condução e encerramento da sessão solene de defesa feito pelo(a) Presidente: **Dr^a. Letusa Albrecht**. Após haver analisado o referido trabalho e arguido a candidata, os membros da banca examinadora deliberaram pela:

) Aprovação da tese por unanimidade

) Aprovação somente após satisfazer as exigências de modificações no prazo fixado pela banca (não superior a noventa dias).

) Reprovação da tese

Na forma regulamentar foi lavrada a presente ata que é abaixo assinada pelos membros da banca, na ordem acima determinada, e pela candidata.

Curitiba, 15 de junho de 2021

Dr^a. Letusa Albrecht – ICC/PR

Dr^a. Karina Alves de Toledo – UNESP

Dr. Daniel Santos Mansur – UFSC



Documento assinado digitalmente

Daniel Santos Mansur
Data: 16/06/2021 10:39:44-0300
CPF: 046.529.716-13
Verifique as assinaturas em <https://v.ufsc.br>

Candidata: Juliana Bernardi Aggio

+55(41)3316-3230

Rua Prof. Algacyr Munhoz Mader, 3775 - CIC 81350-010 Curitiba/PR, Brasil



ACKNOWLEDGMENT

Most of all, I thank my supervisors, Pryscilla Wowk, Tony Rothfuchs, Ana Mosimann, and Brian Ferguson, for always having time to help me with my professional and personal growth, for warmly welcoming me, and for making me feel like I belong to your research groups. Thank you for the flights!

I genuinely thank Veronika Krmeská, Pryscilla, Marisa Oliveira and David Carpentier for the time you sat by my side to teach me and actively help me to produce results. All the adventures that Veronika and Pryscilla made me live are well kept in my heart. My work would not have been possible without the various people who donated or collected blood for me, or just calmed me down during the process. This feeling is extended to the ones who saved me from flow cytometer machines issues, especially Juan Basile and Priscila Hiraiwa (who had to do it late at night too); to Vinicius Gilhen for helping me with anesthesia and cardiac puncture; and to Tabata Klimeck who took the neutrophil pictures. I am glad for the patience of the nice ladies from Karolinska animal facility who taught me to properly grab a mouse (between my blood and tears!).

Also, my thanks to the friendships that brightened my days and kept me on my track in tough times, among whom I cannot fail to mention Nuno Sousa, Thais Lima, Dayana Hristova, Júlia Cerato, Fernanda Tomiotto, Leonie Vetter, Andrea Koishi and Karoline Agostinho.

I feel lucky to have received so much help from many people from many places in the last years, so I thank all the colleagues and staff personnel from Instituto Carlos Chagas, Karolinska Institutet and the Department of Pathology of the University of Cambridge for all the support given to this project during this time. I am going to keep most of you and the beautiful Stockholm in my best memories.

Always all my love to my parents and Bruno for the unconditional support in all my steps.

This work was funded by Fundação Araucária, Coordenação de Aperfeiçoamento de Pessoal de Nível Superior (CAPES), and Conselho Nacional de Desenvolvimento Científico e Tecnológico (CNPq). Part of the work presented in the second chapter of this thesis was financed by Programa de Doutorado Sanduíche no Exterior CAPES (notice nº 47/2017, process nº 88881.189711/2018-01), the Swedish Research Council, and the Karolinska Institutet.

ABSTRACT

Zika virus (ZIKV) is a recent example of an emerging flavivirus affecting humans and highlights the need for a faster action to contain viral epidemics. Filling some gaps in ZIKV immunology knowledge, evidenced in its last outbreak, could assist in understanding particular aspects of ZIKV pathology. In this work, this topic has been addressed exploring two important innate mechanisms during ZIKV infection: neutrophil response and skin leukocyte migration to the draining lymph node (dLN). Neutrophils are abundant and versatile inflammatory cells with controversial actions in viral pathologies. The first section of this thesis reports that human neutrophils were not targets of ZIKV replication, despite some internalized viral particles. No changes were evidenced in cell viability nor activation of human neutrophils in face of ZIKV (absence of surface receptors modulation, secretion of inflammatory cytokines and granule content, production of reactive oxygen species, and neutrophil extracellular traps formation), suggesting viral escape from neutrophil recognition. ZIKV infection in primary innate cells also did not promote a favorable environment to neutrophil migration. However, neutrophil presence in a co-culture infection resulted in lower frequencies of infection in the co-cultured cells. *In vivo*, neutrophil depletion did not contribute to reducing ZIKV spread to dLN. Overall, human neutrophil *in vitro* did not appear to be an essential component of ZIKV clearance or inflammation. Parallel to innate responses efforts against viruses, adaptive responses start to be assembled. Classically, T cell priming requires dendritic cells (DCs) mobilization to the dLN for antigen presentation. Using an *in vivo* fluorochrome-based migration assay, the second section shows that infection with *Vaccinia virus* (VACV) actively inhibited skin DCs migration to dLN, adding one more layer to the immune response suppression mechanisms of VACV. The DCs movement blockage did not impair dLN inflammation or priming of VACV antigen-specific CD4⁺ T cells, but was capable of mitigating responses to a secondary challenge with *Mycobacterium bovis* bacillus Calmette-Guérin (BCG). Moreover, VACV was detected in dLN very early post infection, indicating that the virus retained the capacity to prime T cells in the dLN by accessing the dLN through other means independent of DCs migration. Using the same approach, mobilization of leukocytes from the skin to dLN in immunocompetent mice was investigated after ZIKV infection. Neutrophils infected with ZIKV and prolonged ZIKV persistence in LN had been previously reported. Neutrophil immigrated to the dLN after ZIKV infection. However, this population was not recruited from the infected skin. In contrast to what had been observed for VACV skin infection, ZIKV and *Dengue virus* mobilized CD103⁻CD11b^{high}EpCAM^{low} skin DCs to pLN. The three works that make up this thesis pointed that neutrophil actions and skin DCs migration to LNs, both weakly explored in general virology, are specific for different viruses and models, and should be taken in consideration on efforts against diseases, such antiviral therapies and recombinant vaccines development.

Keyword: Innate immunity, dendritic cells, lymph nodes, migration, neutrophil, *Vaccinia virus*, *Zika virus*.

RESUMO

Zika vírus (ZIKV) é um exemplo recente de um flavivírus emergente que afeta humanos e evidencia a necessidade de ações mais rápidas para conter epidemias virais. Preencher lacunas no conhecimento de imunologia de ZIKV, evidenciadas em seu último surto, pode contribuir para a compreensão de aspectos particulares da patologia de ZIKV. Nesse trabalho, esse tópico foi abordado explorando dois importantes mecanismos inatos durante a infecção de ZIKV: a resposta de neutrófilos e a migração de leucócitos da pele para o linfonodo drenante (dLN). Neutrófilos são células inflamatórias abundantes e versáteis com ações controversas em patologias virais. A primeira seção desta tese reporta que neutrófilos humanos não foram alvos de replicação por ZIKV, apesar da internalização de algumas partículas virais. Nenhuma mudança foi evidenciada na viabilidade celular ou ativação de neutrófilos humanos frente a ZIKV (ausência de modulação de receptores de superfície, secreção de citocinas inflamatórias e conteúdo granular, produção de espécies reativas de oxigênio e formação de armadilhas extracelulares neutrofílicas), sugerindo um escape viral do reconhecimento por neutrófilos. A infecção de ZIKV em células imunes primárias também não promoveu um ambiente favorável à migração de neutrófilos. Entretanto, a presença de neutrófilos em uma cultura infectada resultou em menores frequências de infecção nas células co cultivadas. *In vivo*, a depleção de neutrófilos não contribuiu para a redução da dispersão de ZIKV para o dLN. No geral, neutrófilos humanos *in vitro* não parecem ser componentes essenciais na eliminação ou inflamação de ZIKV. Paralelamente aos esforços da resposta inata contra vírus, respostas adaptativas começam a ser montadas. Classicamente, a ativação de linfócitos T requer a mobilização de células dendríticas (DCs) para o dLN para apresentação de antígenos. Usando um ensaio de migração fluorescente *in vivo*, a segunda seção mostra que a infecção com *Vaccinia vírus* (VACV) inibiu ativamente a migração de DCs da pele para o dLN, adicionando mais uma camada aos mecanismos de supressão da resposta imune do VACV. O bloqueio do movimento de DCs não interferiu na inflamação no dLN ou na ativação de linfócitos CD4 específicos para VACV, mas foi capaz de mitigar respostas para um segundo desafio com *Mycobacterium bovis* bacilo Calmette-Guérin (BCG). Em adição, VACV foi detectado no dLN cedo após a infecção, indicando que o vírus mantém a capacidade de ativar linfócitos no dLN por acessar o dLN de forma independente da migração de DCs. Usando a mesma abordagem, a mobilização de leucócitos da pele para o dLN foi investigada em resposta a ZIKV em camundongos imunocompetentes. Foi previamente relatado a presença de neutrófilos infectados com ZIKV e prolongada persistência de ZIKV no dLN. Neutrófilos migraram para o dLN depois da infecção de ZIKV. Porém, essa população não foi recrutada da pele infectada. Em contraste com o que foi observado para VACV, ZIKV e *vírus da Dengue* mobilizaram CD103⁻CD11b^{high}EpCAM^{low} DCs da pele para o pLN. Os três trabalhos que compõem essa tese mostram que a ação de neutrófilos e a migração de DCs da pele para o pLN, ambos aspectos pouco explorados em virologia, são específicos para diferentes vírus e modelos, e devem ser levados em consideração nos esforços contra doenças, como terapias antivirais e desenvolvimento de vacinas recombinantes.

Palavras-chaves: células dendríticas, imunologia inata, linfonodos, migração, neutrófilos, *Vaccinia vírus*, *Zika vírus*.

SUMMARY

1. INTRODUCTION	9
1.1 ZIKA VIRUS OVERVIEW.....	9
1.2 ZIKA VIRUS INNATE IMMUNE RESPONSE	12
1.2.1 Zika virus sensors and the Interferon system	13
1.2.2 Mouse models	16
1.2.3 Non-human primates models	18
1.2.4 Human patients	19
1.2.5 Human innate cells	20
1.3 GAPS IN ZIKA VIRUS INNATE IMMUNOLOGY	22
1.3.1 Neutrophils	22
1.3.1.1 Neutrophils in virology	25
1.3.1.2 Neutrophils as therapeutic targets for viral diseases	31
1.3.2 Neutrophil and dendritic cell migration to lymph nodes	33
2. AIM	37
3. DEVELOPMENT	39
3.1.CHAPTER 1. Zika virus escapes from human neutrophils (manuscript).....	39
3.2 CHAPTER 2. Cellular migration to the draining lymph nodes in viral infection	76
3.2.1 Vaccinia virus infection inhibits skin dendritic cell migration to draining lymph nodes (paper)	78
3.2.3 Cellular migration to the draining lymph nodes after Zika virus infection	90
3.2.3.1 Methodology	90
3.2.3.2 Results.....	91
4. DISCUSSION	95
5. CONCLUSIONS	100
5.1 PERSPECTIVES	101
6. REFERENCES	102

1. INTRODUCTION

Our culture, traditions and ways of relating (even intimately using condoms) is partly linked to the evolution of viruses. For example, it is believed that a virus is the first of the plagues that struck the ancient western civilization. The Antonine plague, probably the first viral epidemic registered, occurred in the Roman Empire during the reign of Marcus Aurelius (161-180 A.D.) and was caused by smallpox (FEARS, 2004; PIRET; BOIVIN, 2021). It decimated as much as one-third of the population in the area, as well as great part of the Roman army, claiming the life of Marcus Aurelius himself. After other deeply impacting viral outbreaks throughout our history such as Spanish Flu and HIV/AIDS, between the years of 2007 and 2020, only viral diseases were declared Public Health Emergencies of International Concern by the World Health Organization: H1N1 influenza (2009), Ebola (2013-2015 and 2018-2020), poliomyelitis (2014 to present), Zika (2016) and COVID-19 (2020 to present) (WILDER-SMITH; OSMAN, 2020). This work, which was started during the last Zika outbreak and therefore uses *Zika virus* as the main model, aims to contribute to the field of basic immunology of viral infections, indispensable to mitigate viral diseases impacts.

1.1 ZIKA VIRUS OVERVIEW

The *Flaviviridae* family is composed of single stranded positive RNA viruses which have a long history as emerging and re-emerging viruses causing epidemics throughout the world. The genus *Flavivirus* (with 53 species) includes important human pathogens such as *Dengue* (DENV), yellow fever (YFV), *West Nile* (WNV), *Japanese encephalitis* (JEV), and *tick-borne encephalitis virus* (TBEV). Flaviviruses are now globally distributed, predominantly in the equatorial region of the globe that harbors the arthropod vectors required for their transmission. These viruses infect up to 400 million people annually and outbreaks of other less well-characterized flaviviruses, like *Spondweni virus* (SPOV) and *Usutu virus* (USUV), have the potential to pop up in different regions of the world (PIERSON; DIAMOND, 2020). Brazil, where DENV is endemic, totaled 987,173 probable cases of the virus infection in 2020 (MINISTÉRIO DA SAÚDE, 2021a). The epidemic potential of flaviviruses among humans reflects the characteristics of their insect vectors and host reservoirs, a poorly planned urbanization, changing environmental conditions, extensive global travel, virus genetic makeup, and the immune status of the host (PIERSON; DIAMOND, 2020). Since 2007, a hitherto harmless old member of the family, *Zika*

virus (ZIKV), joined the list of emerging viruses causing outbreaks in the human population.

ZIKV is a small spherical (around 50 nm), enveloped virus with an approximately 11 kb positive single stranded RNA genome that encodes a single open reading frame flanked by highly structured untranslated regions. It is translated at the endoplasmic reticulum into one polyprotein, which is post-translationally cleaved by cellular and viral proteases into three structural proteins (capsid; pre-membrane, and envelope) and seven non-structural proteins (NS1, NS2A, NS2B, NS3, NS4A, NS4B, and NS5). The structural proteins are involved in the genome protection and in the virus entry and exit from the host cell, while non-structural proteins are required for viral genome transcription and replication, proteolytic processing of the polyprotein and attenuation of cellular innate immune response (NEUFELDT et al., 2018).

From the first isolation of ZIKV in the Zika Forest in Uganda in 1947, where it circulated between non-human primates and sylvatic *Aedes africanus* mosquitos, until 2007, the virus was sporadically diagnosed in Africa and Southeast Asia as a cause of mild self-limiting febrile disease in humans. In 2007, it caused the first large-scale outbreak in the Yap Island and Guam (Micronesia), where more than 7,000 individuals were estimated to be infected. In 2013/2014, ZIKV appeared in several Pacific Islands (French Polynesia, New Caledonia, the Cook Islands, Tahiti, and Easter Island), where it infected approximately 28,000 individuals and was associated for the first time with increased incidence of Guillain-Barré Syndrome, a debilitating neuronal disease in adults (CAO-LORMEAU et al., 2016; PIERSON; DIAMOND, 2018; TRIPATHI et al., 2017).

On May of 2015, ZIKV was detected for the first time in Brazil, with autochthonous transmission (ZANLUCA et al., 2015), and by late 2015 the virus had spread across South and Central America, the Caribbean and the southern parts of the United States, also reaching Europe. Phylogenetic and molecular analysis showed a single introduction of ZIKV into the Americas estimated to have occurred between May and December 2013, more than one year before the detection of ZIKV in Brazil (FARIA et al., 2016). There are some hypotheses on how ZIKV came to be introduced into Brazil, like large scale patterns in human mobility and sport events held in Brazil with the participation of athletes from French Polynesia (the July 2014 World Cup soccer tournament; the August 2014 Va'a canoe event; or the June 2013 Confederations Cup soccer tournament) (FARIA et al., 2016). From then until 5th of

May of 2021, Brazil notified approximately 260,000 ZIKV cases, the majority concentrated in 2016 and in the northeastern region, with a low adult mortality (Table 1). At that time, ZIKV infections during pregnancy were linked to stillbirth, placental insufficiency, miscarriage and fetal malformations including a wide range of congenital abnormalities, now collectively known as Congenital Syndrome Associated to ZIKV infection (CSZ) (BRASIL et al., 2016; COSTELLO et al., 2016).

Table 1. Number of cases of Zika virus (ZIKV) fever and Congenital Syndrome Associated to ZIKV infection (CSZ) in Brazil from 2015 to May of 2021. Numbers of cases and deaths presented in epidemiological notifications from the Ministry of Health of Brazil. (*) denotes fetus, neonatal, and infant deaths; (-) denotes information not found (MINISTÉRIO DA SAÚDE, 2016, 2017, 2018, 2019a, 2019b, 2020, 2021b, 2021a).

		2015	2016	2017	2018	2019	2020	2021 (until 5 th of May)	total	total deaths
n ^o ZIKV cases	notified cases	-	216,207	17,593	8,680	10,768	7,387	1,442	262,077	18
	positive cases	-	130,701	8,839	3,984	-	-	-	-	
	pregnant patients	-	11,052	949	449	447	609	-	13,506	
n ^o CSZ cases		954	1,927	360	178	55	-	-	3,474	402 *

ZIKV is classified into two distinct genotypes, African and Asian. All the three outbreaks since 2007 were caused by the Asian genotype. A few amino acid changes related to increased virulence and transmission have been identified associated with the spread of the virus from Asia to the Americas (FARIA et al., 2016; LIU; SHI; QIN, 2019).

Primates are the primary vertebrate hosts for ZIKV amplification in the urban and sylvatic transmission cycle. ZIKV is predominantly transmitted among hosts by *Aedes* mosquitos species but also by *Anopheles*, *Mansonia* and *Culex* ssp. (PHUMEE et al., 2019). Moreover, ZIKV sexual and vertical (mother-to-child) transmission has been reported. Virus RNA has also been detected in different body fluids like saliva, urine, tear, aqueous humor, breast milk, semen, and vaginal washes (NGONO; SHRESTA, 2018; PIERSON; DIAMOND, 2018).

Clinical symptoms of acute ZIKV infection in humans are typically absent (asymptomatic infection) or nonspecific, such as self-limiting flu-like fever, headache, myalgia, arthralgia, rash, and conjunctivitis without long-term consequences. Due to factors not yet fully understood (e.g. age, immune-status, comorbidities, virus strains,

microbiome, coinfections) ZIKV symptomatic infection may result in severe and life-threatening visceral disease (injury to male and female reproductive tracts and eye), neurotropic disease (encephalitis, cognitive impairment, and flaccid paralysis), and congenital disease (placental insufficiency, microcephaly, congenital malformations, and fetal demise) (PIERSON; DIAMOND, 2020).

Preferred target cells for ZIKV include skin fibroblasts and endothelial cells, neural progenitor and glia cells, placental macrophages and trophoblasts, testicular cells, uterine fibroblasts and eye-associated tissue (i.e. pantropic). Although no bona fide entry receptor for ZIKV infection in humans is yet known, members of the TIM (T cell immunoglobulin mucin domain protein 1) and TAM (tyrosine protein kinase receptor 3 (TYRO3)-AXL-MER) family of phosphatidylserine receptors (NEUFELDT et al., 2018), and Neural Cell Adhesion Molecule (NCAM1) are potential ZIKV receptors (SRIVASTAVA et al., 2016). The AXL receptor antagonizes type I interferon (IFN) signaling and promotes ZIKV infection in human astrocytes by regulating the expression of the SOCS1 type I IFN suppressor in a signal transducer and activator of transcription proteins (STAT) 1/STAT2-dependent manner (CHEN et al., 2018).

The most definitive current ZIKV diagnostic tool is based on reverse transcription associated to polymerase chain reaction (RT-PCR) (LAZEAR; DIAMOND, 2016). At present, no therapy, antiviral drug or vaccine is available to ZIKV infection. Despite ZIKV infection being resolved in the majority of the cases without residual symptoms, some reports suggest persistence of infected cells for prolonged periods of time, implying the existence of cell and tissue viral reservoirs that resist host immune clearance (CAMPOS et al., 2020). These aspects, the transplacental and sexual transmission, and life-threatening neurological complications, distinguish ZIKV from other flaviviruses and highlight the need for a better understanding of ZIKV evolution, biology, pathogenesis, and immune responses that may operate in these processes.

1.2 ZIKA VIRUS INNATE IMMUNE RESPONSE

It is clear that ZIKV can induce an immune response in hosts that includes both innate and adaptive immune elements, and successfully contain viral infection within a limited time in the majority of cases (ALIOTA et al., 2016; LUCAS et al., 2018; SCHOUEST et al., 2020).

However, it is increasingly evident that ZIKV has developed multiple strategies to reprogram or antagonize the host immunity in favor of the virus (BOS et al., 2020; BOWEN et al., 2017; FOO et al., 2017; HIRSCH et al., 2017; MICHELMAYR et al., 2017; SUN et al., 2017, 2020; VIELLE et al., 2018). It is unclear how ZIKV reaches immune privileged sites within the body and breaches protective blood-testis, placental-fetal, and brain barriers, which lead to sexual transmission and congenital defects. There are also reports of prolonged viremia in infected pregnant women, in semen, and persisting reservoirs of ZIKV infected cells in rare cases, e.g. the genitourinary tract and lymph nodes (PIERSON; DIAMOND, 2018, 2020). Moreover, different data indicate that an aggressive host inflammatory response is the major determinant of ZIKV pathogenicity, more than the infection *per se* (TRIPATHI et al., 2017; WANG et al., 2018). Finally, it remains unclear how the infection could result in an autoimmune disorder. In this context the triggered immune response still needs to be better understood.

The next sections review the identified ZIKV sensors and how ZIKV interacts with the interferon system; the early innate immune events described in mouse models, non-human primate models and human patients, as well as the involvement of human innate cells in ZIKV pathology through *in vitro* studies. The highlights of this review are gathered below (Figure 1).

1.2.1 Zika virus sensors and the Interferon system

The mammalian innate immune system detects and responds to flavivirus infection by recognizing pathogen-associated molecular patterns (PAMPs), such as viral nucleic acid or proteins. The best-characterized viral sensors are pattern-recognition receptors (PRRs), including cell surface and endosomal Toll-like receptors (TLRs); the cytoplasmic RNA sensors, retinoic acid-inducible gene I (RIG-I)-like receptors, the melanoma-associated differentiation antigen 5 (MDA5), NOD-like receptors (NLRs), and C-type lectin receptors (CLRs). Binding of single or double-stranded viral RNA results in the downstream activation of adaptor molecules, such as mitochondrial antiviral-signalling protein (MAVS), myeloid differentiation primary response gene 88 (MyD88), TIR-domain-containing adaptor-inducing IFN- β (TRIF), nuclear translocation of transcription factors such as IFN regulatory transcription factors 3 and 7 (IRF3 and IRF7), and NF- κ B, which induce expression of type I and II IFN, and various other inflammatory cytokines and chemokines that orchestrate the innate and adaptive immune response. The IFN system, comprising

type I (IFN- α/β are the main variants), type II (IFN- γ), and type III (IFN- λ 1-4) interferons, is the primary mechanism through which the innate immune system protects us against viruses. Type I IFNs are the primary IFNs that are generated in most cell types during viral infections and trigger their own transcriptional program, which results in expression of hundreds of IFN-stimulated genes (ISGs). The ISGs influence many cellular processes, including RNA processing, protein stability, and cell viability, thereby directly affecting specific steps of the viral life cycle and replication. Type I IFNs bind to IFNA- α/β receptors (IFNAR) and signal through the Janus kinase and signal transducer and activator of transcription proteins (JAK-STAT) pathway the expression of ISGs (NGONO; SHRESTA, 2018).

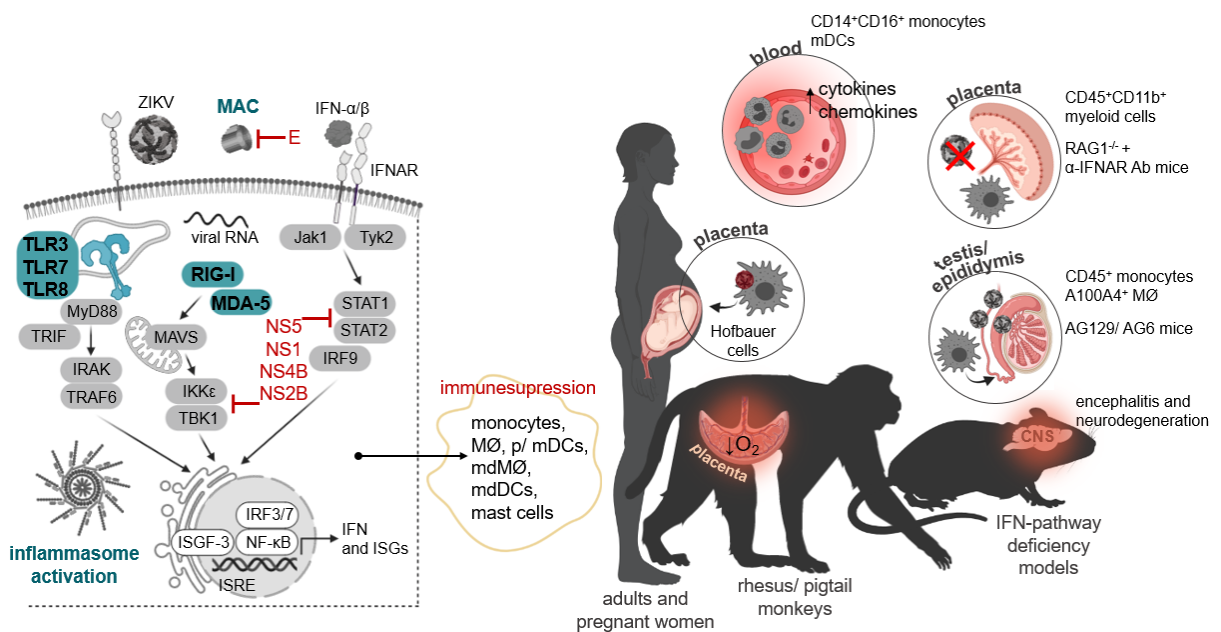


Figure 1. Summary of innate immune components interaction with Zika virus. Identified ZIKV sensors (indicated in blue) and ZIKV antagonism in IFN pathway (topic 1.2.1); innate cells susceptible to ZIKV (topic 1.2.5); and innate immunity action in mouse, non-human primates and humans (topics 1.2.2, 1.2.3 and 1.2.4). MØ=macrophages; pDCs= plasmocytoid dendritic cells; mDCs=myeloid DCs; mdMØ=monocyte derived macrophage; mdDCs=monocyte derived DCs. Designed by the author. Created with Biorender (under licensing and usage conditions).

RIG-I was identified as the major PRR at early time points after ZIKV infection and recognizes the 5' region of the ZIKV genome leading to IFN secretion by infected cells (CHAZAL et al., 2018; ESSER-NOBIS et al., 2019; HERTZOG et al., 2018). Besides RIG-I, ZIKV induces the transcription of TLR3 and MDA5 in human skin fibroblasts (HAMEL et al., 2015). TLR3 and TLR8 are required for triggering type I IFN production in THP-1 (monocytes like) cells upon ZIKV infection, as well as for induction of inflammatory cytokines in HTR8 (trophoblast) cells (LUO et al., 2018).

TLR3 may play a key role in ZIKV-mediated microcephaly, since their activation abrogates the neurodevelopment of infected neural progenitor cells in a human embryonic stem cell-derived cerebral organoid model and dysregulates apoptosis and neurogenesis pathways (DANG et al., 2016).

Moreover, plasmacytoid dendritic cells (pDCs) can sense ZIKV by a specialized synapse upon physical contact with infected cells, during which viral RNA is transferred to pDCs, leading to IFN production via TLR7. It has been previously demonstrated for other viruses that PAMPs could be transferred to pDCs by non-canonical or non-infectious carriers, like exosomes and immature viral particles (ASSIL et al., 2019).

ZIKV can also activate the inflammasome pathways through its NS5 protein, which facilitates the PYD domain-containing protein 3 (NLRP3) inflammasome assembly and leads to pro-caspase-1 cleavage, activation of IL-1 β secretion, and induction of a strong host inflammatory response (WANG et al., 2018). Other groups suggested that ZIKV NLRP3 activation represses IFN- α expression in human monocytes subverting antiviral responses to establish long-term persistence (KHAIBOULLINA et al., 2017).

IFN antiviral responses arguably represent the most critical immune component restricting ZIKV replication, as underscored by the high susceptibility to ZIKV in animal models where the IFN pathway is not functional. IFNAR1^{-/-} mice (lacking type I IFN receptor) or Irf3^{-/-}Irf5^{-/-}Irf7^{-/-} triple knockout mice (little production of IFN- α/β) were susceptible to ZIKV infection in several tissues including brain, spinal cord, and testes, and developed neurological disease (LAZEAR et al., 2016). Similar observations of severe symptoms and detection of viral RNA spread were found using A129 mice (type I IFN receptor deficient) (DOWALL et al., 2016). A129 mice showed ZIKV disease in an age-dependent manner with aged mice not succumbing to infection (ROSSI et al., 2016). In the same way, ZIKV causes high morbidity and mortality in AG129 mice (lack type I and II IFN receptor) (ALIOTA et al., 2016; ROSSI et al., 2016). STAT2^{-/-} mice (subsequent molecule in IFN signaling pathway) recapitulated ZIKV tissue tropism to the central nervous system (CNS), gonads, spleen, and liver and display strain specific severity of neurological symptoms and lethality (TRIPATHI et al., 2017).

Nevertheless, ZIKV has developed strategies to counterbalance host immune mechanisms and its IFN antagonism seems to be cell type/species dependent. ZIKV nonstructural protein NS5 was suggested to antagonize type I IFN signaling by

targeting STAT2 for degradation via proteasome (GRANT et al., 2016), and inhibiting STAT1 phosphorylation (HERTZOG et al., 2018). Other ZIKV non-structural proteins can also interfere with type I IFN production. NS1, NS4, and NS5 can inhibit the induction of IRF3 and NF- κ B signaling and induce proteasome-mediated degradation of STAT2 (KUMAR et al., 2016). NS1, NS4B and NS2B-NS3 can impair TANK-binding kinase 1 (TBK1) and JAK-STAT signaling (WU et al., 2017).

Although ZIKV can antagonize IFN-induced responses after infection by preventing induction of IFNs and disrupting their signaling pathways, IFN still can act restricting ZIKV replication and spread. ZIKV NS5 protein, besides suppression of type I and III IFN signaling, can activate type II IFN signaling (CHAUDHARY et al., 2017). ZIKV is sensitive to the antiviral effects of both type I and II IFN in human skin fibroblasts (HAMEL et al., 2015), and syncytiotrophoblasts (frontline of fetal protection) are refractory to ZIKV infection due to their constitutive release of type III IFN (IFN λ 1), which acts in an autocrine and paracrine manner to induce ISGs and protect non-placental cells from ZIKV infection (BAYER et al., 2016).

1.2.2 Mouse models

ZIKV does not cause infection and disease in immunocompetent adult mice. To overcome this limitation, studies have used immunocompromised, neonatal, special mouse strains or alternative inoculation routes that allow the reproduction of ZIKV pathogenesis consistent with that seen in humans. Mouse models have been useful to demonstrate ZIKV ability to cause fetal abnormalities, deterioration of gonadal tissue, infection through sexual route, and in recapitulating the neurotropic nature of ZIKV infection (TRIPATHI et al., 2017).

Intracranial ZIKV infection in C57BL/6 WT (immunocompetent) or Rag1^{-/-} mice (deficient in mature T and B cells) resulted in a lethal encephalitis with infiltration of macrophages and NK cells and gene expression of pro-inflammatory cytokines correlated with virus spread (IFN $\alpha/\beta/\gamma$, TNF, IL-1 α/β , and IL-6) (HAYASHIDA et al., 2019). On the other hand, neonatal immunocompetent mice challenged subcutaneously with ZIKV elicit T cell infiltration with the predominance of CD8⁺ T cells in the central nervous system, increased expression of IFN- γ , granzyme B, perforin 1, and IL-2 mRNA, and develop slow onset non-lethal encephalitis and neurodegeneration (MANANGEESWARAN; IRELAND; VERTHELYI, 2016). Both works showed that the presence of a functional IFN pathway is not sufficient to control ZIKV replication in the CNS. In contrast, IFNAR^{-/-} mice infected through both routes

showed an accelerated ZIKV spread to peripheral organs in addition to the CNS, where it elicits an inflammatory response characterized by significant increase in mRNA expression of complement C3, COX-2, IL-1 α / β , IL-6, and neutrophils infiltration (HAYASHIDA et al., 2019; MANANGEESWARAN; IRELAND; VERTHELYI, 2016). Curiously, in the brain of STAT2^{-/-} mice subcutaneously infected with ZIKV chemokines associated with T cell infiltration (CCL3, CCL4, CCL5, and CXCL9), monocytes/macrophages infiltration (CCL2 and CCL7), and neutrophil infiltration (CXCL1 and CXCL2, IFN α / β / γ , IL-6, IP-10, and TNF- α) were detected (TRIPATHI et al., 2017). ZIKV intravaginal infection in immunocompetent FVB mice increased transcriptional levels of CCL2, CXCL1 and CXCL10 chemokines in the brain of ZIKV-positive embryos (KHAIBOULLINA et al., 2019).

Late in pregnancy, CD45⁺CD11b⁺ myeloid cells, including neutrophils, monocytes and macrophages from pregnant anti-IFNAR Ab-treated RAG1^{-/-} (AIR) mice, a model of ZIKV vertical transmission, were elevated in the placenta and contained infectious virus. Although the monocyte/macrophage fraction of these myeloid cells have also been reported to contribute to a reduction in viral spread to the fetus during vertical transmission (WINKLER et al., 2020). In contrast, neutrophil recruitment and Ly6C^{mid-hi} monocytes were essential for ZIKV dissemination and pathogenesis. AG129 mice challenged with a recombinant ZIKV that could not replicate in myeloid cells presented no mortality. A complete lack of infectious virus in the sera, no dissemination of virus to peripheral organs (spleen and reproductive tract), no influx of neutrophils to spleen, and no key cytokines involved in leukocyte recruitment during inflammation were also observed. The group also identified Ly6C^{mid-hi} monocyte as the major myeloid cell population that disseminates ZIKV (MCDONALD et al., 2020).

In this same way, CD45⁺ leukocytes, especially monocytes, in the testis and epididymal lumen of AG129 mice contain replicating ZIKV. This finding indicates these cells infection reservoir and trafficking of ZIKV to immunologically privileged sites, and a source of virus particles that are ejaculated allowing for ZIKV sexual transmission (MCDONALD et al., 2018). Still in accordance, bone marrow-derived S100A4⁺ macrophages in AG6 mice were showed to be susceptible to ZIKV and capable, through differentiation into pro-inflammatory M1 macrophages expressing IFN- γ , to increase the permeability of the blood-testis barrier which in turn facilitates S100A4⁺ macrophages invasion into the seminiferous tubules, protecting ZIKV from CD8⁺ T cells action (YANG et al., 2020).

1.2.3 Non-human primates models

Studies in non-human primates (NHP) models have showed an important role of innate immune cells during ZIKV infection, including rapid recruitment and activation of those cells into the blood, signaling pathways regulation, and upregulation of pro-inflammatory cytokines in peripheral blood.

Within 1-2 dpi, a rhesus monkey cohort showed monocytes, NK cells and lymphocytes general activation in the peripheral blood during ZIKV infection (HIRSCH et al., 2017; OSUNA et al., 2016). Minor changes in leukocyte phenotype, and decreased frequencies of CD14⁺CD16⁻ monocytes and myeloid DCs were also described (COFFEY et al., 2017; SILVEIRA et al., 2017). Rhesus monkey developed robust pro-inflammatory response in the first days post ZIKV infection as evidenced by a substantial increase in serum levels of TNF- α , IL-2, IL-10, and IL-12/IL-23 (AID et al., 2017), IL-1RA, CCL2, CXCL10, and CXCL11 (HIRSCH et al., 2017), or CCL2, IL-15, VEGF, IL-10, and IL-1 α (OSUNA et al., 2016). The transcriptome profile in peripheral blood mononuclear cells (PBMC) of these animals showed a robust induction of IFN- α and antiviral pathways, ISGs (OAS2, IFIT1/2/3, ISG15, IRF7, IFI44, MX1, and MX2), components of the inflammasome (NOD2, NLRP3, CXCL10, BTG2, BST2, OSM), proinflammatory cytokines/chemokines (TNF- α , IL-1, IL-18, CCR7, CCL2, and CCL20), and immunomodulatory pathways (IL-10, TGF- β , and T regulatory cells). Acute ZIKV infection also upregulated genes associated with monocyte and T helper cell pathways, but downregulated T cell signaling, B cell signaling, and MHC-I pathways (AID et al., 2017).

ZIKV infection in pigtail macaques induced a robust cellular innate immune response including rapid DC, monocyte and neutrophil recruitment into the blood, mucosal tissues (vagina and intestine), and lymph nodes within the first week of infection and increased plasma pro-inflammatory cytokines/chemokines (IL-1RA, sCD40L, CCL2, and IL-15). Plasmacytoid DCs presence and the production of CCL2 may initiate the recruitment of non-classical monocytes, primary cellular targets for ZIKV infection, and other ZIKV cellular targets to the lymph nodes, resulting in the observed increased viral dissemination and persistence at this site (O'CONNOR et al., 2018).

The available data from NHP studies suggests the contribution of some underlying inflammation to the placental dysfunction in ZIKV-infected pregnancies. Long-term persistence of ZIKV in both pregnant rhesus macaques and fetal tissues was associated with robust maternal and fetal innate and adaptive immune

responses, systemic fetal inflammatory response to congenital infection with ZV, and impairment in transplacental transport of oxygen (uterine vasculitis and placental villous damage), that may result in adverse obstetric outcomes. The inflammatory immune response observed in placenta and fetal tissues is characterized by activation of monocytes/macrophages, myeloid DCs and NK cells, alterations in classical to non-classical monocytes phenotype, and elevated cytokines/chemokines (IL-1RA, IL-1 β , CCL2, IL-12, IFN- γ , and CXCL-10) (HIRSCH et al., 2018).

1.2.4 Human patients

Work from multiple groups has analyzed ZIKV infection and immune responses from human clinical samples. During the acute phase of human ZIKV infection, multiple pro-inflammatory cytokines were increased in the blood, although the cellular sources of these responses remain unknown. Differential cytokine expression may lead to manifestation of different clinical conditions.

Serum cytokine levels of five travelers returning from Asia, the Pacific and Brazil with acute ZIKV showed elevated concentrations of IL-1 β , IL-2, IL-4, IL-6, IL-9, IL-10, IL-13, IL-17, IL-10, RANTES, CCL2, and VEGF (TAPPE et al., 2016). Several immune mediators, such as IL-4, IL-6, IL-7, IL-8, IL-10, IL-18, TNF- α , IFN- γ , GRO- α , IL-1RA, CXCL10, CCL2, MIP-1 β , eotaxin, and SDF-1 α , were higher in 95 acute ZIKV-infected patients from Campinas, Brazil (KAM et al., 2017). Brazilian patients from Rio Grande do Norte have increased mRNA expression of TLR3 and IFN $\alpha/\beta/\gamma$ in peripheral blood, and decreased expression of RIG-1, TLR-8, MYD88, and TNF- α , during acute ZIKV infection. This data suggests a viral escape mechanism is in action (DA SILVA et al., 2019). A cohort of patients with moderate symptoms during a ZIKV outbreak in Singapore/2016 had higher levels of IP-10, CCL2, IL-1RA, IL-8, and PIGF-1, accompanied by a transient leukopenia, except of CD14⁺ monocytes (LUM et al., 2018b).

Using an in vitro model of ZIKV infection of primary human PBMCs obtained from healthy blood donors, the majority of ZIKV-infected cells at 48 hours post-infection were CD14⁺CD16⁺ monocytes. The same was observed for 29 patients in Nicaragua around 3.3 days of acute illness. An analysis of the patients' blood showed that 4.6% of PBMCs become infected, among which 82.6% were monocytes, 10.7% myeloid DCs, 2% NK cells, 0.8% B cells, and 0.6% T cells (MICHLMAYR et al., 2017).

ZIKV infection in myeloid DCs from individuals with acute disease was also characterized by transcriptional changes that suppress IFN-dependent immune responses and impair DCs function in order to increase these cells susceptibility to ZIKV (SUN et al., 2017). But, three individuals diagnosed with ZIKV infection during the 2016 outbreak in Caribbean, showed transcriptional changes of activation in plasmacytoid DCs and upregulation of type I IFN dependent genes (SUN et al., 2020).

Higher levels of IL-22, CCL2, TNF- α , and CXCL10 were observed in ZIKV-infected pregnant women carrying infants with congenital CNS abnormality deformities (KAM et al., 2017). The placenta of a ZIKV infected pregnant patient diagnosed with Guillain-Barré Syndrome that had a spontaneous abortion was inflamed and presented tissue abnormality dysfunction that could be supported by the increased Hofbauer cells, CD8 T cells, and expression of local pro-inflammatory cytokine IFN- γ , TNF- α , RANTES, and VEGFR2 (RABELO et al., 2018). Three ZIKV-infected women in Singapore had different placental infection profiles in acute phase with increased IL-1RA, CXCL10, EGF, and RANTES expression, and neutrophil numbers. Despite that, the placentas showed no anatomic defects and the babies had no congenital anomalies (LUM et al., 2019).

1.2.5 Human innate cells

ZIKV-infected leukocytes could disseminate or serve as a viral reservoir in different compartments of the body, including immune-sheltered tissues, a mechanism known as Trojan horse. Moreover, insights into the specific cellular innate immune responses arising at the earliest stages post-ZIKV exposure have a central role in understanding ZIKV infection, persistence, and pathogenesis. CD14⁺ monocytes, DCs and macrophages are believed to be primary targets of ZIKV infection *in vitro*. Interestingly, ZIKV driven immunosuppression that can favor virus spread as seen in *in vitro* models of infection of these cells. Moreover, the overactivation of key molecules in the innate immune pathways upon ZIKV infection is detrimental to human neuronal differentiation by the induction of pro-aging factors (LIU et al., 2019; PEI et al., 2021).

At 24 hours post infection with an Asian strain of ZIKV lower virus burden in CD14⁺ monocytes from whole blood, non-classical monocytes expansion (CD14^{low}CD16⁺), suppression of the type I IFN-signaling pathway, high IL-10 expression, and an M2-skewed immunosuppression gene expression profile were

reported. Though higher virus burden, high expression of CXCL10, and M1-skewed inflammatory gene expression were associated with African ZIKV strain infection (FOO et al., 2017; LI et al., 2018). The authors also observed heightened sensitivity of maternal monocytes to ZIKV during the first and second trimesters of gestation with a M2-skewed immunosuppression phenotype induced by Asian ZIKV infection (FOO et al., 2017). In line, monocytes from human cord blood were identified as targets for ZIKV infection (KHAIBOULLINA et al., 2017) and could be more prone to infection since they present an impaired production of IL-1 β , IL-10 and MCP-1 and a higher expression of ZIKV entry receptors (YOSHIKAWA et al., 2019). Moreover, ZIKV affected adhesive properties of monocytes enhancing their transmigration through endothelial barriers and viral dissemination to neural cells (AYALA-NUNEZ et al., 2019).

Contemporary and ancestral ZIKV strains productively infect human mdDCs (BOWEN et al., 2017; HAMEL et al., 2015; VIELLE et al., 2018). Low but significant levels of ZIKV infection in immature mdDCs has been reported, whereas mature DCs were not permissive to ZIKV infection (LI et al., 2018). A better ZIKV replication and IFN induction in mdDCs was observed associated to Asian than African strain infection (ÖSTERLUND et al., 2019). However, other studies reported that ZIKV infection does not induce activation or maturation of DCs, and is characterized by limited expression of type I and II IFN and pro-inflammatory cytokines (BOWEN et al., 2017; GARCÍA-NICOLÁS et al., 2019; VIELLE et al., 2018).

Monocyte-derived macrophages are susceptible to Asian and African ZIKV strains (KHAIBOULLINA et al., 2017). The transcriptomic profile after ZIKV infection showed activation of cross-talk pathways between monocyte-derived macrophages and NK cells, suggesting that immune cells can act in combination to orchestrate host immune responses and drive disease progression (LUM et al., 2018a). Other study reported ZIKV attenuated replication in macrophages (ÖSTERLUND et al., 2019). ZIKV infects and replicates in primary human placental macrophages, called Hofbauer cells, *in vitro* and in placenta explants, suggesting an intrauterine transmission mechanism (DE NORONHA et al., 2016; JURADO et al., 2016; LUM et al., 2019; QUICKE et al., 2016; TABATA et al., 2016). Upon infection, Hofbauer cells are modestly activated, produce IFN- α and other pro-inflammatory cytokines (IL-6, MPC-1 and IL-10), and upregulate RIG-I-like receptor transcription expression and downstream antiviral effector genes, confirming a ZIKV-antiviral response is activated in these cells (QUICKE et al., 2016).

Mast cells were identified positive to ZIKV infection in the placenta of two women seropositive for ZIKV infection. Also, a human mast cell lineage (HMC-1) was permissive to ZIKV, degranulated and released TNF- α , IL-6, IL-10, and VEGF in the presence of virus suggesting these cells as source of mediators that can activate other immune cells and contribute in viral spread in vertical transmission (RABELO et al., 2020).

Beyond that cellular overview, it is worth mentioning that ZIKV neutralization can be mediated by the human classical complement pathway, driven by IgM antibodies, leading to the membrane-attack complex (MAC) formation (SCHIELA et al., 2018). but ZIKV envelope (E) protein binds to terminal pathway complement proteins and interferes with the formation of MAC (MALEKSHAHI et al., 2020).

1.3 GAPS IN ZIKA VIRUS INNATE IMMUNOLOGY

Within the presented context, we detected a lack of studies assessing two relevant components of the innate immune system that may impact the development of ZIKV disease and ensuing responses: first, the neutrophil; and second, cell migration, specially DCs and neutrophils, to the draining lymph nodes after skin ZIKV infection. In this thesis we set out to contribute knowledge to help fill these gaps.

Chapter 1 of this thesis presents work on human neutrophil *in vitro* response to ZIKV (submitted manuscript). Chapter 2 elucidates the unprecedented inhibition role of *vaccinia virus* in the migration of dendritic cells to the draining lymph node (paper), making use of a fluorochrome-based migration *in vivo* assay. This was later used as a tool to start assessing cellular migration in response to ZIKV infection.

In the next sections an overview of the current knowledge on the role played by neutrophils in viral infections as well as DCs and neutrophil migration to lymph nodes is presented.

1.3.1 Neutrophils

Mature neutrophils are abundant (50-70% of circulating leukocytes in humans), short-lived terminally differentiated polymorphonuclear leukocytes (with fully formed cytoplasmic granules - filled with more than 700 proteins, secretory vesicles, and segmented nuclei), and major effectors recruited to sites of acute inflammation. Neutrophils are continuously generated in the bone marrow from myeloid precursors and recruited to the circulation, a process called granulopoiesis (canonically involving IL-23, IL-17 and GM-CSF) (MAYADAS; CULLERE; LOWELL,

2014). Under physiological conditions, they can also be found in the bone marrow, spleen, liver and lung (reservoirs of mature neutrophils). Neutrophils (senescent or dead on inflammation) die through apoptosis and are removed by tissue macrophages and dendritic cells primarily in the liver, spleen and bone marrow, a process termed efferocytosis (KOLACZKOWSKA; KUBES, 2013; KRUGER et al., 2015).

Inflammation develops in response to PAMPs (e.g. lipopolysaccharide, peptidoglycan, lipoteichoic acids, double-stranded viral RNA, and bacterial DNA) and injured tissue damage-associated molecular patterns (DAMPs) that trigger activation of PRRs. Tissue resident macrophages and mast cells act as sentinel cells that initiate neutrophil recruitment by controlling and inducing various processes, such as an increase in permeability of local blood vessels and the release of attractive factors. Chemokines, lipid mediators, complement fragments, and tissue breakdown products (e.g. TNF- α , IL-1, IL-6, CXCL1, CXCL2, CXCL8, C5a, GM-CSF and leukotriene B4) (GALANI; ANDREAKOS, 2015), trigger changes on the surface of endothelium like the expression of adhesion molecules (e. g selectins) and conformational changes of neutrophil surface integrins (e.g. LFA1 and MAC1) with higher affinity for immunoglobulin-like cell adhesion molecules (CAMs). Following a chemotactic gradient along the endothelium to the required site, neutrophil recruitment cascade involves tethering, rolling, adhesion, crawling and transmigration at endothelial cell-cell junctions through regions of basement membrane that exhibit low levels of extracellular matrix molecules and gaps between pericyte regions. Neutrophil recruitment is not limited to infectious conditions and also occurs in sterile environments (KOLACZKOWSKA; KUBES, 2013).

Circulating neutrophils are quiescent and their activation is usually a multistep process, with them becoming fully activated in response to pro-inflammatory stimuli in the tissue, a state in which neutrophils reach their full pathogen-destruction capacity. Neutrophils are relatively unresponsive to a single stimulus, but exposure to one stimulus (e.g. lipopolysaccharide, TNF, chemokines, growth factors and adhesion), know as neutrophil priming, enhances the ability of the cell to mount an activation response to a second stimulation (MAYADAS; CULLERE; LOWELL, 2014). Neutrophils recognize pathogens via classes of cell surface and intracellular PRRs (TLRs, CLRs, RLRs, NLRs) that bind to pathogen-specific molecules, opsonic receptors (Fc γ Rs and complement receptors) that recognize host proteins such as IgG and complement, and G protein-coupled receptors (GPCRs), involved mainly in

guiding neutrophil migration. These receptors induce intracellular signals that lead to full neutrophil activation (TAKEUCHI; AKIRA, 2010).

Neutrophils can readily eliminate pathogens by multiple means, both intra- and extracellular. After phagocytosis (upon ligation of opsonic receptors), neutrophils kill microorganisms using NADPH oxygenase-dependent mechanisms (reactive oxygen species (ROS)) or antibacterial proteins and enzymes (e.g. cathepsins, calprotectins, defensins, proteinases, lactoferrin, lipocalin, lysozyme, elastase, and myeloperoxidase), the latter can be released into the phagosomes or into the extracellular milieu (KRUGER et al., 2015). Oxygen derivatives kill through decarboxylation, deamination, or peroxidation of pathogen proteins and lipids; and most peptides in neutrophil granules cause disruption of bacterial membranes, inhibition of microbial iron uptake, cleavage of cell wall peptidoglycans, interference in nucleic acids biosynthesis, and disruption of bacterial biofilm (KRUGER et al., 2015; MAYADAS; CULLERE; LOWELL, 2014). Also, highly activated neutrophils can eliminate extracellular microorganisms by releasing neutrophil extracellular traps (NETs): a core of DNA element to which histones, granule proteins and enzymes are attached to immobilize and eventually kill the trapped pathogen (BRINKMANN et al., 2004; KENNY et al., 2017; PAPAYANNOPOULOS, 2018).

Neutrophils have classically been referred with a restrict set of pro-inflammatory functions. With new technologies such as intravital microscopy and the availability of transgenic mice, recently it has become apparent that they are more complex multitasking cells capable of a vast array of specialized functions, contributing to chronic inflammatory conditions, adaptive immune responses and presenting anti-inflammatory or healing characteristics (KOLACZKOWSKA; KUBES, 2013). Neutrophil cross talk with other immune cells is mediated by their ability to secrete a bunch of cytokines and express a large number of cell surface molecules. Neutrophils can promote DCs maturation and provide access to neutrophil captured pathogen products (ALFARO et al., 2011); present antigens capable of priming Th1- and Th17-acquired immune responses (ABDALLAH et al., 2011); migrate to lymph nodes and cross-prime CD8⁺ T cells (BEAUVILLAIN et al., 2007, 2011); transport antigens from the dermis to the bone marrow, initiating memory CD8⁺ T cells (DUFFY et al., 2012); and splenic neutrophils can induce immunoglobulin class switching, somatic hypermutation and antibody production by activating marginal zone B cells (PUGA et al., 2012). Moreover, neutrophils can participate in NK cells regulation

(COSTANTINI et al., 2011; JAEGER et al., 2012; SPÖRRI et al., 2008) and macrophages regulation (FILARDY et al., 2010).

Although neutrophil recruitment during infection is likely to be essential for protective immunity, neutrophil improper or prolonged activation during a sterile injury or a dysregulated infection may be detrimental (release of oxidants, proteases, feeding of neutrophil recruitment loop) and cause perpetual or non-resolving bystander injury. Several chronic inflammatory disease conditions are characterized by a sustained influx of neutrophils, such as cystic fibrosis, chronic obstructive pulmonary disease, rheumatoid arthritis, nephritis, systemic lupus erythematosus, and cardiovascular diseases. A balance between beneficial and detrimental effects of neutrophil initiated inflammatory responses must be maintained for tissue homeostasis (DRESCHER; BAI, 2013; KOLACZKOWSKA; KUBES, 2013; KRUGER et al., 2015).

1.3.1.1 Neutrophils in virology

The role of neutrophils in bacterial, fungal, and protozoan infections is crucial and has been well characterized. However, it remains unclear how critical neutrophils are for antiviral immunity or if they even present virus-directed responses. Conventionally, due to the abundance of neutrophils reaching the site of infection and their mechanisms of action, a contribution to viral clearance is expected. Moreover, neutrophil protective effects during antiviral defense are controversial since they have been reported to mediate both beneficial and detrimental effects to the host, and no pattern of action is observed within a group of viruses. A summary on the current knowledge of the role of neutrophils in viral infections is presented in Table 2. Also, the accumulated knowledge of neutrophil involvement in ZIKV infection since its last outbreak is illustrated in Figure 2.

In summary, neutrophils can phagocytose virus or become activated by PRRs and initiate an antiviral program, produce antimicrobial agents that inactivate the virus, and neutrophils through NETs can entrap the virus and inactivate it. On the other hand, neutrophils can propagate viral infections; become excessively activated, triggering overt immune activation leading to host tissue damage. It is also important to note that neutrophils are well known to be infiltrated during many types of lung diseases associated with acute respiratory distress syndrome (ARDS) and severe pneumonia (CAMP; JONSSON, 2017). Such observations confirm the importance of neutrophils in viral infections.

Table 2. Neutrophils involvement in viral infection. Neutrophil positive or negative actions in the host perspective during various virus infections. In vivo works are indicated in orange (and by the symble ■), in vitro studies are in blue (and by the symble ●), and studies in patients in green (and by the symble ◆). (-) indicates that the consequences of neutrophil actions were not investigated.

	Neutrophil contributions to the host	Virus	Observations	References
Respiratory viruses	<u>Negative:</u> NETs have a detrimental role in the pathophysiology of COVID-19	<i>Severe acute respiratory syndrome-related to coronavirus 2 (SARS-CoV-2)</i>	◆ Sera from patients with COVID-19 had elevated levels of cell-free DNA, MPO, and citrullinated histone H3. NETs were consistently increased in hospitalized patients receiving mechanical ventilation or in intensive care units. NETs were associated with inflammation and microvascular thrombosis.	(BARNES et al., 2020; LEPPKES et al., 2020; MIDDLETON et al., 2020; SKENDROS et al., 2020; VERAS et al., 2020; ZUO et al., 2020)
	<u>Positive:</u> control of viral replication <u>Negative:</u> contribution to lung pathology	<i>Rat coronavirus (RCoV)</i>	■ PMN-depleted rats infected with RCoV had increased mortality and morbidity and prolonged pulmonary viral replication. PMN were required for the production of chemokines in airways. However, the presence of PMN was correlated with haemorrhagic lesions, epithelial barrier permeability and cellular inflammation in the lungs.	(HAICK et al., 2014)
	<u>Positive:</u> limitation of viral replication and disease and reduction of the risk of a secondary infection. Contribution in the progression of immune response <u>Negative:</u> instigation of alveolar-capillary damage and viral dissemination	<i>Influenza virus</i>	■ Neutrophils ameliorated vascular permeability and pulmonary inflammation post intermediate or high virulence strains of influenza virus infection limiting extrapulmonary spread of the virus. Excessive neutrophil infiltration in lungs of influenza A virus infected mice resulted in alveolar damage, increased viral loads and progression into ARDS-like pathology. Neutrophil depletion resulted in mild lung pathology. Moreover, NETs formation was linked with lung damage. Influenza A virus infection induced neutrophil dysfunction (impaired phagocytosis) due to reduced G-CSF production in the lung.	(TATE et al., 2009, 2011; TUMPEY et al., 2005) (NARASARA JU et al., 2011) (ISHIKAWA et al., 2016)

		<ul style="list-style-type: none"> ● Human neutrophils are infected by influenza virus, activating TLR7 and TLR8 and producing inflammatory cytokines. (WANG et al., 2008) ● Neutrophils in the lungs infected with influenza A virus acted as antigen presenting cells for antiviral CD8⁺ T cells. (HUFFORD et al., 2012) ● Human neutrophils peptides induced aggregation of influenza A virus and bacteria, which increased their uptake by neutrophils. The antimicrobial peptide LL-37 did not alter neutrophil uptake of IAV, but increased neutrophil oxidative response and boosted NETs formation by the virus. (TECLE et al., 2007; TRIPATHI et al., 2014) ◆ Neutrophils were infected with avian Influenza virus in the placental blood of a pregnant woman. (ZHAO et al., 2008)
<p><u>Positive:</u> viral restraint</p> <p><u>Negative:</u> obstruction and damage of airways</p>	<p><i>Respiratory syncytial virus (RSV)</i></p>	<ul style="list-style-type: none"> ■ RSV induced NETs formation in human neutrophils that trap viral particles. However, NETs were detected occluding the airways in the lung of patients with severe lower respiratory tract disease caused by RSV. (CORTJENS et al., 2016a)
		<ul style="list-style-type: none"> ● RSV induced neutrophil degranulation (MPO) and chemokines release (IL-8, MIP-1α, MIP-1β). (JAOVISIDH A et al., 1999)
		<ul style="list-style-type: none"> ● RSV triggered ROS-dependent NETosis in human neutrophils. Those NETs were capable of trapping RSV decreasing cellular damage by interfering with viral fusion protein. Neutrophils also released NETs in response to RSV-infected cells. (FUNCHAL et al., 2015; MURARO et al., 2018; SOUZA et al., 2018)
		<ul style="list-style-type: none"> ● Neutrophil migration and adherence to RSV-infected airway epithelial cells was associated with greater epithelial cell damage, neutrophil degranulation and reduction in infectious viral load. These effects were mediated in part by β_2-integrin ligand LFA-1 on neutrophil binding to ICAM receptor on nasal epithelial cells. (DENG et al., 2020; HERBERT et al., 2020)

			<p>◆ RSV proteins were detected in neutrophils in cases of severe RSV bronchiolitis in infants.</p>	(HALFHIDE et al., 2011)
Other viruses	<p><u>Positive:</u> protection of infected tissue and contribution in the progression of immune response</p>	<p><i>Vaccinia virus (VACV)</i></p>	<p>■ Ly6C⁺Ly6G⁺ cells infiltrated in VACV infected skin later than monocytes and produced IFN-I and ROS. The depletion of neutrophils resulted in increased tissue damage.</p>	(FISCHER et al., 2011)
			<p>◆ VACV activated oxidative metabolism in neutrophils. Neutrophils uptaked VACV without phagocytosis.</p>	(JONES, 1982; WEST et al., 1987)
			<p>■ Intranasal infection with <i>Modified vaccinia virus Ankara (MVA)</i> induced early immigration of neutrophils to the lungs (dependent on the complement component C5, but in a C3-independent manner).</p>	(PRICE et al., 2015)
			<p>■ After intradermal injection, neutrophils migrated from skin to bone marrow, carrying MVA and activating CD8⁺ T cells.</p>	(DUFFY et al., 2012)
	<p><u>Positive:</u> viral restraint</p>	<p><i>Myxoma virus (MYXV)</i></p>	<p>■ Systemic intravenous MYXV infection induced neutrophil and platelets recruitment to the liver microvasculature. There, the interaction between neutrophils and platelets facilitated the release of NETs, which contributed in reducing the number of liver infected cells.</p>	(JENNE et al., 2013)
<p><u>Positive:</u> reduction in the risk of a secondary infection, reduced mortality in patients, and viral restraint</p>	<p><i>Human immunodeficiency virus 1 (HIV-1) and Feline immunodeficiency virus (FIV)</i></p>	<p>■ HIV patients and FIV infected animals showed a profound defect in the chemotaxis of neutrophils (rolling, adhesion and emigration) in response to inflammatory signals. Neutropenia and neutrophil defects are common complications of infections by lentivirus due to altered neutrophil development caused by HIV infection of bone marrow stem cells, stroma cells, macrophages and resident CD4⁺ cells, altered cytokine milieu in the bone marrow, and suppression of hematopoiesis by viral proteins and antiretroviral drugs. Also HIV protease inhibitors could directly induce neutrophils apoptosis.</p>	(HADAD et al., 2007; HEIT et al., 2006; KUBES et al., 2003; PRICE et al., 2015)	

		<ul style="list-style-type: none"> ● Neutrophils sense HIV-1 by TLR7 and TLR8, and generate ROS that trigger NETs formation. NETs captured HIV-1 and promoted its elimination through myeloperoxidase and α-defensin. ● Different components of HIV-1 induced activation of neutrophils by modulating the expression of TLR2, TLR4, and TLR7, CD62 and CD11b, promoting the secretion of IL-6 and TNF-α, and altering ROS production. 	(SAITOH et al., 2012)
			(GIRALDO et al., 2016)
<u>Positive:</u> viral restraint	<i>Herpes simplex virus type-1 (HSV-1)</i>	■ Depletion of neutrophils induced higher HSV-1 titers in the eyes and spread to skin and brain of mice that became more susceptible to encephalitis and had increased mortality.	(TUMPEY et al., 1996)
-	<i>Epstein-Barr virus (EBV)</i>	<ul style="list-style-type: none"> ● EBV binding to human PMN resulted in the activation of intracellular events involved and release of pro-inflammatory lipid mediators. ● EBV infected human neutrophils and induced its apoptosis. 	(GOSSELIN et al., 2001)
			(LAROCHELLE et al., 1998)
<u>Negative:</u> viral dissemination	<i>Cytomegalovirus (CMV)</i>	<ul style="list-style-type: none"> ● CMV infection of endothelial cells induced enhanced production of IL-8, CXCL1 and neutrophil chemotaxis. During transmigration, neutrophils acquired CMV particles that could later be transmitted to fibroblasts. ● Human retinal pigment epithelial cells infected with human CMV induced neutrophil chemotaxis, but the binding and the transepithelial neutrophil penetration were impaired by up-regulation of Fas ligand in the retinal cells as a result of virus infection. 	(GRUNDY et al., 1998)
			(CINATL et al., 2000)
-	<i>Hepatitis B virus (HBV)</i>	◆ Impaired NETs released in patients with chronic HBV infection. HBV proteins C and E were responsible for this inhibition by decreasing ROS production and autophagy.	(HU et al., 2019)

	<u>Negative:</u> NETs exacerbation of asthma	<i>Sendai virus (Sev)</i>	<ul style="list-style-type: none"> ■ Sev infection induced NET formation in the lung of mice and alveolar inflammation. NETs also primed bone marrow-derived cells to release cytokines that can amplify the inflammatory cascade. 	(AKK; SPRINGER; PHAM, 2016)
	<u>Negative:</u> contribution to the kidney damage and NETs association with disease	<i>Hantavirus (HTNV)</i>	<ul style="list-style-type: none"> ■ Elevated levels of circulating and tissue-localized myeloperoxidase, elastase, IL-8 and histones in acute hemorrhagic fever with renal syndrome. Primary blood microvascular endothelial cells acquired a pro-inflammatory phenotype during hantavirus infection and are responsible to attract and activate neutrophils through surface receptors in an IL-8 dependent mechanism. Hantavirus alone did not activate neutrophils <i>in vitro</i>. ● HTNV use of $\beta 2$ integrin receptors CR3 and CR4 as entry receptors at the same time strongly induces both ROS production and NET formation. Also, HTNV infection induced high systemic levels of circulating NETs and autoantibodies to nuclear antigens in patients. 	(STRANDIN et al., 2018)
Alphavirus and Flavivirus	<u>Positive:</u> viral restraint	<i>Chikungunya virus (CHIKV)</i>	<ul style="list-style-type: none"> ■ Neutrophils expression of IFN reduced mortality of zebra fish infected with CHIKV. ● NETs neutralized CHIKV <i>in vitro</i> and reduced mice susceptibility. CHIKV activated NETs through activation of TLR7 and ROS <i>in vivo</i>. 	(PALHA et al., 2013)
	-	<i>Japanese encephalitis virus (JEV)</i>	<ul style="list-style-type: none"> ● Neutrophils degraded JEV by oxidation. 	(SRIVASTAV A et al., 1999)
	-	<i>Tick-borne encephalitis virus (TBEV)</i>	<ul style="list-style-type: none"> ● TBEV infected neutrophils and induced their apoptosis. 	(PLEKHOVA et al., 2012)

	<p><u>Negative:</u> enhancement of neuroinvasive disease</p>	<p><i>West Nile virus</i> (WNV)</p>	<p>■ In early infection, neutrophils are rapidly recruited to the site of infection, used as reservoirs for viral replication and act as Trojan horse carrying the virus into the central nervous system. Neutrophil depletion prior to WNV infection results in reduced viremia and enhanced survival of the host.</p>	<p>(BAI et al., 2010; PAUL et al., 2017)</p>
	<p>-</p>	<p>Dengue virus (DENV)</p>	<p>● Neutrophils respond to DENV-2 by increasing mRNA level of the antimicrobial peptides α-defensins and cathelicidin LL-37.</p>	<p>(CASTAÑED A-SÁNCHEZ et al., 2016)</p>
			<p>◆ Patients had increased serum levels of IL-8, elastase, TNF-α, reactive oxygen species, markers for NETs, neutrophil gelatinase-associated lipocalin, and several canonical proteins associated with neutrophils degranulation. It was also reported severe neutropenia in a cohort of adult DENV patients.</p>	<p>(DEVIGNOT et al., 2010; HOANG et al., 2010; JUFFRIE et al., 2000; LIU et al., 2016; OPASAWAT CHAI et al., 2019; THEIN et al., 2014)</p>

1.3.1.2 Neutrophils as therapeutic targets for viral diseases

Clinical manipulation of neutrophils to control viral infection is not trivial and should be cautiously evaluated once it may cause opportunistic infections or immunopathology. However, this does not preclude exploring therapies that have neutrophils as targets in infections and chronic diseases. HSV-1 infection can cause stromal keratitis lesions, a chronic inflammation of the eye, with risk of intraocular pressure elevation and formation of cataracts. The disease can be partially controlled with the administration of a resolvin agent, RvE1, which are mediators derived from omega-3 fatty acids eicosapentaenoic and docosahexaenoic acid. RvE1 was showed to inhibit the production of IFN- γ , IL-6 and IL-17, which was correlated with a reduced influx of neutrophils in the neovascular system where lesions occurred (DRESCHER; BAI, 2013; RAJASAGI et al., 2011). In the same line, WNV in a milieu deficient in the chemokine receptor gene *Cxcr2* results in reduced viremia and enhanced survival of the host (BAI et al., 2010) being possibly amenable to a similar therapeutic approach.

Other explored approaches are blocking neutrophil transendothelial migration, inhibition of neutrophil elastase, and decreasing ROS activity (VAN DER LINDEN; MEYAARD, 2016). NETs can also be targeted by existing drugs through several means. Neutrophil elastase, peptidyl arginine deiminase type 4 (PAD4), and gastermin D inhibitors can prevent NET formation. DNase has been used safely to

digest NETs in the mucous secretions of the airways of cystic fibrosis patients (BARNES et al., 2020). Colchicine is an existing drug that could inhibit both neutrophil recruitment to sites of inflammation and the secretion of IL-1 β , and trials in COVID-19 are underway (BARNES et al., 2020).

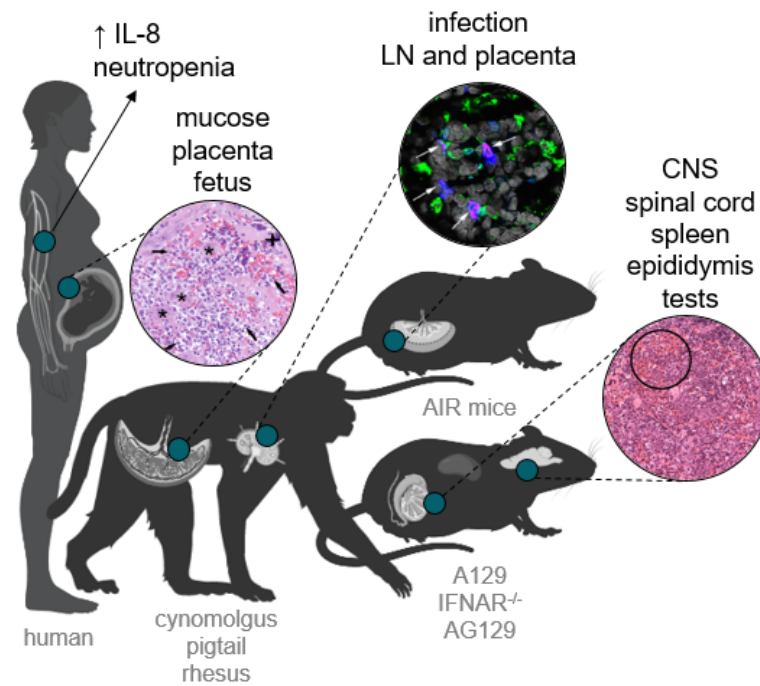


Figure 2. Neutrophils in Zika virus infection. There are sparse evidences supporting a role for neutrophils in ZIKV infection. Neutrophils may be permissive to ZIKV as viral RNA was found in myeloperoxidase⁺ neutrophils in lymph nodes 7 days after infection in cynomolgus macaques (OSUNA et al., 2016), and in CD45⁺CD11b⁺ neutrophil myeloid cells in the placenta of anti-IFNAR Ab-treated RAG1^{-/-} (AIR) mice, a model of ZIKV vertical transmission (WINKLER et al., 2020). IFN receptor deficient mouse models showed enhanced neutrophil inflammation in the CNS following ZIKV infection and in other relevant structures such as spleen, spinal cord, epididymis and testes (ALIOTA et al., 2016; DOWALL et al., 2016; HAYASHIDA et al., 2019; MANANGEESWARAN; IRELAND; VERTHELYI, 2016; MCDONALD et al., 2018; ZUKOR et al., 2018). Neutrophils infiltrations were also present in mucosal, placental and fetal tissues during acute ZIKV infection in humans, pigtail and rhesus macaques (LUM et al., 2019; NGUYEN et al., 2017; O’CONNOR et al., 2018). ZIKV patients presented elevated IL-8 serum levels in the acute or convalescent phases of the disease (KAM et al., 2017; LUM et al., 2018b; TAPPE et al., 2016). Monocytes infected *in vitro* for 24 and 48 hours had IL-8 upregulated in the transcriptional profile compared to monocytes from healthy uninfected dblood donors (MICHLMAYR et al., 2017). Neutropenia was detected in the blood of patients in acute phase and in the first week after ZIKV infection in rhesus monkeys (DUDLEY et al., 2016; LUM et al., 2018b; PANTOJA et al., 2017). Moreover, lethal challenge of AG129 mice with a recombinant ZIKV that could not replicate in myeloid cells, resulted in no viral infection and dissemination to peripheral organs, and no influx of neutrophils to spleen and key cytokines involved in leukocyte recruitment, suggesting an essential role for neutrophils recruitment in ZIKV pathogenesis (MCDONALD et al., 2020). Designed by the author. Created with Biorender (under licensing and usage conditions).

1.3.2 Neutrophil and dendritic cell migration to lymph nodes

Beyond the bloodstream, pathogens can spread in the host using lymphatic vessels (started in open-ended capillaries). The lymphatic system has as major function to transport interstitial fluids from tissues back to the circulatory system, and is largely used by the immune system as a migratory via for immune cells surveillance. As a countermeasure to possible unwanted passers-by, all lymphatic fluid is filtered in the lymph nodes (LNs), widely distributed in several points along the system (450 ones in adults), where resident and recruited cells can contain pathogen dissemination. In a very clever way, lymph nodes evolved to also work as an important site of antigen presentation, lymphocytes priming and tolerance (HAMPTON; CHTANOVA, 2019).

LNs are secondary lymphoid organs highly compartmentalized, kidney-shaped encapsulated bodies. Lymphatic fluid coming from the draining area via the afferent lymphatics enters the LN into the subcapsular sinus, bypassing LN follicles through the medullary sinus until efferent lymphatics. The bottom of the subcapsular sinus is composed by sinus-lining cells and a large population of macrophages and lymphoid tissue-resident DCs (that capture antigens and either eliminate or present them and create cytokine-rich surroundings), and works as a shield to the lymphoid compartment, allowing the active passage of cells. Fluid and molecules <70 kDa can enter only via small collagen tubules originating between the sinus-lining cells. Antigen-loaded DCs reach the lymphoid compartment/outer cortex/lymphoid follicle through the reticular conduit system (a road-like cellular three dimensional network formed by fibroblastic reticular cells that provides essential chemotactic, survival, and regulatory signals for immune cells) and present their antigens to T cells in the paracortex or B cells in follicles, developing into germinal centers. The LN paracortex is vascularized by high endothelial venules (HEV), to allow active immigration of lymphocytes from the blood into this compartment (NOVKOVIC et al., 2020; ROOZENDAAL; MEBIUS; KRAAL, 2008).

DCs are the most potent and versatile antigen-presenting cells, and comprise a heterogeneous population distributed across various organs (different origins, functions, and surface marker expression). DCs in the skin are diverse: some are resident in the dermis, some are resident in the epidermis (Langerhans cells), and others are recruited from the blood and remain only transiently in the skin before entering lymphatic vessels. Since DCs discovery in 1973 by Ralph Steinman, several DCs subsets have been described based on ontogeny. Conventional DCs (cDCs)

represent the prototypical antigen-presenting cell type of the immune system. In mouse, among Langerhans cells, there are at least four cDCs subsets recognized within the dermis on the basis of the expression of CD207 (Langerin), CD11b and CD103 (HENRI et al., 2010; KUSHWAH; HU, 2011).

DCs probably enter the lymph through the initial lymphatic vessel (during inflammation, infection or in steady state) in a passive way through gaps between lymphatic endothelial cells or squeezing themselves between closed junctions. To migrate through peripheral lymphatic vessels, DCs need to express their main LN homing chemokine receptor, CC-chemokine receptor 7 (CCR7), induced together with the maturation of human DCs, while the expression of other chemokine receptors is downregulated. DCs respond to a chemotactic gradient of CCR7 ligands, CCL19 and/or CCL21. Even inside the LN, DCs continue to follow a CCL21 gradient until the T cell zone. Other factors were associated with DCs migration to LN: intracellular adhesion molecule 1 (ICAM1); junctional adhesion molecule 1 (JAM1); integrin lymphocyte function-associated antigen 1 (LFA1); lipid mediators like cysteinyl leukotrienes and prostaglandin E₂; pro-inflammatory cytokines such as IL-1; ADP-ribosyl cyclase; matrix metalloproteinase (MMP) 9 and 2 (PLATT; RANDOLPH, 2013; RANDOLPH; ANGELI; SWARTZ, 2005; WORBS; HAMMERSCHMIDT; FÖRSTER, 2017).

As already mentioned, neutrophils are well known for performing their functions following recruitment into inflamed tissue before dying *in situ*. As neutrophils in inflamed tissues exhibited extended lifespan of up to 5 days, a possible involvement in other activities, such as shaping of innate and adaptive immune responses has been proposed (MANTOVANI et al., 2011). Moreover, observations suggest that neutrophils can re-enter the vasculature from inflamed tissue via reverse transmigration (BUCKLEY et al., 2006).

It was very elegantly showed by Kastenmüller *et al.* (KASTENMÜLLER et al., 2012) that a network of diverse lymphoid cells are spatially prepositioned close to lymphatic sinus-lining sentinel macrophages where they can rapidly and efficiently receive inflammasome-generated IL-18 and additional cytokine signals from the pathogen-sensing phagocytes. This leads to rapid IFN- γ secretion by lymphocytes, fostering antimicrobial resistance in the macrophage population. Moreover, subcapsular sinus macrophages orchestrate a complex interplay involving the recruitment of neutrophils that provides a rapid and robust response to lymph-borne pathogens, especially extracellular bacteria. Neutrophils were recruited to the

subcapsular, medullary, and interfollicular areas of the dLN 4 hours after infection with *Pseudomonas aeruginosa*, representing 2-3% of the total hematopoietic cell population. Neutrophil recruitment was dependent on inflammasome-mediated activation of macrophages and caspase-1-dependent cytokine production, in this case more likely on production of IL-1, rather than IL-18 (KASTENMÜLLER et al., 2012).

Other reports indicate similar migration of neutrophils to LNs. As a consequence of *Staphylococcus aureus* presence in LNs, a neutrophil influx from bone marrow arriving via HEVs and the B cells-neutrophil interactions within the LN parenchyma limited the subsequent humoral immune response (KAMENYEVA et al., 2015). Neutrophils also accumulated in the subcapsular sinus of the draining lymph node after infection with *Toxoplasma gondii* and formed persistent swarms that removed macrophages in the subcapsular sinus (CHTANOVA et al., 2008). After influenza virus vaccination with UV-inactivated virus, neutrophils containing influenza are rapidly recruited to LNs via HEVs dependent on CXCL1 and IL-1 α . In the initial stage, the majority of neutrophils aggroup in the subcapsular sinus of the LN and are associated with macrophages (PIZZAGALLI et al., 2019). MVA intradermal administration induced an influx of neutrophils to dLN and MVA was found associated with these cells in the subcapsular sinus (ABADIE et al., 2009).

The possibility that neutrophils may also emigrate from inflamed tissue via lymphatics has also been supported after *Staphylococcus aureus* infection (HAMPTON et al., 2015). The migration was dependent on CD11b and CXCR4 but not CCR7 (HAMPTON et al., 2015), as previously suggested (BEAUVILLAIN et al., 2011). Interestingly, these skin egressing neutrophils were able to augment lymphocytes proliferation in LN (HAMPTON et al., 2015). Neutrophils can migrate to LNs through lymphatics also in response to ovalbumin emulsified in complete Freund's adjuvant (BEAUVILLAIN et al., 2011; GORLINO et al., 2014), IL-17 and GM-CSF (BEAUVILLAIN et al., 2011), *Mycobacterium bovis* BCG (neutrophils carriage of live bacteria) (ABADIE et al., 2005), and *Salmonella abortusovis* (BONNEAU et al., 2006).

Although molecular mechanisms involved in leukocytes trafficking across HEVs are well described, the molecules that control movement of immune cells into LNs through lymphatic vessels are not fully defined. In the migratory pattern to LNs, neutrophils used CD11b/Mac-1, LFA-1, CXCR4, E-selectin, ICAM-1, VCAM-1, and CXCL8 molecules (GORLINO et al., 2014; RIGBY et al., 2015).

In comparison to DCs, the significance and extent of neutrophil lymphatic migration are incompletely understood. Since neutrophils reach LN early from inflamed tissues and often carry microbes, neutrophil lymphatic migration can exert considerable influence on the subsequent adaptive immune response. Neutrophils appear to exert an immunoregulatory role in both peripheral sites and lymph nodes (MANTOVANI et al., 2011). The functional relevance of neutrophils that have migrated to LN was assessed in mice and showed that the cells suppressed the B cell and CD4⁺ T cell responses, interfered with the ability of DCs and macrophages to present antigen shortly after their migration into the LNs by competition for the available antigen (YANG et al., 2010).

Some of the methodologies to evaluate leukocytes entry in afferent lymphatic vessels and migration to draining lymph node are *in vitro* and *ex vivo* models of adhesion and transmigration, including explanted skin, and *in vivo* analysis like transfer of immune cells into the skin, image-based/intravital imaging approaches, lymphatic cannulation and the classic application of fluorescent sensitizers to the skin to label cells and induce inflammation. Most of what is known about the mechanisms of DC migration to LNs is derived from studies of the mobilization of murine DCs from the skin, derived from the fluorescein isothiocyanate (FITC) painting assay, and most focus on Langerhans cells. Consequently, there is a large gap in the knowledge of how leukocytes directly interact with, enter and travel through lymphatic vessels to finally become positioned in the LN (HAMPTON; CHTANOVA, 2019; RANDOLPH; ANGELI; SWARTZ, 2005).

2. AIM

Explore human neutrophils action and the leukocyte migration (specially dendritic cells (DCs) and neutrophils) to the draining lymph node (dLN) in response to *Zika virus* (ZIKV) infection.

Aims chapter 1:

- 1.** To determine the *in vitro* viability of neutrophils challenge with ZIKV strains at different time points;
- 2.** To determine the *in vitro* neutrophil susceptibility to ZIKV, and the virus replication and release of infectious viral particles after ZIKV infection;
- 3.** To characterize the profile expression of relevant neutrophils surface molecules after *in vitro* interaction with ZIKV;
- 4.** To characterize the profile of released pro-inflammatory cytokines by neutrophils after *in vitro* interaction with ZIKV;
- 5.** To determine the levels of elastase secretion by neutrophils after *in vitro* interaction with ZIKV;
- 6.** To determine the neutrophil intracellular formation of reactive oxygen species after *in vitro* interaction with ZIKV;
- 7.** To determine the *in vitro* formation and blockage of neutrophil extracellular traps (NETs) by ZIKV, and the potential of pre-induced NETs to capture viral particles;
- 8.** To characterize the profile of released chemokines by human PBMCs and mdDCs after *in vitro* challenge with ZIKV;
- 9.** To determine the *in vitro* migration of neutrophils in response to different concentrations of recombinant human IL-8 and A549 cells culture after ZIKV infection;
- 10.** To determine the susceptibility to ZIKV infection and viability of A549 cells cultivated during different times in the presence of neutrophils (pre-activated or not), and the activation profile of neutrophils after that interaction;
- 11.** To determine ZIKV titers in the peripheral organs after different times of subcutaneous infection;
- 12.** To characterize neutrophil antibody-mediated depletion in wild type C57BL/6 mice;
- 13.** To compare ZIKV titers in the draining lymph nodes after subcutaneous infection in an inflamed site between wild type C57BL/6 mice and neutrophil-depleted mice.

Aims chapter 2:

- 1.** To produce and purify *vaccinia virus* (VACV) Western reserve strain, VACV deletion mutants ($\Delta A49$, $\Delta B13$ and $\Delta B15$), and *modified vaccinia virus Ankara* (MVA) stocks;
- 2.** To quantify the *in vivo* skin DCs migration to the popliteal lymph node (pLN) in response after subcutaneous infection to different VACV doses and in different days in comparison with *Mycobacterium bovis* bacillus Calmette-Guérin (BCG);
- 3.** To determine other skin migratory cell populations in response to VACV infection after infection;
- 4.** To characterize cellular populations in the pLN after VACV and BCG infection;
- 5.** To quantify skin DCs migration to pLN after infection with non-replicative VACV (inactivated VACV and MVA) in comparison with BCG;
- 6.** To compare the migratory skin DCs subsets in the pLN between non-replicative VACV and BCG;
- 7.** To determine skin DCs migration to pLN, BCG loads in the pLN, and proliferation of CD4⁺ T cells from P25 TCRTg RAG-1^{-/-} EGFP mice after BCG infection upon pre-treatment with VACV or i-VACV;
- 8.** To quantify skin DCs migration to pLN after infection with zymosan and *Herpes simplex virus-1*, also in a upon pre-treatment with VACV;
- 9.** To determine the skin inflammatory cytokines and CCR7 in the skin after 24 hours of VACV, i-VACV and MVA in comparison to BCG infection;
- 10.** To quantify skin DCs migration after infection with VACV deletion mutants to IL-1 signaling components;
- 11.** To determine VACV and BCG loads in the pLN over time after infection;
- 12.** To produce, confirm, expand and purify a recombinant VACV expressing the Ag85B from BCG (rVACV-Ag85B);
- 13.** To determine the proliferation of CD4⁺ T cells from P25 TCRTg RAG-1^{-/-} EGFP mice after rVACV-Ag85B infection;
- 14.** To characterize cellular populations in the pLN after flavivirus subcutaneous infection;
- 15.** To standardize the *in vivo* fluorochrome-based migration assay at Instituto Carlos Chagas;
- 16.** To determine skin DCs migration to pLN after subcutaneous flavivirus infection in comparison with BCG;

3. DEVELOPMENT

3.1.CHAPTER 1. Zika virus escapes from human neutrophils (manuscript)

The data from this section is present in form of a manuscript which will be submitted to the journal *Frontiers in Immunology*.

Title: Zika Virus Escapes from Human Neutrophils

Authors: Juliana Bernardi Aggio, Barbara Nery Porto, Claudia Nunes Duarte dos Santos, Ana Luiza Pamplona Mosimann and Priscilla Fanini Wowk

Resumo: A emergência de *Zika vírus* (ZIKV) destacou a necessidade de um conhecimento aprofundado para o desenvolvimento de terapias virais. Seis anos após o último surto que deixou inesperadas sequelas neurológicas e congênitas em humanos, ainda há uma grande lacuna de conhecimento de imunologia de ZIKV. Este trabalho abordou a resposta de neutrófilos, uma importante célula efetora da imunidade inata, para cepas asiáticas e africanas de ZIKV. Neutrófilos são células abundantes e versáteis que entram em contato com vírus na corrente sanguínea ou em tecidos afetados. Entretanto, a função desempenhada por neutrófilos em infecções virais é ainda controversa. Nossos resultados mostram que neutrófilos humanos não foram alvos da replicação de ZIKV, e que o vírus não ativou respostas antivirais em neutrófilos. Rastreamos mecanismos de ação de neutrófilos contra ZIKV nas primeiras 12 horas depois da estimulação *in vitro*, descobrimos que neutrófilos não parecem ser componentes essenciais dessa resposta de defesa do hospedeiro. As células não foram ativadas ou agiram contra o vírus conforme avaliado através da ausência de fosfatidilserina e modulação de receptores de superfície, secreção de citocinas inflamatórias e conteúdo granular, produção de espécies reativas de oxigênio e formação de armadilhas extracelulares neutrofilicas. No geral, a presença de neutrófilos não afetou a infectividade de ZIKV. Além disso, a infecção de ZIKV em células imunes inatas primárias não foi suficiente para promover um ambiente favorável para a migração de neutrófilos. A depleção de neutrófilos de camundongos imunocompetentes também não afetou a disseminação de ZIKV para o linfonodo drenante. Resumindo, esses dados sugerem que ZIKV escapa do reconhecimento de neutrófilos humanos e não exercem uma função antiviral benéfica ou contribuem para um ambiente inflamatório, somando à discussão do papel de neutrófilos durante infecções virais.

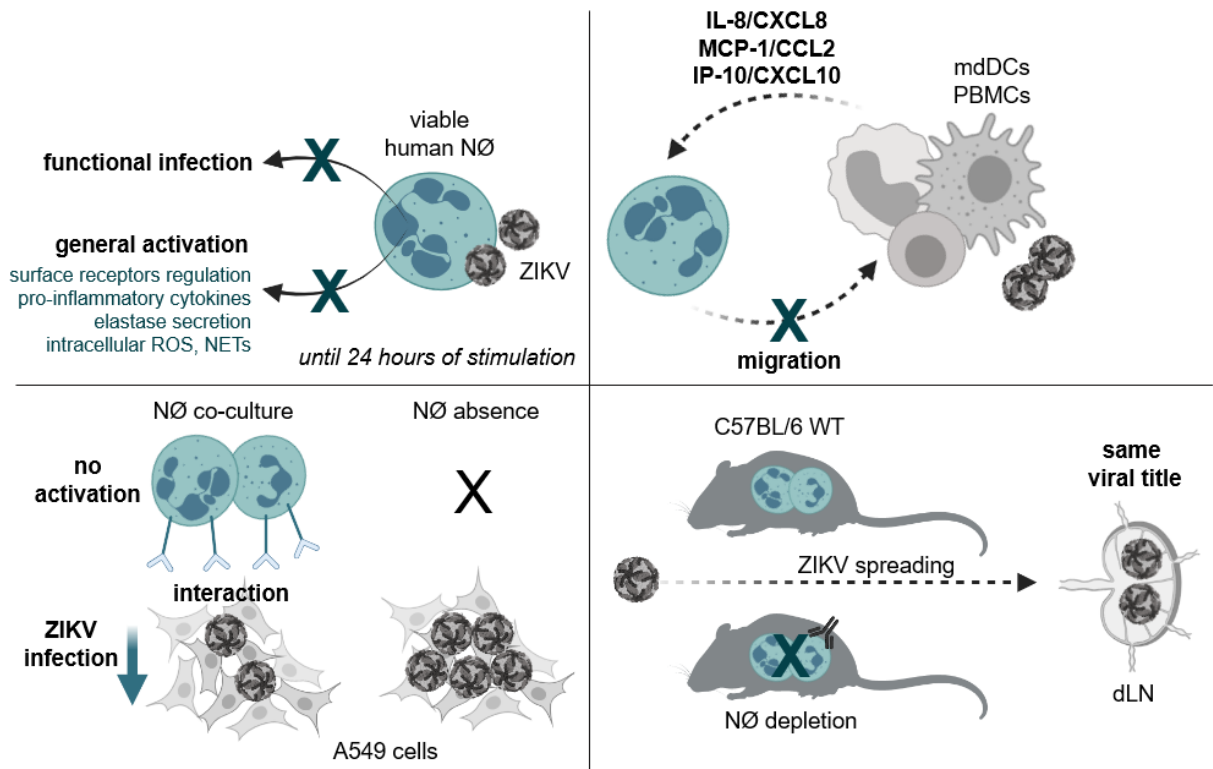


Figure 3. Graphical abstract of the manuscript *Zika virus escapes from human neutrophils*.

Zika Virus Evades Human Neutrophil Response

1 **Juliana Bernardi Aggio¹, Bárbara Nery Porto², Claudia Nunes Duarte dos Santos¹, Ana Luiza**
2 **Pamplona Mosimann^{1†}, Priscilla Fanini Wowk^{1†*}**

3 ¹ Laboratório de Virologia Molecular, Instituto Carlos Chagas, Fundação Oswaldo Cruz (FIOCRUZ),
4 Curitiba, Brazil

5 ² Program in Translational Medicine, Hospital for Sick Children, Toronto, Canada

6 [†] These authors have contributed equally to this work and share last authorship.

7 * Correspondence:

8 Priscilla Fanini Wowk, Ana Luiza Pamplona Mosimann

9 priscilla.wowk@fiocruz.br, anamosimann@fiocruz.br

10 **Keywords: neutrophils, Zika virus, innate immunity, NETs, migration.**

11 Abstract

12 *Zika virus* (ZIKV) emergence highlighted the need for a deeper understanding on virus-host
13 interaction to pave the development of antiviral therapies. The present work addressed the response
14 of neutrophils to ZIKV, an important effector cell in innate immunity that showed relevant
15 participation in other neurotropic arbovirus. Our results indicate that human neutrophils are not
16 permissive to Asian and African ZIKV strains replication and the interaction with the virus does not
17 activate antiviral response in neutrophils. Indeed, after *in vitro* challenge with ZIKV, neutrophils
18 were not primed or acted against the virus as evaluated by the absence of phosphatidylserine and
19 surface receptors modulation, secretion of inflammatory cytokines and granule content, production of
20 reactive oxygen species and neutrophil extracellular traps formation. Moreover, ZIKV infection of
21 primary innate immune cells was not sufficient to trigger a favorable environment for neutrophil
22 migration. However, neutrophil presence in a co-culture infection resulted in lower frequencies of
23 infection on the co-cultured cells, but neutrophil depletion from immunocompetent mice did not
24 affect ZIKV spreading to the draining lymph nodes. The data suggest that ZIKV escapes from
25 directly human neutrophils response and neutrophil do not play a beneficial antiviral role *per se*, but
26 these cells can participate on an infected environment.

27

28 Number of words: 6,926

29 Number of figures: 8 and 4 supplementary

30 1 Introduction

31 *Zika virus* (ZIKV) is an enveloped vector-borne RNA virus, member of the genus *Flavivirus* which
32 includes important human pathogens. The epidemic potential of flaviviruses is related to the
33 particulars and global distribution of their arthropod vectors (mainly *Aedes* spp.), as well as human
34 population density, mobility and anthropogenic interventions (1). Furthermore, genetic changes in the
35 viral genome and the host immune-status may also contribute to viral spread and pathogenesis (2).
36 After decades of sparse reports of infection in Africa and Asia, since 2007 the ZIKV Asian genotype
37 has been implicated in larger outbreaks in human populations, starting at Southeast Asia, spreading
38 throughout the Americas and reaching Europe (3). In Brazil, ZIKV was first detected in 2015 and

39 recognized as a Public Health Emergency in 2016 around 220,000 cases confirmed and the
40 infection was associated with Congenital Syndrome Associated to ZIKV infection during
41 pregnancy and to the Guillain-Barré Syndrome in adults (4–6).

42 Typically ZIKV infection results in mild clinical symptoms and the infection is rapidly counter-acted
43 by different arms of the immune response such as interferon (IFN) type I, neutralizing antibodies,
44 and specific T cells (7–9). Furthermore, ZIKV infection has been reported to trigger a rapid
45 recruitment and activation of monocytes, NK cells, plasmacytoid dendritic cells and lymphocytes,
46 and the upregulation of multiple signaling pathways, like pro-inflammatory cytokines and
47 chemokines in the blood of macaques and humans (10–15). Among innate immune cells, monocytes,
48 dendritic cells and macrophages have been described as targets of ZIKV infection and replication
49 (16–19).

50 It had been suggested that the ensuing innate immune response is linked to particular and not well
51 determined aspects of ZIKV infection that define the fate of the disease. Cellular infiltration and
52 inflammation at ZIKV infection sites contributed to placental dysfunctions (20) and encephalitis (21–
53 23). The overactivation of key molecules in the innate immune pathways upon ZIKV infection is
54 detrimental to human neuronal differentiation (24). Moreover, ZIKV affects adhesive properties of
55 monocytes, enhancing their transmigration through endothelial barriers and viral dissemination to
56 neural cells (25). Neutrophils, Ly6C^{mid-hi} monocyte, and CD45⁺ monocytes in AG129 mice (type I
57 and II IFN receptor deficient), and bone marrow-derived S100A4⁺ macrophages in AG6 mice (type
58 I, II and III IFN receptor deficient) were showed to be essential for ZIKV dissemination and
59 pathogenesis in peripheral organs and testis (26–28). CD45⁺CD11b⁺ monocytes and macrophages
60 play an important role in containing ZIKV spread in the placenta (29), while infected human
61 placental macrophages (Hofbauer cells) might gain access to the fetus (30). In this context, the role
62 played by neutrophils during ZIKV infection remains underdetermined. Elucidating mechanisms by
63 which neutrophils mediate antiviral activity might enable the development of therapies that retain
64 antiviral functions but limit inflammation-associated damage.

65 Mature neutrophils are the most abundant granulocytes in the bloodstream and the major effectors
66 during inflammation and infection. Once in the infection site, neutrophils can fastly eliminate intra-
67 and extracellular pathogens by phagocytosis, oxidative burst, multiple granule proteolytic enzyme,
68 antimicrobial peptides and neutrophil extracellular traps (NETs) release (31,32). Neutrophils have
69 been also recognized as multitasking cells capable of cross talk with adaptive responses, for example,
70 presenting antigens during viral infections (33,34). The relevance of neutrophils during flavivirus
71 infection was demonstrated for *West Nile virus* (WNV) infections, where neutrophils are recruited to
72 the site of infection, used as reservoirs for viral replication and act as Trojan horses carrying the virus
73 into the central nervous system (CNS) enhancing WNV neuroinvasive disease (35). Neutrophil
74 depletion prior to WNV infection resulted in reduced viremia and enhanced survival of the host (36).

75 Here, we address the role of neutrophils on ZIKV pathogenesis by the *in vitro* screening of classical
76 human neutrophil defense mechanisms after stimulation with different ZIKV strains and a recent
77 clinocal isolate. We report that neutrophils are not targets for ZIKV replication. In accordance, we
78 did not evidence changes in cell viability nor in the expression of human neutrophil activation
79 markers after interaction with ZIKV, suggesting viral escape from neutrophil recognition. ZIKV
80 infection of monocyte derived dendritic cells (DCs) and peripheral blood mononuclear cells
81 (PBMCs) also did not trigger a favorable environment for neutrophil migration. Neutrophil presence
82 in a co-culture infection assay seems to reduce ZIKV infection in susceptible cells, but did not
83 contribute to reducing ZIKV spread to peripheral organs *in vivo*.

84 2 Materials and Methods

85 2.1 Cells

86 Peripheral blood was obtained by intravenous puncture from healthy volunteers (both genders, aged
87 between 21-42 years old and without clinical evidence of disease) upon written consent. The
88 procedures were in accordance with Fundação Oswaldo Cruz (FIOCRUZ) research ethics committee
89 under the number CAAE 60643816.6.0000.5248. Human neutrophils were isolated from peripheral
90 blood by negative selection with magnetic microspheres MACSxpress Neutrophil Isolation Kit and
91 MACSxpress Separator (Miltenyi Biotec), according to the manufacturer instructions. Cell viability
92 was determined by Trypan blue exclusion counting and the neutrophil status was confirmed by flow
93 cytometry and cytospin slides (Cytospin 4; Thermo Fisher Scientific) visualized by deconvolution
94 microscopy (LEICA AF6000 Modular System).

95 Peripheral blood mononuclear cells (PBMCs) were isolated using Histopaque density 1.077 g/mL
96 (Lonza). CD14⁺ cells were sorted with the MACS system (Miltenyi Biotec), according to the
97 manufacturer instructions and seeded at 5x10⁵ cells/mL in RPMI-1640 media with L-glutamine
98 (Lonza) supplemented with 10% fetal bovine serum (FBS; Gibco), 25 µg/mL gentamicin (Gibco),
99 100 IU/µg/mL penicillin-streptomycin (Sigma-Aldrich), 12.5 ng/mL recombinant human GM-CSF
100 (PeproTech), and 25 ng/mL recombinant human IL-4 (PeproTech). The cells were incubated during 7
101 days at 37°C, 5% CO₂ and humid atmosphere. On the third day of incubation, fresh supplemented
102 medium was added to the cell culture. Human monocyte-derived dendritic cells (mdDCs)
103 differentiation was confirmed by flow cytometry (CD11c^{+high} CD14^{+low}).

104 Human A549 lung epithelial cells (ATCC CCL-185) were maintained in RPMI-1640 media
105 supplemented with 10% FBS, 25 µg/mL gentamicin, and 100 IU/µg/mL penicillin-streptomycin at
106 37°C, 5% CO₂ and humid atmosphere. *Aedes albopictus* mosquito C6/36 cells (ATCC: CLR-1660)
107 were grown in Leibovitz's media (L-15; Gibco) supplemented with 5% FBS, 25 µg/mL gentamicin,
108 and 0.26% tryptose (Sigma-Aldrich) at 28°C.

109 2.2 Zika virus

110 Viral stocks of the *Zika virus* (ZIKV) Asian strains, the clinical isolate BR 2015/15261 (37) and the
111 laboratory-adapted PE243 (38), and the ZIKV ancestral African isolate MR766 (39) were prepared in
112 C6/36 cells. Seven days post-infection the cell culture supernatant was collected, clarified by
113 centrifugation and later titrated by foci-forming immunodetection assay in C6/36 cells (40). In
114 parallel, C6/36 cells were maintained in the same conditions without viral addition. This conditioned
115 supernatant, hereby called mock, was used as a negative control of activation and infection.

116 2.3 Cell interaction with ZIKV

117 Neutrophils at 2.5x10⁵ cells/200 µL of RPMI-1640 media supplemented with 25 µg/mL gentamicin
118 and 100 IU/µg/mL penicillin-streptomycin were incubated during 2 hours with ZIKV strains (BR
119 2015/15261, PE243 and MR766) using a multiplicity of infection (MOI) of 1 at 37°C, 5% CO₂ and
120 humid atmosphere under agitation. Neutrophils were also stimulated in the same conditions with
121 mock, 200 IU/mL IFN-α2A (Blau Farmacêutica), 100 ng/mL of *Escherichia coli* lipopolysaccharide
122 (LPS-EK, InvivoGen) and 16 nM of phorbol 12-myristate 13-acetate (PMA; Sigma-Aldrich) as
123 controls of activation. After the 2h incubation period, neutrophils were washed twice (250 x g; 7
124 minutes) in non-supplemented media and plated in 96 well plates in RPMI-1640 media supplemented
125 with 10% FBS, gentamicin and penicillin-streptomycin. Medium collected at this point was called

126 input and used as a control to account for any remaining viruses in the neutrophil culture after
 127 washing out the initial inoculum. Two (input), 6, 12 and 24 hours after the beginning of challenge,
 128 neutrophils and the culture supernatant were harvested and assessed. To exclude non-internalized
 129 virus binding in their surface, neutrophils were treated after the wash steps with 0.05% trypsin-EDTA
 130 (Gibco) during 10 minutes at room temperature (41), washed and suspended in the new media.
 131 Where indicated, neutrophils did not have the stimuli removed after 2 hours and were immediately
 132 plated in the same conditions for 6 hours.

133 PBMCs at 1×10^6 cells/500 μ L of RPMI-1640 media supplemented with 25 μ g/mL of gentamicin and
 134 100 IU/ μ g/mL of penicillin-streptomycin were stimulated with mock, ZIKV strains at an MOI of 1,
 135 and LPS at 37°C, 5% CO₂ and humid atmosphere under agitation for 2 hours. The cells were then
 136 washed twice (300 x g; 10 minutes) with non-supplemented media and plated in 24 well plates in the
 137 same conditions and concentration during 24 and 48 hours when the supernatant was recovered for
 138 chemokines quantification. With the same purpose, mdDCs were plated at 1×10^6 cells/500 μ L of
 139 RPMI-1640 supplemented with gentamicin and penicillin-streptomycin and rested during 24 hours at
 140 37°C, 5% CO₂ and humid atmosphere before undergoing the same stimulation.

141 A549 cells were seeded 16 hours before infection in 24 well plates at 1×10^5 cells in RPMI-1640
 142 media supplemented with 10% of FBS, gentamicin, and penicillin-streptomycin at 37°C, 5% CO₂ and
 143 humid atmosphere. A549 cells were incubated during 2 hours with ZIKV strains at an MOI of 1 (or
 144 different stimulations when indicated) in 400 μ L of RPMI-1640 media supplemented with
 145 gentamicin and penicillin-streptomycin. After the incubation period, cells were washed twice with
 146 non-supplemented media and kept in RPMI-1640 media supplemented with 10% FBS, gentamicin,
 147 and penicillin-streptomycin at 37°C, 5% CO₂ and humid atmosphere during the indicated times.
 148 C6/36 were infected following the same protocol described above for A549 cells but using L-15
 149 media supplemented with 5% FBS, 25 μ g/mL gentamicin, and 0.26% tryptose at 28°C.

150 **2.4 RT-qPCR**

151 Neutrophil RNA was extracted using the RNeasy Mini Kit (Qiagen) according to the manufacturer's
 152 instructions. RT-qPCR to detect ZIKV was performed in a 20 μ L one-step RT-qPCR master mix
 153 (Promega) containing 25 ng of sample RNA, 500 nM of the ZIKV1086 and ZIKV1162c
 154 oligonucleotides and 200 nM of ZIKV1107-FAM probe according to a previously described protocol
 155 (42). RNase P (*RPPH1*) was used as a reference gene (43). The expression of human gene *IRF3* was
 156 determined using the forward primer 5' CGCTCTGCCCTCAACCGCAA 3'; and the reverse primer
 157 5' CCACCCAGGCAGCTCAGCAC 3'. *RPPH1* primer was used to normalize gene expression. One-
 158 step SYBR Green RT-qPCR master mix (Sigma) was used with 25 ng of sample RNA and 10 pmoles
 159 of each primer pair following manufacturer recommendations. The following cycling conditions were
 160 used: reverse transcription at 42°C for 30 min, denaturation and RT inactivation at 94°C for 30 sec,
 161 followed by 40 cycles of denaturation at 94°C for 10 sec, annealing at 55°C for 10 sec, extension at
 162 72°C for 30 sec, and plate read (acquisition of fluorescent data). A melting curve analysis was
 163 performed after the amplification steps were completed by continuously recording the fluorescence
 164 while increasing the temperature. The fluorescence threshold limit of the SYBR Green was set
 165 automatically by the Light Cycler software (Roche). The relative expression of those molecules was
 166 determined by the $2^{(-\Delta\Delta C_t)}$ method, in which samples were normalized to RNase P and expressed as
 167 fold change over mock cells.

168 **2.5 Flow cytometry**

169 Neutrophils and A549 cells viability was determined at the indicated time points using Annexin V
170 (ImmunoTools) and 7-Amino-Actinomycin (7-AAD; BD Bioscience) according to instructions of the
171 PE Annexin V Apoptosis Detection Kit (BD Bioscience). The frequency of ZIKV antigen positive
172 neutrophils, A549 cells and C6/36 cells was measured through staining with a Flavivirus E protein
173 monoclonal antibody 4G2 (ATCC HB-112) (40). Briefly, at the designated time points, the cells were
174 detached (A549 cells with trypsin and C6/36 with cell scrapper) from the cell culture flask, blocked
175 (5% FBS and 1% human AB serum in PBS) during 20 minutes at room temperature, fixed and
176 permeabilized using the Cytotfix/Cytoperm Fixation/Permeabilization Kit (BD Biosciences), and
177 stained with 4G2-FITC conjugated antibody during 45 minutes at 37°C. Alternatively, these cells
178 were labeled with 4G2, goat anti-mouse Alexa Fluor 488 secondary antibody (Thermo Fisher
179 Scientific) and Vybrant DyeCycleViolet Stain (Thermo Fisher Scientific), and fixed in slides pre-
180 treated with poly-L-lysine (Sigma-Aldrich) to be visualized by confocal microscopy (LEICA SP5
181 AOBs). For surface markers staining, neutrophils were blocked and incubated with fluorochrome-
182 conjugated mouse anti-human monoclonal antibodies specific for CD11b (clone ICRF44), CD16
183 (3G8), CD32 (FLI8.26), CD62L (DREG-56), CD182 (6C6) (BD Biosciences) and Hu Axl
184 (D57HAXL) (eBioscience), for 20 minutes at room temperature. Cytokines and chemokines in
185 neutrophils, PBMCs and mdDCs culture supernatants were quantified through the Cytometric Bead
186 Array (CBA) method using the Human Inflammatory Cytokines Kit and Human Chemokine Kit (BD
187 Biosciences) as per manufacturer instructions. To measure intracellular oxygen species, the infection
188 was labeling during 45 minutes at room temperature with 0.5 μ M of 5-(and-6)-chloromethyl-2',7'-
189 dichlorodihydrofluorescein diacetate, acetyl ester (CM-H₂DCFDA) probe (Invitrogen). Flow
190 cytometry was performed on a FACS Canto II with BD FACSDiva software (BD Biosciences) and
191 the acquired data analyzed on FlowJoV10 (BD Biosciences).

192 **2.6 Neutrophil elastase measurement**

193 Elastase in neutrophil culture supernatant at 6 hours post stimulation was detected using the Human
194 PMN-Elastase ELISA Kit (Invitrogen). Cell culture supernatant (100 μ L) was added to a microwell
195 plate coated with anti-human polymorphonuclear elastase polyclonal antibody and incubated at room
196 temperature during 1 hour with a Horseradish peroxidase-conjugated anti- α 1-proteinase inhibitor
197 antibody. The immunocomplex was detected by adding tetramethyl-benzidine substrate solution and
198 the absorbance determined at 450 nm on a microplate reader (BioTek Synergy H1 Hybrid).

199 **2.7 Neutrophil Extracellular Traps Assessment**

200 Neutrophils at 2×10^5 cells/200 μ L of RPMI-1640 media supplemented with 25 μ g/mL gentamicin
201 and 100 IU/ μ g/mL penicillin-streptomycin were incubated during 5 hours with either mock, ZIKV
202 strains (BR 2015/15261, PE243 and MR766) at an MOI of 1, or 160 nM of PMA in 96 well plates at
203 37°C, 5% CO₂ and humid atmosphere. In another setting, neutrophils were first incubated during 1
204 hour with mock or ZIKV strains under agitation, washed twice (250 x g, 7 minutes) and incubated 5
205 hours with PMA. Following the stimulation period, neutrophils were treated with 0.04 U/ μ L of Turbo
206 DNase (Thermo Fisher Scientific) during 10 minutes at 37°C. The enzymatic digestion was stopped
207 with 5 mM EDTA, the culture was centrifuged (300 x g for 1 minute) and the supernatant collected
208 and 5-fold diluted. Free double-stranded DNA (dsDNA) was quantified using Quant-IT PicoGreen
209 dsDNA kit (Invitrogen) in a Qubit 2.0 fluorometer (Invitrogen) according to the manufacturer's
210 recommendations.

211 For neutrophil extracellular traps (NETs) detection, neutrophils were stimulated during 5 hours as
212 described above on Lab-Tek chamber slides (Thermo Fisher Scientific) pre-treated with poly-L-
213 lysine. Afterwards, the supernatant was carefully removed and the cells were treated with 3%

214 paraformaldehyde (Sigma-Aldrich) and stained with an acetyl-histone H3 polyclonal antibody
 215 (Sigma) followed by a mouse anti-rabbit Alexa Fluor 488 secondary antibody (Sigma) and Vybrant
 216 DyeCycleViolet Stain (Thermo Fisher Scientific) during 45 minutes at 37°C. The slides were sealed
 217 with n-propyl gallate (Sigma-Aldrich) and NETs quantified by confocal microscopy (LEICA SP5
 218 AOBS). To evaluate the effect of NET on viral clearance, neutrophils were stimulated during 5 hours
 219 with media or PMA using the same conditions described above. Cells were then incubated for 1 hour
 220 with ZIKV (1 MOI) after which the cell culture was centrifuged (300 x g for 1 minute) and the
 221 supernatant with virus not attached to the traps collected and quantified by foci-forming
 222 immunodetection assay in C6/36 cells.

223 **2.8 Migration assay**

224 Neutrophils at 3×10^5 cells/200 μ L of RPMI-1640 media supplemented with 25 μ g/mL gentamicin
 225 and 100 IU/ μ g/mL penicillin-streptomycin were seeded on a 3 μ m pore Thin Cert insert (Greiner
 226 Bio-One) coupled to a 24 well plate. To the well underneath the insert were added 600 μ L of RPMI-
 227 1640 media containing 1,000 or 50,000 pg of recombinant human (rh-) IL-8 (PeproTech) or A549
 228 cells culture previously infected during 48 hours with mock or ZIKV (1 MOI). For this specific
 229 experiment, infected A549 cells were maintained in the absence of FBS. RPMI-1640 media and
 230 A549 cells stimulated with mock were used as a negative control of cell migration. After 2 hours at
 231 37°C, 5% CO₂ and humid atmosphere, migrated neutrophils were collected from the bottom part of
 232 the transwell system and the cellular concentration determined by Turk dye exclusion counting. The
 233 chemotactic index was calculated as the ratio of the number of migrated neutrophils in each condition
 234 and the number of neutrophils that migrated in the negative control (44).

235 **2.9 Co-culture assay**

236 A549 cells at 1×10^5 cells per well of 24 well plates in RPMI-1640 media supplemented with 25
 237 μ g/mL gentamicin and 100 IU/ μ g/mL penicillin-streptomycin were stimulated during 2 hours with
 238 mock and ZIKV (1 MOI) in the absence or presence of neutrophils in a ratio of 1:5. To evaluate if
 239 neutrophils were physically interacting with A549 cells through a surface protein, neutrophils were
 240 treated with trypsin during 10 minutes at room temperature, washed and suspended in fresh media
 241 before addition to A549 cells in the same ratio. After the incubation period A549 cells culture was
 242 washed twice and kept in 500 μ L of RPMI-1640 media supplemented with 10% FBS, gentamicin and
 243 penicillin-streptomycin for 14 hours. At this point, A549 cells were assessed for viability and
 244 intracellular ZIKV antigen by flow cytometry as described above. In a second co-culture experiment
 245 setting, A549 cells were incubated during 2 hours with mock or ZIKV (1 MOI), washed twice and
 246 kept in the described conditions during 24 hours. Next, neutrophils in a ratio of 1:5, LPS only or
 247 neutrophils plus LPS were added or not to these cultures. A549 cells were evaluated 16 hours later
 248 for viability and frequency of ZIKV antigen positive cells. At the end of interaction, neutrophils
 249 present in the culture were checked for surface markers by flow cytometry as described above.

250 **2.10 *In vivo* ZIKV infection model**

251 C57BL/6 mice were obtained from Instituto Carlos Chagas/FIOCRUZ-PR animal facility, and
 252 maintained and handled according to the directives of the Guide for the Care and Use of Laboratory
 253 Animals of the Brazilian National Council of Animal Experimentation. The protocols were approved
 254 by the Committee on the Ethics of Animal Experimentation from Fundação Oswaldo Cruz –
 255 CEUA/FIOCRUZ (license LW 03-19). Both male and female mice between 8-12 week-old mice
 256 were used. ZIKV PE243 (1.3×10^6 FFU, 10 μ L) spread to tissues were determined in blood, spleen,
 257 kidney and lymph nodes (popliteal (pLN), lumbar aortic (laLN), and sciatic lymph nodes (sLN)) after

258 10 minutes, 1, 3, 6 and 24 hours of viral subcutaneous footpad injection. The organs were aseptically
259 removed, gently homogenized using a tissue grinder, submitted to three freeze-thaw cycles and the
260 viral load measured by foci-forming immunodetection assay in C6/36 cells. The blood samples were
261 collected through cardiac puncture and the plasma were titered in C6/36 cells. To deplete peripheral
262 neutrophils, animals were inoculated intraperitoneally with 200 μ L of PBS containing 400 μ g of anti-
263 mouse Ly6G (1A8; BioxCel) or mouse IgG2a isotype control (C1.18.4; BioxCel). Control animals
264 received 200 μ L of PBS only. After 18 hours, the frequency of neutrophils in total blood was
265 evaluated through flow cytometry by surface staining with fluorochrome-conjugated anti-mouse
266 monoclonal antibodies specific for CD11b (M1/70), Ly6C/G (RB6-8C5), CD3 (145-2C11) and CD8
267 (53-6-7) (1:100; BD Biosciences). Neutrophils depleted animals were inoculated in the hind footpad
268 with PBS containing 1,000 ng of LPS (to induce an inflammatory environment) or PBS. After 3
269 hours, the mice were inoculated with 10 μ L of ZIKV PE243 (1.3×10^6 FFU) in the same footpad. One
270 hour later, popliteal lymph nodes (pLNs) were harvested and the viral title determined as above.

271 **2.11 Statistical Analyses**

272 Analyses were performed using GraphPad Prism 6 (GraphPad Software, Inc., USA). Wilcoxon
273 matched-pairs signed rank test (nonparametric paired t-test) was used in the analysis of the *in vitro*
274 experiments with primary human cells to clarify individual patterns. One-way Anova with Tukey's
275 multiple comparison test was used in animal experiments to compare the average of groups. A cut-off
276 of $p < 0.05$ was considered significant.

277 **3 Results**

278 **3.1 ZIKV does not trigger human neutrophil cell death**

279 Cell death is a mechanism through which viruses may deplete cell populations and imbalance
280 immune response. Conversely, the induction of anti-apoptotic signals may extend the availability of
281 cellular substrates for viral replication (45). Therefore, our first aim was to assess if ZIKV
282 stimulation affects the viability of human neutrophils. No morphological changes in neutrophils were
283 observed after ZIKV challenge (Figure 1A). The neutrophils viability during the first 24 hours after
284 interaction with different ZIKV strains were investigated by annexin V and 7-AAD labeling (Figure
285 1B-C). As expected, over time, an increased expression of phosphatidylserine in the control mock-
286 stimulated neutrophils were observed (Figure 1). In the absence of inflammation, neutrophils have a
287 short life span of 8-12 hours in circulation and undergo constitutive apoptosis (46). The observed
288 decrease in viability was not attributed to the neutrophil isolation methodology (Figure 1C, dashed
289 line). In accordance with previous reports (47), LPS, a positive control of neutrophil activation,
290 inhibited apoptosis at the late time points (Figure 1C). In the first 6 hours post virus interaction,
291 neutrophils expressed phosphatidylserine in higher frequencies than the mock control (Figure 1C).
292 This is suggestive of an early stress induced by the virus presence, but with low impact in the
293 neutrophil apoptotic state. In our model, we considered neutrophils functional until 24 hours after
294 ZIKV interaction due to the low loss of cellular integrity indicated by 7-AAD uptake (Figure 1C) and
295 used this time frame to evaluate other aspects of neutrophil biology.

296 **3.2 ZIKV does not establish a productively infection in human neutrophils**

297 In addition to subverting the target cell into a reservoir for virus replication and dissemination, viral
298 infection may use the infected cells as a Trojan horse to overcome physiological host defense barriers
299 (35). It can also result in the inhibition of important cell signal transduction pathways (19). To
300 address this issue, we next sought to understand whether human neutrophils are susceptible to and

301 sustain ZIKV infection. No positive cells were detected for intracellular staining of the envelope
302 protein (4G2 monoclonal antibody) through immunofluorescence or flow cytometry 24 hours after
303 incubation with all three ZIKV strains tested (Figure 2A, panels a-d, and 2B). Also, no signal was
304 detected at early time points (data not showed). The possibility of an active internalization of a few
305 viral particles by neutrophils via receptors or phagocytosis could not be excluded. Low frequency
306 events may not result in a signal strong enough to allow the detection with used techniques, in
307 contrast with observed in the positive control, the highly susceptible and permissive mosquito cell
308 line C6/36 (Figure 2A, panels i-l). Corroborating with this hypothesis, ZIKV RNA could be detected
309 in the cells that had been incubated with the virus, however we did not observe an increase in ZIKV
310 RNA levels over time (Figure 2C) or the release of functional viral particles in loads greater than the
311 input (Figure 2D). Treatment of neutrophils with trypsin after the wash steps resulted in the reduction
312 but not in the abolishment of virus RNA levels (Figure 2E). This suggests that the low RNA levels
313 measured cannot be fully attributed to viral inoculum leftover that could not be completely washed
314 away, and at least partially, could be explained by the virus particles that stick at the cell membrane.
315 Moreover, the expression of *IRF3* mRNAs, an important factor whose translation is induced when
316 endosomal sensors recognize viral RNA, indicate that there is some degree of intracellular
317 recognition of ZIKV antigens over time, although not significant nor different from the positive
318 control, IFN- α (Figure 2F).

319

320 **3.3 Human neutrophils are not responsive to ZIKV**

321 The recognition of viral elements in the cell cytosol triggers the development of defense mechanism
322 involved in viral replication control and inflammation. However, a significant part of neutrophil
323 activation mechanisms is coordinated through the signaling of cell surface pattern-recognition
324 receptors (46). Thus, we evaluated the modulation of neutrophil surface receptors after ZIKV
325 challenge as a measurement of activated phenotype in neutrophils. The adhesion integrin CD11b, the
326 Fc γ RII CD32, and the chemokine receptor CD182/CXCR2 were upregulated over time following
327 LPS stimulation, while the selectin adhesion receptor CD62L was downregulated (Figure 3A-B),
328 indicating priming of neutrophils (48,49). Nevertheless, only slight differences were observed in the
329 expression of these molecules between mock- and the ZIKV strains-stimulated neutrophils. No
330 significant differences were observed in the IL-8/CXCL8 levels secreted by neutrophils after 12
331 hours of stimulation with mock or ZIKV (Figure 3C). Similar results were obtained for IL-1 β , IL-6
332 and IL-10 (data not showed). Corroborating these findings, no elastase was detected in neutrophil
333 supernatant culture after 6 hours of stimulation with ZIKV BR 2015/15261 (Figure 3D). It was also
334 noted a general lack of intracellular ROS production in neutrophils, measured by the oxidation of
335 chloromethyl-H₂DCFDA, in contrast to the oxidative stress generated by phorbol 12-myristate 13-
336 acetate (PMA) stimulation, a well-known ROS inducer (Figure 3E).

337 Next, we evaluated the generation of NETs in the context of ZIKV infection. NETs formation are
338 dependent on ROS (50) and the lack of intracellular ROS in neutrophils previously stimulated with
339 ZIKV (Figure 3E) indicated an impairment to its formation. Moreover, neutrophils nuclei and
340 membrane integrity after contact with ZIKV (Figure 1A) indicated this defense mechanism was not
341 being activated. We confirmed that NETs were not induced by any ZIKV strains tested after 5 hours
342 of stimulation through the quantification of free double-stranded DNA in neutrophil supernatants
343 (Figure 4A), and the absence of web-link extracellular structures colocalizing with DNA and histone
344 (Figure 4B). PMA, a well-known potent mitogen and a robust NET inducer over a 3-4 hour time
345 course (50), as observed here (Figure 4A-B). When neutrophils were first stimulated for 1 hour with
346 ZIKV followed by PMA for 5 hours, no difference were observed in the levels of free DNA in

347 neutrophil culture when compared with PMA treatment of mock-stimulated cells (Figure 4C),
 348 suggesting that ZIKV also does not interfere with NETs formation by other stimuli. Moreover, no
 349 less free viral particles were detected when ZIKV was incubated with PMA-induced NETs (Figure
 350 4D), which suggests that ZIKV is not trapped and neutralized by the DNA fibers in a scenario where
 351 a secondary stimulus triggered NETs.

352 To confirm that neutrophil does not impact ZIKV particles, neutrophil were incubated for either 2 or
 353 6 hours with ZIKV. These virus did not have impaired infectivity during subsequent infection of the
 354 susceptible A459 cells (Figure 5).

355 **3.4 ZIKV infection does not provide a favorable environment for human neutrophil** 356 **migration**

357 Although neutrophils are circulatory cells and therefore have the potential to encounter viruses in the
 358 bloodstream, their fate is to contribute to the inflammation process on the infected tissue. In fact, the
 359 priming of neutrophils in the circulation by an isolated stimulus is insufficient, and their complete
 360 activation to full capacity is a multistep process achieved after their transmigration through the
 361 endothelium following a chemotactic gradient (46). Secretion of IL-8/CXCL8, an important
 362 neutrophil chemoattractant, was measured after stimulating mdDCs and PBMCs with ZIKV for 24
 363 and 48 hours. LPS was used as a positive control of activation and boosted the chemokines
 364 production (Figure 6A-B). Similar levels of IL-8 were detected for the monocyte chemoattractant
 365 protein-1 (MCP-1/CCL2) and IFN-inducible protein 10 (IP-10/CXCL10) in mdDCs at the same time
 366 points (Figure 6A). A concentration of recombinant human IL-8 (rhIL-8) corresponding
 367 approximately to the ones detected in the PBMCs and mdDCs supernatant (1,000 pg) was not enough
 368 to induce neutrophil migration in a transwell assay (Figure 6C). Neutrophils migrated with a 50-fold
 369 higher rhIL-8 concentration (Figure 6C). Interestingly, A549A cells infected with ZIKV PE243 for
 370 48 hours, which could generate a rich environment to neutrophil migration due to higher replication,
 371 also did not promote neutrophil migration (Figure 6C).

372 To mimic a situation where neutrophils reached an infected environment after migration, we co-
 373 cultured neutrophils with A549 cells in two situations. First, to assess neutrophil influence during the
 374 infection, neutrophils were added to A549 cells concomitant with ZIKV infection. Both stimuli were
 375 maintained for 2 hours and then removed. The A549 cells infection frequency was evaluated after 16
 376 hours by the detection of ZIKV envelope protein (4G2) (Figure 7A). The second situation aimed to
 377 observe neutrophil role to an established ZIKV infection. A549 cells were infected for 24 hours with
 378 ZIKV strains and after this time neutrophils were added for 16 hours when A549 cells infection
 379 frequency was measured (Figure 7B). A significant reduction in A549 cell infection was observed
 380 when neutrophils were present in both conditions (Figure 7A-D). We did not detect an increase in the
 381 frequency of A549 cells annexin V⁺-AAD⁻ due to neutrophil presence pointing to no loss in A549
 382 cell viability (Supplementary Figure 1A-B). We hypothesized that a small number of particles might
 383 have been internalized by neutrophils (Figure 2) and a reduced fraction of the virus particles could be
 384 binding to the surface of neutrophils (Figure 2D-E). Nevertheless, such a small reduction in the
 385 number of free viral particles is not enough to explain the decrease in the infection rate seen in the
 386 co-cultures (Figure 5). Neutrophils co-cultured with A549 cells infected for 24 hours also did not
 387 exhibit modulation of surface receptors, indicating non-activation (Supplementary Figure 1C).
 388 Moreover, the addition of neutrophils previously activated with LPS to the infected A549 cells had
 389 no effect on the frequency of infected cells in comparison with the conditions where resting
 390 neutrophils were added to the co-culture (Supplementary Figure 1D), reinforcing that the reduction of
 391 the infection is not due to neutrophils activation. Since neutrophil treatment with trypsin before

392 addition to A549 cells restored A549 cells infection frequencies (Figure 7E), we hypothesized that
 393 neutrophils were interacting with A459 cells through surface protein membrane components,
 394 impairing ZIKV infection. The treatment with trypsin did not significantly affect the viability of
 395 neutrophils (annexin V⁻-AAD⁺) or the average expression of CD11b and CD32 receptors, but did
 396 reduce the expression of CD62L and CD182, suggesting an impact on neutrophil surface proteins by
 397 trypsin (data not showed).

398 **3.5 Neutrophil depletion does not alter ZIKV titers in the draining lymph node**

399 Next, we investigated contribution of the neutrophils to virus clearance in a local ZIKV infection. In
 400 C57BL/6 immunocompetent model, we only detected ZIKV PE243 in the lymph nodes (popliteal
 401 (pLN), lumbar aortic, and sciatic lymph nodes) until 3 hours post infection (Supplementary Figure
 402 2A). Therefore, we used the pLN after 1 hour of ZIKV infection as a viral spread site in our studies.
 403 C57BL/6 mice had the number of neutrophils significantly reduced through a monoclonal antibody
 404 targeting Ly6G (clone 1A8) (Supplementary Figure 2B-C), and were inoculated subcutaneously in
 405 the hind footpad with LPS to stimulate neutrophil migration to the injection site 3 hours previously
 406 viral subcutaneous infection. The animals treated with the anti-Ly6G antibody (Ly6G x LPS)
 407 presented similar titers of ZIKV in the pLN than animals that received no antibody treatment (PBS x
 408 LPS) (Figure 8). The slightly reduced titers in the pLN seen in mice that received LPS in comparison
 409 with the ones that received PBS in the footpad were attributed to the inflammatory context. This
 410 result suggests that, in this model, the presence of neutrophils was not essential to contain ZIKV
 411 spreading to the draining lymph node.

412 **4 Discussion**

413 Neutrophil-inflammatory responses triggered by viral infection are necessary for the initiation of
 414 effective antiviral immunity (51–54), but can also become dysregulated and result in tissue injury
 415 (55,56). Due to its dual nature, a complete understanding of neutrophil functions during viral
 416 infections may lead to the design of therapeutic strategies that exploit the beneficial functions of
 417 neutrophils while limiting their damaging effects. It could be extended to ZIKV pathology, in which
 418 neutrophils could be associated with the virus congenital and neurotropic nature, the ability to cause
 419 injury to the reproductive tract and be sexually transmitted, as well as the long-term viral persistence
 420 in some body fluids and tissues (3). In order to investigate these possibilities we interrogated the
 421 response of human neutrophils to Asian and African ZIKV strains in different experimental settings.

422 Neutrophils were suggested to be permissive to ZIKV as viral RNA was found in myeloperoxidase⁺
 423 neutrophils present in the lymph nodes of cynomolgus macaques 7 days post-infection (12), and in
 424 CD45⁺CD11b⁺ neutrophil-myeloid cells in the placenta of AIR mice (vertical transmission in a *Rag1*-
 425 deficient mouse model) (29). In contrast to those previous findings, our results showed that human
 426 neutrophils are not targets of ZIKV replication and do not represent a remarkable ZIKV reservoir.
 427 This is in agreement with previous reports showing that ZIKV preferentially targets human PBMCs,
 428 specially CD14⁺CD16⁺ monocytes (18). We reported the absence of AXL in the surface of human
 429 neutrophils (Supplementary Figure 3), a TAM family tyrosine kinase that has been described as a
 430 facilitator to ZIKV infection due to attenuation of type I IFN (57), but other known or unknown
 431 receptors could mediate viral endocytosis or phagocytosis in neutrophils.

432 Surprisingly, neutrophil stimulation with ZIKV did not promote cell activation or any of the classical
 433 pathways of neutrophil microbicide mechanisms as noted by the absence of phosphatidylserine and
 434 surface receptors modulation, secretion of inflammatory cytokines and granule content, production of
 435 reactive oxygen species and NETs. A prolonged continued stimulation of 6 hours did not change this

436 scenario (Supplementary Figure 4). These results indicate neutrophils presented a non-responsive
 437 phenotype in our experimental settings and would not be the major source of mediators during ZIKV
 438 infection. Other virus, such as *Human immunodeficiency virus-1*, induced activation on neutrophils
 439 by modulating the expression of TLR2, TLR4, and TLR7, CD62 and CD11b, promoting the secretion
 440 of IL-6 and TNF- α , and altering ROS production (58). ZIKV and Dengue virus type 2 (DENV-2)
 441 were showed previously not able to provoke NETs induction in mouse neutrophils (59) and humans
 442 (60), but DENV-2 triggered spontaneous decondensation of neutrophil nuclei in patients during acute
 443 phase of infection and the *in vitro* incubation of NETs with DENV-2 significantly decreased DENV
 444 infectivity (61).

445 A viral escape from innate immune components could result in delayed immune responses favoring
 446 virus spread. Furthermore, we cannot rule out a possible suppression of neutrophil action by ZIKV,
 447 as already showed to primary monocytes, mdDCs and plasmacytoid DCs that have their maturation
 448 and activation impaired during ZIKV replication (16,18,19,62). Moreover, a cohort of rhesus
 449 monkeys produced minimal systemic cytokine response to ZIKV infection (11). In accordance, Asian
 450 ZIKV strains triggered a non-classical monocyte expansion and M2-skewed gene expression,
 451 characteristic of anti-inflammatory responses (17). In patients infected by ZIKV, myeloid DCs and
 452 PBMCs showed suppression of antiviral IFN immune responses and innate immune sensors,
 453 suggesting that ZIKV creates an intracellular milieu conducive to supporting the infection (63,64).

454 However, several reports indicate neutrophil migration during ZIKV infection, it is likely that
 455 neutrophils exercise their actions at the site of infection rather than directly on the virus. IFN receptor
 456 deficient mouse models show enhanced neutrophils infiltration in the CNS following ZIKV infection
 457 and in other relevant structures such as spleen, spinal cord, epididymis and testis (9,21,22,27,65).
 458 Neutrophil infiltrations were also present in mucosal, placental and fetal tissues during acute ZIKV
 459 infection in humans, pigtail and rhesus macaques (13,66,67). ZIKV patients in acute or recovery
 460 disease phase, THP-1 cells and monocytes presented elevated IL-8/CXCL8 levels after ZIKV
 461 infection (14,15,18,68), and neutropenia was detected in the blood of patients in acute phase and in
 462 the first week after ZIKV infection in rhesus monkeys (15,69,70). Moreover, lethal AG129 mice
 463 model challenged with a recombinant ZIKV that did not replicate in myeloid cells, resulted in no
 464 viral infection, no cytokines involved in leukocytes recruitment, and no viral dissemination to
 465 peripheral organs (26). Despite these reports, in our settings, 48 hours of ZIKV infection of mdDCs
 466 and PBMCs did not induce sufficient levels of IL-8 to promote neutrophil migration. This might be
 467 due to limitations of our *in vitro* model. Even ZIKV infection in A549 cells that endure high levels of
 468 ZIKV replication and can generate a more complex environment did not promote neutrophil
 469 migration. Frumence *et al.* showed the secretion of soluble IL-8 in ZIKV infected A549 cells (71),
 470 however at lower levels required to promote neutrophil migration *in vitro*.

471 Emerging evidence points out to a secondary action of neutrophils in the site of infection, not directly
 472 primed by the virus, but possibly dependent on the mosquito saliva components. Mosquito-sourced
 473 factors at bite sites enhanced *Semliki Forest virus* infection specifically by promoting a counter-
 474 productive neutrophil-dependent inflammation. The mosquito bite induced at the site of infection an
 475 increase in neutrophil chemoattractants CXCL1, CXCL2, CXCL3, CXCL5, IL-1 β and IL-6, which
 476 cause an influx of inflammatory neutrophils expressing IL-1 β . These infiltrating neutrophils helped
 477 coordinate the entry of myeloid cells, via CCR2, that are permissive to viral infection (72). The
 478 neutrophil stimulation factor 1 (NeSt1), a recently identified *Aedes aegypti* salivary gland protein,
 479 could contribute to this process. It activates neutrophils in the bite site increasing IL-1 β and CXCL2,
 480 and promotes the recruitment of susceptible macrophages to the bite site, which in turn increases
 481 ZIKV replication and leads to increased viral pathogenesis in AG129 mice (73). In an attempt to

482 assess the putative impact of neutrophil migration to infected tissues *in vitro*, we used a co-culture
483 system with A549 cells. Our results show a reduction on ZIKV infection of A549 cells when
484 neutrophils are present that it seems to be due to the interaction between the two cells, but not related
485 to neutrophil activation. It has been showed that cell-to-cell contact between neutrophils and A549
486 cells leads to a pro-proliferative effect on tumor cells involving the release of elastase and COX-2
487 products (74). Also, the direct cell-cell contact between neutrophils and A549 cells was a prerequisite
488 for an increased production of IL-6 and IL-8 by A549 cells (75). Apoptotic neutrophils induced A549
489 cell death mediated by soluble Fas ligand (76), or arrested its cell cycle, which can be dependent on
490 cell contact (77). It was not the case in our model, where neutrophils presence did not affect A549
491 cell viability. It remains to be defined what molecules and pathways might be involved during those
492 cell interactions that potentially contribute to the reduction of viral infection or proliferation.

493 In order to gain a better understanding on the role played by neutrophils in ZIKV clearance at the
494 inflammation site, we depleted neutrophils from C57BL/6 mice. In this scenario, we did not observe
495 a direct action of neutrophils in preventing ZIKV spread to the lymph nodes in the first hour after
496 ZIKV inoculation in a setting where an inflammatory environment had been previously induced by
497 LPS injection. Interestingly, other authors reported that besides extensive neutrophil recruitment to
498 the inflammation site after certain virus infections (*Respiratory syncytial virus*, *Herpes simplex virus*
499 *type 1* and *Coxsackievirus B3*), neutrophils did not play an important role in viral replication and
500 disease susceptibility, which in turn was exerted by monocytes and macrophages (78–81).

501 Immunocompetent mice, like C57BL/6 strain, readily resolve ZIKV infection and are a limited
502 model to answer long-term questions. However, IFN pathway deficient models, despite being
503 valuable tools to study ZIKV pathology, could alter the kinetic of neutrophil recruitment. Intracranial
504 ZIKV infection in C57BL/6 WT or *Rag1*^{-/-} mice (deficient in mature T and B cell) resulted in a lethal
505 encephalitis with infiltration of macrophages and NK cells (21). Neonatal immunocompetent mice
506 challenged subcutaneously with ZIKV elicit CD8⁺ T cells to the CNS (22). In contrast, *IFNAR*^{-/-} mice
507 (IFN type I and II receptor deficient) infected by both routes, showed an accelerated ZIKV spread to
508 peripheral organs and to the CNS, where it elicits an inflammatory response characterized by
509 neutrophils infiltration (21,22). Curiously, chemokines associated with neutrophil infiltration, besides
510 T cell, monocytes and macrophages were also detected in the brain of *STAT2*^{-/-} mice subcutaneously
511 infected with ZIKV (23). In the context of infection with the pulmonary bacteria *Francisella*
512 *tularensis* and *Influenza virus*, the absence of IFN result in higher neutrophil recruitment (82,83). It
513 would be of considerable interest to assess the production of neutrophil chemoattractants, such as
514 CXCL1 and CXCL2 in the CNS of humans following ZIKV infection, since ZIKV antagonizes
515 human IFN-I.

516 In conclusion, the results indicate that human neutrophils are slightly activated by direct contact with
517 the ZIKV. Thus, the direct interaction between ZIKV and neutrophils does not contribute to the viral
518 replication or to the inflammatory disease associate with the virus infection. On the other hand, *in*
519 *vitro*, neutrophils are able to reduce the ZIKV infection/replication on A549 cells. Is not clear how
520 neutrophils play this role and also, this data needs *in vivo* validation. Finally, despite not being a cell
521 target for the ZIKV infection it seems that, *in vitro*, neutrophils play a role in shaping the ZIKV
522 infection in other target cells.
523

524 **Conflict of Interest**

525 The authors declare that the research was conducted in the absence of any commercial or financial
526 relationships that could be construed as a potential conflict of interest.

527 **Author Contributions**

528 JBA and PFW conceptualized, designed, and performed the experiments and data analysis. BNP and
529 ALMP contributed in the interpretation and discussion of the data. CNDS contributed with her
530 expertise in virology. All authors prepared the manuscript.

531 **Funding**

532 This research was funded by the Conselho Nacional de Desenvolvimento Científico e Tecnológico
533 (CNPq-Universal - 444857/2014-1) and by Instituto Carlos Chagas/Fiocruz-PR (CNPq – PROEP-
534 ICC 442356/2019-6). CNDS (307176/2018-5) is CNPq fellow.

535 **Acknowledgments**

536 We thank Instituto Carlos Chagas's staff for technical assistance, especially our colleagues at the
537 Molecular Virology Laboratory and Juliano Bordignon for critical reading. We also thank the
538 Program for Technological Development in Tools for Health – PDTIS-FIOCRUZ for the use of the
539 Flow Cytometry (RPT08L) Microscopy (RPT07C), and Animal facilities at Instituto Carlos
540 Chagas/Fiocruz-PR.

541 **References**

- 542 1. Olson MF, Juarez JG, Kraemer MUG, Messina JP, Hamer GL. Global patterns of aegyptism
543 without arbovirus. *PLoS Negl Trop Dis* (2020) **15**:e0009397. doi:10.1101/2020.07.20.212209
- 544 2. Pierson TC, Diamond MS. The continued threat of emerging flaviviruses. *Nat Microbiol*
545 (2020) **5**:796–812. doi:10.1038/s41564-020-0714-0
- 546 3. Pierson TC, Diamond MS. The emergence of Zika virus and its new clinical syndromes.
547 *Nature* (2018) **560**:573–581. doi:10.1038/s41586-018-0446-y
- 548 4. Cugola FR, Fernandes IR, Russo FB, Freitas BC, Dias JLM, Guimarães KP, Benazzato C,
549 Almeida N, Pignatari GC, Romero S, et al. The Brazilian Zika virus strain causes birth defects
550 in experimental models. *Nature* (2016) **534**:267–271. doi:10.1038/nature18296
- 551 5. Cao-Lormeau VM, Blake A, Mons S, Lastère S, Roche C, Vanhomwegen J, Dub T, Baudouin
552 L, Teissier A, Larre P, et al. Guillain-Barré Syndrome outbreak associated with Zika virus
553 infection in French Polynesia: a case-control study. *Lancet* (2016) **387**:1531–1539.
554 doi:10.1016/S0140-6736(16)00562-6
- 555 6. Faria NR, Do Socorro Da Silva Azevedo R, Kraemer MUG, Souza R, Cunha MS, Hill SC,
556 Thézé J, Bonsall MB, Bowden TA, Rissanen I, et al. Zika virus in the Americas: Early
557 epidemiological and genetic findings. *Science* (80-) (2016) **352**:345–349.
558 doi:10.1126/science.aaf5036
- 559 7. Schouest B, Fahlberg M, Scheef EA, Ward MJ, Headrick K, Szeltner DM, Blair R V., Gilbert
560 MH, Doyle-Meyers LA, Danner VW, et al. Immune outcomes of Zika virus infection in

- 561 nonhuman primates. *Sci Rep* (2020) **10**:13069. doi:10.1038/s41598-020-69978-w
- 562 8. Lucas CGO, Kitoko JZ, Ferreira FM, Suzart VG, Papa MP, Coelho SVA, Cavazzoni CB,
563 Paula-Neto HA, Olsen PC, Iwasaki A, et al. Critical role of CD4+ T cells and IFN γ signaling
564 in antibody-mediated resistance to Zika virus infection. *Nat Commun* (2018) **9**:3136.
565 doi:10.1038/s41467-018-05519-4
- 566 9. Aliota MT, Caine EA, Walker EC, Larkin KE, Camacho E, Osorio JE. Characterization of
567 Lethal Zika Virus Infection in AG129 Mice. *PLoS Negl Trop Dis* (2016) **10**:e0004682.
568 doi:10.1371/journal.pntd.0004682
- 569 10. Aid M, Abbink P, Larocca RA, Boyd M, Nityanandam R, Nanayakkara O, Martinot AJ,
570 Moseley ET, Blass E, Borducchi EN, et al. Zika Virus Persistence in the Central Nervous
571 System and Lymph Nodes of Rhesus Monkeys. *Cell* (2017) **169**:610–620.
572 doi:10.1016/j.cell.2017.04.008
- 573 11. Hirsch AJ, Smith JL, Haese NN, Broeckel RM, Parkins CJ, Kreklywich C, DeFilippis VR,
574 Denton M, Smith PP, Messer WB, et al. Zika Virus infection of rhesus macaques leads to viral
575 persistence in multiple tissues. *PLoS Pathog* (2017) **13**:e1006219.
576 doi:10.1371/journal.ppat.1006219
- 577 12. Osuna CE, Lim SY, Deleage C, Griffin BD, Stein D, Schroeder LT, Omange R, Best K, Luo
578 M, Hraber PT, et al. Zika viral dynamics and shedding in rhesus and cynomolgus macaques.
579 *Nat Med* (2016) **22**:1448–1455. doi:10.1038/nm.4206
- 580 13. O'Connor MA, Tisoncik-Go J, Lewis TB, Miller CJ, Bratt D, Moats CR, Edlefsen PT,
581 Smedley J, Klatt NR, Gale M, et al. Early cellular innate immune responses drive Zika viral
582 persistence and tissue tropism in pigtail macaques. *Nat Commun* (2018) **9**:3371.
583 doi:10.1038/s41467-018-05826-w
- 584 14. Kam Y-W, Leite JA, Lum FM, Tan JLL, Lee B, Judice CC, De Toledo Teixeira DA, Andreata-
585 Santos R, Vinolo MA, Angerami R, et al. Specific Biomarkers Associated With Neurological
586 Complications and Congenital Central Nervous System Abnormalities From Zika Virus-
587 Infected Patients in Brazil. *J Infect Dis* (2017) **216**:172–181. doi:10.1093/infdis/jix261
- 588 15. Lum FM, Lye DCB, Tan JLL, Lee B, Chia PY, Chua TK, Amrun SN, Kam YW, Yee WX,
589 Ling WP, et al. Longitudinal Study of Cellular and Systemic Cytokine Signatures to Define
590 the Dynamics of a Balanced Immune Environment During Disease Manifestation in Zika
591 Virus-Infected Patients. *J Infect Dis* (2018) **218**:814–824. doi:10.1093/infdis/jiy225
- 592 16. Bowen JR, Quicke KM, Maddur MS, O'Neal JT, McDonald CE, Fedorova NB, Puri V,
593 Shabman RS, Pulendran B, Suthar MS. Zika Virus Antagonizes Type I Interferon Responses
594 during Infection of Human Dendritic Cells. *PLoS Pathog* (2017) **13**:e1006164.
595 doi:10.1371/journal.ppat.1006164
- 596 17. Foo S-S, Chen W, Chan Y, Bowman JW, Chang L-C, Choi Y, Yoo JS, Ge J, Cheng G, Bonnin
597 A, et al. Asian Zika virus strains target CD14+ blood monocytes and induce M2-skewed
598 immunosuppression during pregnancy. *Nat Microbiol* (2017) **2**:1558–1570.
599 doi:10.1038/s41564-017-0016-3

- 600 18. Michlmayr D, Andrade P, Gonzalez K, Balmaseda A, Harris E. CD14+CD16+ monocytes are
601 the main target of Zika virus infection in peripheral blood mononuclear cells in a paediatric
602 study in Nicaragua. *Nat Microbiol* (2017) **2**:1462–1470. doi:10.1038/s41564-017-0035-0
- 603 19. Vielle NJ, Zumkehr B, García-Nicolás O, Blank F, Stojanov M, Musso D, Baud D,
604 Summerfield A, Alves MP. Silent infection of human dendritic cells by African and Asian
605 strains of Zika virus. *Sci Rep* (2018) **8**:5440. doi:10.1038/s41598-018-23734-3
- 606 20. Hirsch AJ, Roberts VHJ, Grigsby PL, Haese N, Schabel MC, Wang X, Lo JO, Liu Z, Kroenke
607 CD, Smith JL, et al. Zika virus infection in pregnant rhesus macaques causes placental
608 dysfunction and immunopathology. *Nat Commun* (2018) **9**:263. doi:10.1038/s41467-017-
609 02499-9
- 610 21. Hayashida E, Ling ZL, Ashhurst TM, Viengkhou B, Jung SR, Songkhunawej P, West PK,
611 King NJC, Hofer MJ. Zika virus encephalitis in immunocompetent mice is dominated by
612 innate immune cells and does not require T or B cells. *J Neuroinflammation* (2019) **16**:177.
613 doi:10.1186/s12974-019-1566-5
- 614 22. Manangeeswaran M, Ireland DDC, Verthelyi D. Zika (PRVABC59) Infection Is Associated
615 with T cell Infiltration and Neurodegeneration in CNS of Immunocompetent Neonatal
616 C57Bl/6 Mice. *PLoS Pathog* (2016) **12**:e1006004. doi:10.1371/journal.ppat.1006004
- 617 23. Tripathi S, Balasubramaniam VRMT, Brown JA, Mena I, Grant A, Bardina S V., Maringer K,
618 Schwarz MC, Maestre AM, Sourisseau M, et al. A novel Zika virus mouse model reveals
619 strain specific differences in virus pathogenesis and host inflammatory immune responses.
620 *PLoS Pathog* (2017) **13**:e1006258. doi:10.1371/journal.ppat.1006258
- 621 24. Pei X, Gao J, Shan C, Dunn TJ, Xie X, Xia H, Zou J, Thames BH, Sajja A, Yu Y, et al.
622 Inhibition of innate immune response ameliorates Zika virus-induced neurogenesis deficit in
623 human neural stem cells. *PLoS Negl Trop Dis* (2021) **15**:e0009183.
624 doi:10.1371/journal.pntd.0009183
- 625 25. Ayala-Nunez NV, Follain G, Delalande F, Hirschler A, Partiot E, Hale GL, Bollweg BC,
626 Roels J, Chazal M, Bakoa F, et al. Zika virus enhances monocyte adhesion and transmigration
627 favoring viral dissemination to neural cells. *Nat Commun* (2019) **10**:4430.
628 doi:10.1038/s41467-019-12408-x
- 629 26. McDonald EM, Anderson J, Wilusz J, Ebel GD, Brault AC. Zika virus replication in myeloid
630 cells during acute infection is vital to viral dissemination and pathogenesis in a mouse model.
631 *J Virol* (2020) **94**:e00838-20. doi:10.1128/JVI.00127-20
- 632 27. McDonald EM, Duggal NK, Ritter JM, Brault AC. Infection of epididymal epithelial cells and
633 leukocytes drives seminal shedding of Zika virus in a mouse model. *PLoS Negl Trop Dis*
634 (2018) **12**:e0006691. doi:10.1371/journal.pntd.0006691
- 635 28. Yang W, Wu YH, Liu SQ, Sheng ZY, Zhen Z Da, Gao RQ, Cui XY, Fan DY, Qin ZH, Zheng
636 AH, et al. S100A4+ macrophages facilitate zika virus invasion and persistence in the
637 seminiferous tubules via interferon-gamma mediation. *PLoS Pathog* (2020) **16**:e1009019.
638 doi:10.1371/journal.ppat.1009019

- 639 29. Winkler CW, Evans AB, Carmody AB, Peterson KE. Placental Myeloid Cells Protect against
640 Zika Virus Vertical Transmission in a Rag1-Deficient Mouse Model. *J Immunol* (2020)
641 **205**:143–152. doi:10.4049/jimmunol.1901289
- 642 30. de Noronha L, Zanluca C, Azevedo MLV, Luz KG, dos Santos CND. Zika virus damages the
643 human placental barrier and presents marked fetal neurotropism. *Mem Inst Oswaldo Cruz*
644 (2016) **111**:287–293. doi:10.1590/0074-02760160085
- 645 31. Brinkmann V, Reichard U, Goosmann C, Fauler B, Uhlemann Y, Weiss DS, Weinrauch Y,
646 Zychlinsky A. Neutrophil Extracellular Traps Kill Bacteria. *Science* (80-) (2004) **303**:1532–
647 1535. doi:10.1126/science.1092385
- 648 32. Kruger P, Saffarzadeh M, Weber ANR, Rieber N, Radsak M, von Bernuth H, Benarafa C,
649 Roos D, Skokowa J, Hartl D. Neutrophils: Between Host Defence, Immune Modulation, and
650 Tissue Injury. *PLoS Pathog* (2015) **11**:e1004651. doi:10.1371/journal.ppat.1004651
- 651 33. Duffy D, Perrin H, Abadie V, Benhabiles N, Boissonnas A, Liard C, Descours B, Reboulleau
652 D, Bonduelle O, Verrier B, et al. Neutrophils Transport Antigen from the Dermis to the Bone
653 Marrow, Initiating a Source of Memory CD8+ T Cells. *Immunity* (2012) **37**:917–929.
654 doi:10.1016/j.immuni.2012.07.015
- 655 34. Hufford MM, Richardson G, Zhou H, Manicassamy B, García-Sastre A, Enelow RI, Braciale
656 TJ. Influenza-Infected Neutrophils within the Infected Lungs Act as Antigen Presenting Cells
657 for Anti-Viral CD8+ T Cells. *PLoS One* (2012) **7**:e46581. doi:10.1371/journal.pone.0046581
- 658 35. Paul AM, Acharya D, Duty L, Thompson EA, Le L, Stokic DS, Leis AA, Bai F. Osteopontin
659 facilitates West Nile virus neuroinvasion via neutrophil “Trojan horse” transport. *Sci Rep*
660 (2017) **7**:4722. doi:10.1038/s41598-017-04839-7
- 661 36. Bai F, Kong K, Dai J, Qian F, Zhang L, Brown CR, Fikrig E, Montgomery RR. A Paradoxical
662 Role for Neutrophils in the Pathogenesis of West Nile Virus. *J Infect Dis* (2010) **202**:1804–
663 1812. doi:10.1086/657416
- 664 37. Strottmann DM, Zanluca C, Mosimann ALP, Koishi AC, Auwerter NC, Faoro H, Cataneo
665 AHD, Kuczera D, Wowk PF, Bordignon J, et al. Genetic and biological characterization of
666 Zika virus isolates from different Brazilian regions. *Mem Inst Oswaldo Cruz* (2019)
667 **114**:e190150. doi:10.1590/0074-02760190150
- 668 38. Donald CL, Brennan B, Cumberworth SL, Rezelj V V., Clark JJ, Cordeiro MT, Freitas de
669 Oliveira França R, Pena LJ, Wilkie GS, Da Silva Filipe A, et al. Full Genome Sequence and
670 sfRNA Interferon Antagonist Activity of Zika Virus from Recife, Brazil. *PLoS Negl Trop Dis*
671 (2016) **10**:e0005048. doi:10.1371/journal.pntd.0005048
- 672 39. Dick GWA, Kitchen SF, Haddow AJ. Zika virus isolation and serological specificity. *Trans R*
673 *Soc Trop Med Hyg* (1952) **46**:509–520.
- 674 40. Cataneo AHD, Kuczera D, Koishi AC, Zanluca C, Silveira GF, Arruda TB de, Suzukawa AA,
675 Bortot LO, Dias-Baruffi M, Verri WA, et al. The citrus flavonoid naringenin impairs the in
676 vitro infection of human cells by Zika virus. *Sci Rep* (2019) **9**:16348. doi:10.1038/s41598-019-
677 52626-3

- 678 41. Dejarnac O, Hafirassou ML, Chazal M, Versapuech M, Gaillard J, Perera-Lecoin M, Umana-
679 Diaz C, Bonnet-Madin L, Carnec X, Tinevez JY, et al. TIM-1 Ubiquitination Mediates
680 Dengue Virus Entry. *Cell Rep* (2018) **23**:1779–1793. doi:10.1016/j.celrep.2018.04.013
- 681 42. Lanciotti RS, Kosoy OL, Laven JJ, Velez JO, Lambert AJ, Johnson AJ, Stanfield SM, Duffy
682 MR. Genetic and Serologic Properties of Zika Virus Associated with an Epidemic, Yap State,
683 Micronesia, 2007. *Emerg Infect Dis* (2008) **14**:1232–1239. doi:10.3201/eid1408.080287
- 684 43. Emery SL, Erdman DD, Bowen MD, Newton BR, Winchell JM, Meyer RF, Tong S, Cook BT,
685 Holloway BP, McCaustland KA, et al. Real-Time Reverse Transcription-Polymerase Chain
686 Reaction Assay for SARS-associated Coronavirus. *Emerg Infect Dis* (2004) **10**:311–316.
687 doi:10.3201/eid1002.030759
- 688 44. Porto BN, Alves LS, Fernández PL, Dutra TP, Figueiredo RT, Graça-Souza A V., Bozza MT.
689 Heme Induces Neutrophil Migration and Reactive Oxygen Species Generation through
690 Signaling Pathways Characteristic of Chemotactic Receptors. *J Biol Chem* (2007) **282**:24430–
691 24436. doi:10.1074/jbc.M703570200
- 692 45. Pan Y, Cheng A, Wang M, Yin Z, Jia R. The Dual Regulation of Apoptosis by Flavivirus.
693 *Front Microbiol* (2021) **12**:654494. doi:10.3389/fmicb.2021.654494
- 694 46. Mayadas TN, Cullere X, Lowell CA. The Multifaceted Functions of Neutrophils. *Annu Rev*
695 *Pathol Mech Dis* (2014) **9**:181–218. doi:10.1146/annurev-pathol-020712-164023
- 696 47. Sabroe I, Prince LR, Jones EC, Horsburgh MJ, Foster SJ, Vogel SN, Dower SK, Whyte MKB.
697 Selective Roles for Toll-Like Receptor (TLR)2 and TLR4 in the Regulation of Neutrophil
698 Activation and Life Span. *J Immunol* (2003) **170**:5268–5275.
699 doi:10.4049/jimmunol.170.10.5268
- 700 48. Kishimoto T, Jutila M, Berg E, Butcher E. Neutrophil Mac-1 and MEL-14 Adhesion Proteins
701 Inversely Regulated by Chemotactic Factors. *Science* (80-) (1989) **245**:1238–1241.
702 doi:10.1126/science.2551036
- 703 49. Zhou X, Gao XP, Fan J, Liu Q, Anwar KN, Frey RS, Malik AB. LPS activation, of Toll-like
704 receptor 4 signals CD11b/CD18 expression in neutrophils. *Am J Physiol - Lung Cell Mol*
705 *Physiol* (2005) **288**:L655-62. doi:10.1152/ajplung.00327.2004
- 706 50. Papayannopoulos V. Neutrophil extracellular traps in immunity and disease. *Nat Rev Immunol*
707 (2018) **18**:134–147. doi:10.1038/nri.2017.105
- 708 51. Fischer MA, Davies ML, Reider IE, Heipertz EL, Epler MR, Sei JJ, Ingersoll MA, van
709 Rooijen N, Randolph GJ, Norbury CC. CD11b+, Ly6G+ Cells Produce Type I Interferon and
710 Exhibit Tissue Protective Properties Following Peripheral Virus Infection. *PLoS Pathog*
711 (2011) **7**:e1002374. doi:10.1371/journal.ppat.1002374
- 712 52. Tate MD, Ioannidis LJ, Croker B, Brown LE, Brooks AG, Reading PC. The Role of
713 Neutrophils during Mild and Severe Influenza Virus Infections of Mice. *PLoS One* (2011)
714 **6**:e17618. doi:10.1371/journal.pone.0017618
- 715 53. Saitoh T, Komano J, Saitoh Y, Misawa T, Takahama M, Kozaki T, Uehata T, Iwasaki H,

- 716 Omori H, Yamaoka S, et al. Neutrophil Extracellular Traps Mediate a Host Defense Response
717 to Human Immunodeficiency Virus-1. *Cell Host Microbe* (2012) **12**:109–116.
718 doi:10.1016/j.chom.2012.05.015
- 719 54. Muraro SP, De Souza GF, Gallo SW, Da Silva BK, De Oliveira SD, Vinolo MAR, Saraiva
720 EM, Porto BN. Respiratory Syncytial Virus induces the classical ROS-dependent NETosis
721 through PAD-4 and necroptosis pathways activation. *Sci Rep* (2018) **8**:14166.
722 doi:10.1038/s41598-018-32576-y
- 723 55. Middleton EA, He XY, Denorme F, Campbell RA, Ng D, Salvatore SP, Mostyka M, Baxter-
724 Stoltzfus A, Borczuk AC, Loda M, et al. Neutrophil Extracellular Traps (NETs) Contribute to
725 Immunothrombosis in COVID-19 Acute Respiratory Distress Syndrome. *Blood* (2020)
726 **136**:1169–1179. doi:10.1182/blood.2020007008
- 727 56. Heit B, Jones G, Knight D, Antony JM, Gill MJ, Brown C, Power C, Kubes P. HIV and Other
728 Lentiviral Infections Cause Defects in Neutrophil Chemotaxis, Recruitment, and Cell
729 Structure: Immunorestorative Effects of Granulocyte-Macrophage Colony-Stimulating Factor.
730 *J Immunol* (2006) **177**:6405–6414. doi:10.4049/jimmunol.177.9.6405
- 731 57. Chen J, Yang YF, Yang Y, Zou P, Chen J, He Y, Shui SL, Cui YR, Bai R, Liang YJ, et al.
732 AXL promotes Zika virus infection in astrocytes by antagonizing type I interferon signalling.
733 *Nat Microbiol* (2018) **3**:302–309. doi:10.1038/s41564-017-0092-4
- 734 58. Giraldo DM, Hernandez JC, Velilla P, Urcuqui-Inchima S. HIV-1–neutrophil interactions
735 trigger neutrophil activation and Toll-like receptor expression. *Immunol Res* (2016) **64**:93–
736 103. doi:10.1007/s12026-015-8691-8
- 737 59. Hiroki CH, Toller-Kawahisa JE, Fumagalli MJ, Colon DF, Figueiredo LTM, Fonseca BALD,
738 Franca RFO, Cunha FQ. Neutrophil Extracellular Traps Effectively Control Acute
739 Chikungunya Virus Infection. *Front Immunol* (2020) **10**:3108. doi:10.3389/fimmu.2019.03108
- 740 60. Moreno-Altamirano MMB, Rodríguez-Espinosa O, Rojas-Espinosa O, Pliego-Rivero B,
741 Sánchez-García FJ. Dengue Virus Serotype-2 Interferes with the Formation of Neutrophil
742 Extracellular Traps. *Intervirology* (2015) **58**:250–259. doi:10.1159/000440723
- 743 61. Opasawatchai A, Amornsupawat P, Jiravejchakul N, Chan-in W, Spoerk NJ,
744 Manopwisedjaroen K, Singhasivanon P, Yingtaweesak T, Suraamornkul S, Mongkolsapaya J,
745 et al. Neutrophil Activation and Early Features of NET Formation Are Associated With
746 Dengue Virus Infection in Human. *Front Immunol* (2019) **10**:3007.
747 doi:10.3389/fimmu.2018.03007
- 748 62. Bos S, Poirier-Beaudouin B, Seffer V, Manich M, Mardi C, Desprès P, Gadea G, Gougeon M-
749 L. Zika Virus Inhibits IFN- α Response by Human Plasmacytoid Dendritic Cells and Induces
750 NS1-Dependent Triggering of CD303 (BDCA-2) Signaling. *Front Immunol* (2020)
751 **11**:582061. doi:10.3389/fimmu.2020.582061
- 752 63. Sun X, Hua S, Chen HR, Ouyang Z, Einkauf K, Tse S, Ard K, Ciaranello A, Yawetz S, Sax P,
753 et al. Transcriptional Changes during Naturally Acquired Zika Virus Infection Render
754 Dendritic Cells Highly Conducive to Viral Replication. *Cell Rep* (2017) **21**:3471–3482.
755 doi:10.1016/j.celrep.2017.11.087

- 756 64. Sun X, Hua S, Gao C, Blackmer JE, Ouyang Z, Ard K, Ciaranello A, Yawetz S, Sax PE,
757 Rosenberg ES, et al. Immune-profiling of ZIKV-infected patients identifies a distinct function
758 of plasmacytoid dendritic cells for immune cross-regulation. *Nat Commun* (2020) **11**:2421.
759 doi:10.1038/s41467-020-16217-5
- 760 65. Dowall SD, Graham VA, Rayner E, Atkinson B, Hall G, Watson RJ, Bosworth A, Bonney LC,
761 Kitchen S, Hewson R. A Susceptible Mouse Model for Zika Virus Infection. *PLoS Negl Trop*
762 *Dis* (2016) **10**:e0004658. doi:10.1371/journal.pntd.0004658
- 763 66. Lum FM, Narang V, Hue S, Chen J, McGovern N, Rajarethinam R, Tan JLL, Amrun SN, Chan
764 YH, Lee CYP, et al. Immunological observations and transcriptomic analysis of trimester-
765 specific full-term placentas from three Zika virus-infected women. *Clin Transl Immunol*
766 (2019) **8**:e1082. doi:10.1002/cti2.1082
- 767 67. Nguyen SM, Antony KM, Dudley DM, Kohn S, Simmons HA, Wolfe B, Salamat MS,
768 Teixeira LBC, Wiepz GJ, Thoong TH, et al. Highly efficient maternal-fetal Zika virus
769 transmission in pregnant rhesus macaques. *PLoS Pathog* (2017) **13**:e1006378.
770 doi:10.1371/journal.ppat.1006378
- 771 68. Wang W, Li G, De W, Luo Z, Pan P, Tian M, Wang Y, Xiao F, Li A, Wu K, et al. Zika virus
772 infection induces host inflammatory responses by facilitating NLRP3 inflammasome assembly
773 and interleukin-1 β secretion. *Nat Commun* (2018) **9**:106. doi:10.1038/s41467-017-02645-3
- 774 69. Pantoja P, Pérez-Guzmán EX, Rodríguez I V., White LJ, González O, Serrano C, Giavedoni L,
775 Hodara V, Cruz L, Arana T, et al. Zika virus pathogenesis in rhesus macaques is unaffected by
776 pre-existing immunity to dengue virus. *Nat Commun* (2017) **8**:15674.
777 doi:10.1038/ncomms15674
- 778 70. Dudley DM, Aliota MT, Mohr EL, Weiler AM, Lehrer-Brey G, Weisgrau KL, Mohns MS,
779 Breitbach ME, Rasheed MN, Newman CM, et al. A rhesus macaque model of Asian-lineage
780 Zika virus infection. *Nat Commun* (2016) **7**:12204. doi:10.1038/ncomms12204
- 781 71. Frumence E, Roche M, Krejbich-Trotot P, El-Kalamouni C, Nativel B, Rondeau P, Missé D,
782 Gadea G, Viranaicken W, Desprès P. The South Pacific epidemic strain of Zika virus
783 replicates efficiently in human epithelial A549 cells leading to IFN- β production and apoptosis
784 induction. *Virology* (2016) **493**:217–226. doi:10.1016/j.virol.2016.03.006
- 785 72. Pinggen M, Bryden SR, Pondeville E, Schnettler E, Kohl A, Merits A, Fazakerley JK, Graham
786 GJ, McKimmie CS. Host Inflammatory Response to Mosquito Bites Enhances the Severity of
787 Arbovirus Infection. *Immunity* (2016) **44**:1455–1469. doi:10.1016/j.immuni.2016.06.002
- 788 73. Hastings AK, Uraki R, Gaitsch H, Dhaliwal K, Stanley S, Sproch H, Williamson E, MacNeil
789 T, Marin-Lopez A, Hwang J, et al. *Aedes aegypti* NeSt1 Protein Enhances Zika Virus
790 Pathogenesis by Activating Neutrophils. *J Virol* (2019) **93**:e:00395-19. doi:10.1128/jvi.00395-
791 19
- 792 74. Hattar K, Franz K, Ludwig M, Sibelius U, Wilhelm J, Lohmeyer J, Savai R, Subtil FSB,
793 Dahlem G, Eul B, et al. Interactions between neutrophils and non-small cell lung cancer cells:
794 enhancement of tumor proliferation and inflammatory mediator synthesis. *Cancer Immunol*
795 *Immunother* (2014) **63**:1297–1306. doi:10.1007/s00262-014-1606-z

- 796 75. Grandel U, Heygster D, Sibelius U, Fink L, Sigel S, Seeger W, Grimminger F, Hattar K.
797 Amplification of Lipopolysaccharide-Induced Cytokine Synthesis in Non-Small Cell Lung
798 Cancer/Neutrophil Cocultures. *Mol Cancer Res* (2009) **7**:1729–1735. doi:10.1158/1541-
799 7786.MCR-09-0048
- 800 76. Serrao KL, Fortenberry JD, Owens ML, Harris FL, Brown LAS. Neutrophils induce apoptosis
801 of lung epithelial cells via release of soluble Fas ligand. *Am J Physiol - Lung Cell Mol Physiol*
802 (2001) **280**:L298-305. doi:10.1152/ajplung.2001.280.2.l298
- 803 77. Sun B, Qin W, Song M, Liu L, Yu Y, Qi X, Sun H. Neutrophil suppresses tumor cell
804 proliferation via Fas/Fas ligand pathway mediated cell cycle arrested. *Int J Biol Sci* (2018)
805 **14**:2103–2113. doi:10.7150/ijbs.29297
- 806 78. Xu D, Wang P, Yang J, Qian Q, Li M, Wei L, Xu W. Gr-1+ Cells Other Than Ly6G+
807 Neutrophils Limit Virus Replication and Promote Myocardial Inflammation and Fibrosis
808 Following Coxsackievirus B3 Infection of Mice. *Front Cell Infect Microbiol* (2018) **8**:157.
809 doi:10.3389/fcimb.2018.00157
- 810 79. Kirsebom F, Michalaki C, Agueda-Oyarzabal M, Johansson C. Neutrophils do not impact viral
811 load or the peak of disease severity during RSV infection. *Sci Rep* (2020) **10**:1110.
812 doi:10.1038/s41598-020-57969-w
- 813 80. Cortjens B, Lutter R, Boon L, Bem RA, Van Woensel JBM. Pneumovirus-Induced Lung
814 Disease in Mice Is Independent of Neutrophil-Driven Inflammation. *PLoS One* (2016)
815 **11**:e0168779. doi:10.1371/journal.pone.0168779
- 816 81. Wojtasiak M, Pickett DL, Tate MD, Londrigan SL, Bedoui S, Brooks AG, Reading PC.
817 Depletion of Gr-1+, but not Ly6G+, immune cells exacerbates virus replication and disease in
818 an intranasal model of herpes simplex virus type 1 infection. *J Gen Virol* (2010) **91**:2158–
819 2166. doi:10.1099/vir.0.021915-0
- 820 82. Seo SU, Kwon HJ, Ko HJ, Byun YH, Seong BL, Uematsu S, Akira S, Kweon MN. Type I
821 Interferon Signaling Regulates Ly6Chi Monocytes and Neutrophils during Acute Viral
822 Pneumonia in Mice. *PLoS Pathog* (2011) **7**:e1001304. doi:10.1371/journal.ppat.1001304
- 823 83. Furuya Y, Steiner D, Metzger DW. Does type I interferon limit protective neutrophil responses
824 during pulmonary *Francisella tularensis* infection? *Front Immunol* (2014) **5**:355.
825 doi:10.3389/fimmu.2014.00355

826 Figure Captions

827 Figure 1. ZIKV strains do not affect human neutrophils viability. (A) Neutrophils morphological
828 features showed by flow cytometry and deconvolution microscopy (bright-field) after *in vitro*
829 stimulation during 2 hours with mock (C6/36 cells conditioned media in equivalent volume of ZIKV
830 strains), LPS (100 ng/mL), ZIKV BR 2015/15261, ZIKV PE243 and ZIKV MR766 (1 MOI). The
831 cells were washed to remove the stimuli (indicated by ▼) and evaluated right after that (2 hours) and
832 at 6, 12 and 24 hours after stimulation. The image shows a representative dot plot and cell image of
833 neutrophils after 6 hours of interaction with ZIKV PE243. Bar=25 μm; magnification=100x. (B)
834 Contour plots depicting the frequency of annexin V⁺ and 7-AAD⁺ in the neutrophils gated population
835 at 6 hours after stimulation with mock, LPS and ZIKV PE243. This is a representative plot of the

836 ZIKV strains's effects. Mock-unstained condition was used as a negative control of fluorescence to
 837 set the gates. **(C)** Frequency of annexin V⁺ and annexin V⁺7-AAD⁺ neutrophils at 2, 6, 12 and 24
 838 hours after stimulation with mock, LPS and ZIKV strains. The dashed line represents annexin V⁺ and
 839 annexinV⁺/7-AAD⁺ frequency right after neutrophil purification from blood. Three independent
 840 experiments are showed (n=11). Bars indicate standard error of the mean (SEM). The asterisk (*)
 841 denotes statistical difference between mock and LPS and the number sign (#) between mock and all
 842 the three ZIKV strains in the condition.

843 Figure 2. ZIKV strains do not replicate in human neutrophils. **(A)** Immunostaining of neutrophils
 844 with 4G2 at 24 hours after ZIKV PE243 (1 MOI) (a-d) or mock (e-h) stimulation. Nuclei were
 845 stained withVybrant DyeCicleViolet. Merge of these stainings and the bright-field colocalization are
 846 also showed. C6/36 cells (l-p) were used as an infection positive control. Bar=50 μ m;
 847 magnification=40x. **(B)** Histograms showing 4G2 immunostaing of neutrophils at 24 hours after
 848 mock and ZIKV PE243 stimulation as measured through flow cytometry. Mock-unstained cells were
 849 used as a negative fluorescence control. One representative result of three independent experiments is
 850 showed. **(C)** RNA levels of ZIKV BR 2015/15261, ZIKV PE243 and ZIKV MR766 (1 MOI)
 851 represented by Δ Ct (Ct ZIKV –Ct RNase P) in neutrophils at 2, 6, 12 and 24 hours after stimulation
 852 with the different strains. One independent experiment is showed (n=3). **(D)** ZIKV loads on
 853 neutrophil culture supernatant after 6, 12 and 24 hours of stimulation with ZIKV strains. The dashed
 854 line named input represents the mean of the titers of the three ZIKV strains still detected on the
 855 supernatant after the stimuli removal after 2 hours of stimulation. Four independent experiments are
 856 showed (n=15). **(E)** RNA levels of ZIKV represented by Δ Ct (Ct ZIKV –Ct RNase P)detected 2
 857 hours after stimulation with ZIKV PE243 (1 MOI) in neutrophils treated or not with trypsin. Three
 858 independent experiments are showed (n=9). **(F)** mRNA levels of *IRF3*, in neutrophils at 2, 6, 12 and
 859 24 hours after stimulation with IFN- α (200 U/mL), ZIKV PE243, and ZIKV MR766 (MOI 1) relative
 860 to the non-stimulated cells (represented as $2^{-\Delta\Delta$ Ct}). All data was normalized to human RNase P
 861 expression levels. One independent experiment is showed (n=3). Bars indicate SEM.

862 Figure 3. ZIKV strains do not promote regulation of surface molecules expression, cytokines,
 863 elastase secretion, and intracellular reactive oxygen species production in human neutrophils. **(A)**
 864 Contour plots depicting the frequency of CD16⁺CD11b⁺ neutrophils 6 hours after stimulation with
 865 mock, LPS and ZIKV PE243 (1 MOI). Isotype control antibodies were used as a negative
 866 fluorescence control to set the gates. Histograms of representative results of the CD16⁺CD11b⁺ and
 867 CD11b fluorescence intensity are showed. **(B)** Expression of CD11b, CD32, CD182 and CD62L,
 868 represented by the mean fluorescence intensity (MFI), in neutrophils at 2, 6 and 12 hours after
 869 stimulation with mock, LPS and ZIKV strains. The dashed line represents the respective markers
 870 MFI right after neutrophil obtaining from blood. Two independent experiments are showed (n=8).
 871 **(C)** IL-8 levels in neutrophil culture supernatant after 6 and 12 hours of stimulation with mock, LPS
 872 (100 ng/mL), ZIKV BR 2015/15261, ZIKV PE243 and ZIKV MR766 (1 MOI). Three independent
 873 experiments are showed (n=12). **(D)** Elastase levels in neutrophil culture supernatant after 6 hours of
 874 stimulation with mock, LPS and ZIKV BR 2015/15261 (1 MOI). Two independent experiments are
 875 showed (n=6). **(E)** Chloromethyl-H₂DCFDA dye fluorescence in neutrophils 6 hours after
 876 stimulation with mock, PMA (16 nM) and ZIKV PE243 (1 MOI), and the frequency of neutrophils
 877 chloromethyl-H₂DCFDA⁺ at 2 and 6 hours after stimulation with mock, PMA and ZIKV strains.
 878 Two independent experiments are showed (n=6). Bars indicate SEM. The asterisk (*) denotes
 879 statistical difference between mock and LPS (B-D) or PMA (E) and the number sign (#) between
 880 mock and all the three ZIKV strains in the condition (B).

881 Figure 4. ZIKV strains do not induce, block or are impacted by NETs. **(A)** Free double stranded
 882 DNA (dsDNA) on neutrophil culture supernatant after 5 hours of stimulation with mock, PMA (160
 883 nM), ZIKV BR 2015/15261, ZIKV PE243 and ZIKV MR766 (1 MOI). Three independent
 884 experiments are showed (n=9). The asterisk (*) denotes statistical difference between mock and
 885 PMA. **(B)** Immunostaining of neutrophils with anti-acetyl-histone H3, after 5 hours of stimulation
 886 with mock (a-d), PMA (e-h) and ZIKV PE243 (1 MOI) (i-l). DNA was stained using Vybrant
 887 DyeCicleViolet. Merge of these stainings and the bright-field colocalization are also showed. Bar=50
 888 μm ; magnification=60x. ZIKV PE243 is showed as representative of the ZIKV strains' effects. One
 889 representative of three independent experiments is showed. **(C)** Free dsDNA on neutrophil culture
 890 supernatant after 1 hour of stimulation with mock and ZIKV strains plus 5 hours of stimulation with
 891 PMA. Two independent experiments are showed (n=6). **(D)** ZIKV titers on neutrophil culture
 892 supernatant stimulated or not with PMA during 5 hours followed by 1 hour of interaction with ZIKV
 893 strains. Two independent experiments are showed (n=6). Bars indicate SEM.

894 Figure 5. ZIKV interaction with human neutrophils does not affect the viral infectivity. Flow
 895 cytometry plots depicting the frequency of 4G2⁺ A549 cells at 36 **(A)** or 32 hours **(B)** after infection
 896 with ZIKV PE243 (1 MOI) previously incubated 2 or 6 hours, respectively, in the presence (+NØ) or
 897 absence of neutrophils. Mock condition was used as a negative fluorescence control and ZIKV
 898 PE243 is showed as a representative of the ZIKV strains's effects. Frequency of 4G2⁺ A549 cells
 899 infected during 36 **(C)** or 32 hours **(D)** with ZIKV strains (1 MOI) previously incubated 2 or 6 hours
 900 in the presence or not of neutrophils. Two independent experiments are showed (n=9). Bars indicate
 901 SEM. NØ, neutrophils. (▼) indicates the moment cells were washed to remove the stimuli.

902 Figure 6. ZIKV infection in human primary cells or highly susceptible cell lines does not promote
 903 human neutrophils migration. IL-8, MCP-1 and IP-10 levels in mdDCs **(A)** and IL-8 in PBMCs **(B)**
 904 culture supernatant after 24 and 48 hours of stimulation with mock, LPS (100 ng/mL), ZIKV BR
 905 2015/15261, ZIKV PE243 and ZIKV MR766 (1 MOI). Three independent experiments are showed
 906 (n=9). The asterisk (*) denotes statistical difference between mock and LPS. The number sign (#)
 907 between mock and all the three ZIKV strains in the condition. **(C)** Chemotactic index of neutrophils
 908 after 2 hours of stimulation with 1,000 or 50,000 pg of rhIL-8 and ZIKV PE243 infected A459 cells
 909 at 48 hours post-infection. Two independent experiments are showed (n=6). Bars indicate SEM.

910 Figure 7. Neutrophils presence during or after ZIKV infection in susceptible cells impacts the
 911 intracellular viral burden. **(A)** Flow cytometry plots depicting the frequency of 4G2⁺ A549 cells when
 912 neutrophils (+NØ) or neutrophils pre-treated with trypsin (+NØ +trypsin) were added or not only
 913 during the 2 hours of interaction with ZIKV PE243 (1 MOI). Mock condition was used as a negative
 914 fluorescence control. ZIKV PE243 is showed as representative of the ZIKV strains' effects. (▼)
 915 indicate the moment cells were washed to remove the stimuli. **(B)** Flow cytometry plots depicting the
 916 frequency of 4G2⁺ A549 cells when neutrophils were added (+NØ) during the last 16 hours to an
 917 A549 cell culture previously infected during 24 hours with ZIKV PE243. Frequency of 4G2⁺ A549
 918 cells when neutrophils were added or not during ZIKV strain infection (1 MOI) **(C)** or 24 hours after
 919 ZIKV infection **(D)**. Four independent experiments are showed (n=12). The asterisk (*) denotes
 920 statistical difference between the absence and presence of neutrophils to each ZIKV strain. **(E)**
 921 Frequency of 4G2⁺ A549 cells when neutrophils were treated with trypsin and added during ZIKV
 922 infection (1 MOI). Two independent experiments are showed (n=6). Bars indicate SEM. NØ=
 923 neutrophils.

924 Figure 8. A systemic reduction of neutrophils does not restrict ZIKV relocation to draining lymph
 925 nodes. After neutrophils depletion, mice received footpad s.c. injection of PBS or LPS (1000 ng) and

926 3 hours later, ZIKV PE243 (5×10^5 FFU). One hour later, pLNs were harvested and pooled to
927 determine ZIKV loads. Three animals per group were used in each experiment. One of three
928 independent experiments is showed. Bars indicate SEM.

929 Supplementary Figure 1. ZIKV lower infection in A549 cells in the presence of neutrophils is not due
930 to viability reduction in A549 cells or neutrophils activation. Frequency of A549 cells annexin V-7-
931 AAD⁻ after stimulation with mock or ZIKV BR 2015/15261, ZIKV PE243 and ZIKV MR766 (1
932 MOI) in the presence or not of neutrophils added during infection (A) or 24 hours after ZIKV
933 infection (B). (C) Expression (MFI) of CD11b in neutrophils or neutrophils treated with LPS (100
934 ng/mL) co-cultured 24 hours with A549 cells infected with mock or ZIKV strains (1 MOI). (D)
935 Frequency of 4G2⁺ A549 cells when neutrophils were added 24 hours after ZIKV strains infection in
936 the presence or absence of LPS. Three independent experiments are showed (n=9). Bars indicate
937 SEM. The asterisk (*) denotes statistical difference between mock and LPS (C) and between the
938 absence and presence of neutrophils to each ZIKV strain (D). NØ= neutrophils.

939 Supplementary Figure 2. Neutrophil depletion mediated by anti-Ly6G monoclonal antibody. (A)
940 ZIKV titer detected in the pool of both popliteal (pLN), sciatic (sLN) and lumbar aortic (laLN) lymph
941 nodes per animal after 10 minutes, 1 and 3 hours of ZIKV PE243 (5×10^5 FFU) injection in the
942 footpad. (B) Flow cytometry plots depicting the frequency of CD11b⁺Ly6C/G⁺ polymorphonuclear
943 leukocytes (PMN) and CD8⁺CD3⁺ lymphocytes population in the total blood of C57BL/6 mice
944 treated with PBS or Ly6G (400 µg) i.p. during 18 hours. (C) Frequency of CD11b⁺Ly6C/G⁺ cells in
945 the PMN population in mice treated with PBS or Ly6G. The dashed line indicates the isotype control.
946 The asterisk (*) denotes statistical difference between PBS and Ly6G. Three animals per group were
947 used in each experiment. One of three independent experiments is showed. Bars indicate SEM

948 Supplementary Figure 3. Absence of AXL expression in human neutrophils. AXL fluorescence in
949 neutrophils (first line). An isotype control antibody was used as a negative fluorescence control and
950 A549 cells as a positive control (second line). One representative of two independent experiments is
951 showed.

952 Supplementary Figure 4. A prolonged ZIKV stimulation does not impact the viability, surface
953 receptors expression, and intracellular reactive oxygen species production in human neutrophils.
954 Contour plots depicting the frequency of annexin V⁺ and 7-AAD⁺ neutrophils (A), CD16⁺CD11b⁺
955 and CD11b fluorescence intensity (B), and Chloromethyl-H₂DCFDA⁺ (C) after 6 hours of constant
956 stimulation with mock, LPS (100 ng/mL) or PMA (16 nM) and ZIKV PE243 (1 MOI). Mock-
957 unstained condition or the isotype control were used as negative control to set the gates. ZIKV PE243
958 is showed as a representative of the ZIKV strains's effects. One representative of two independent
959 experiments is showed.

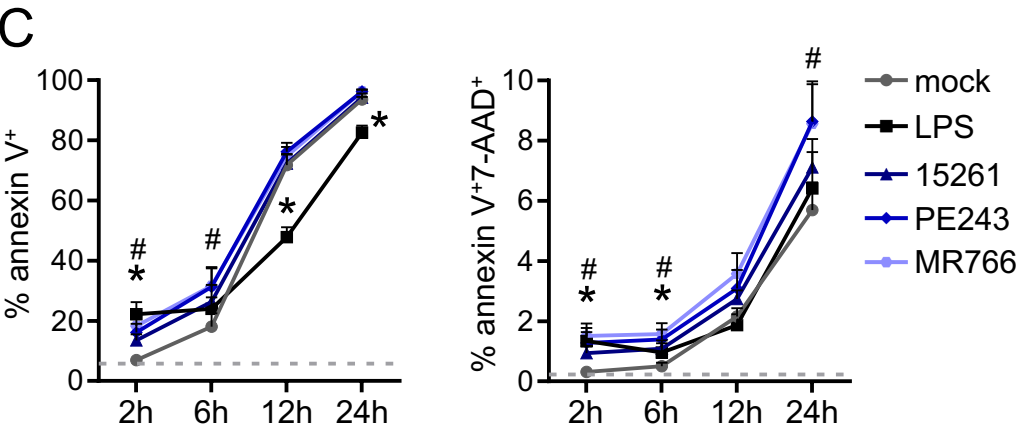
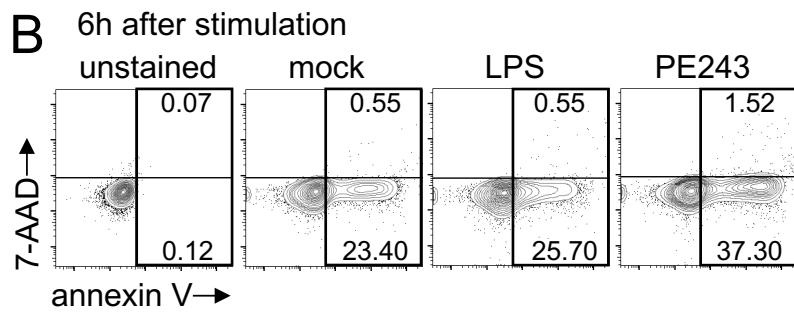
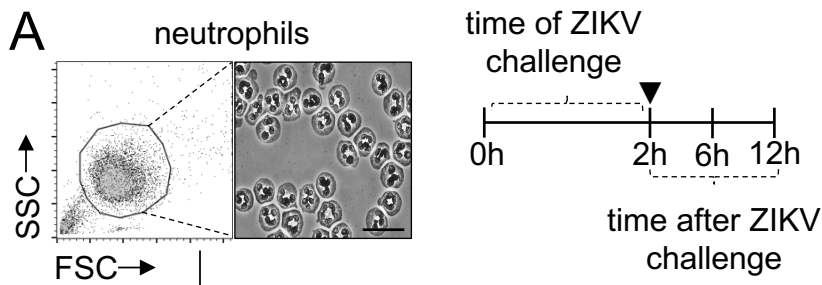


FIGURE 1

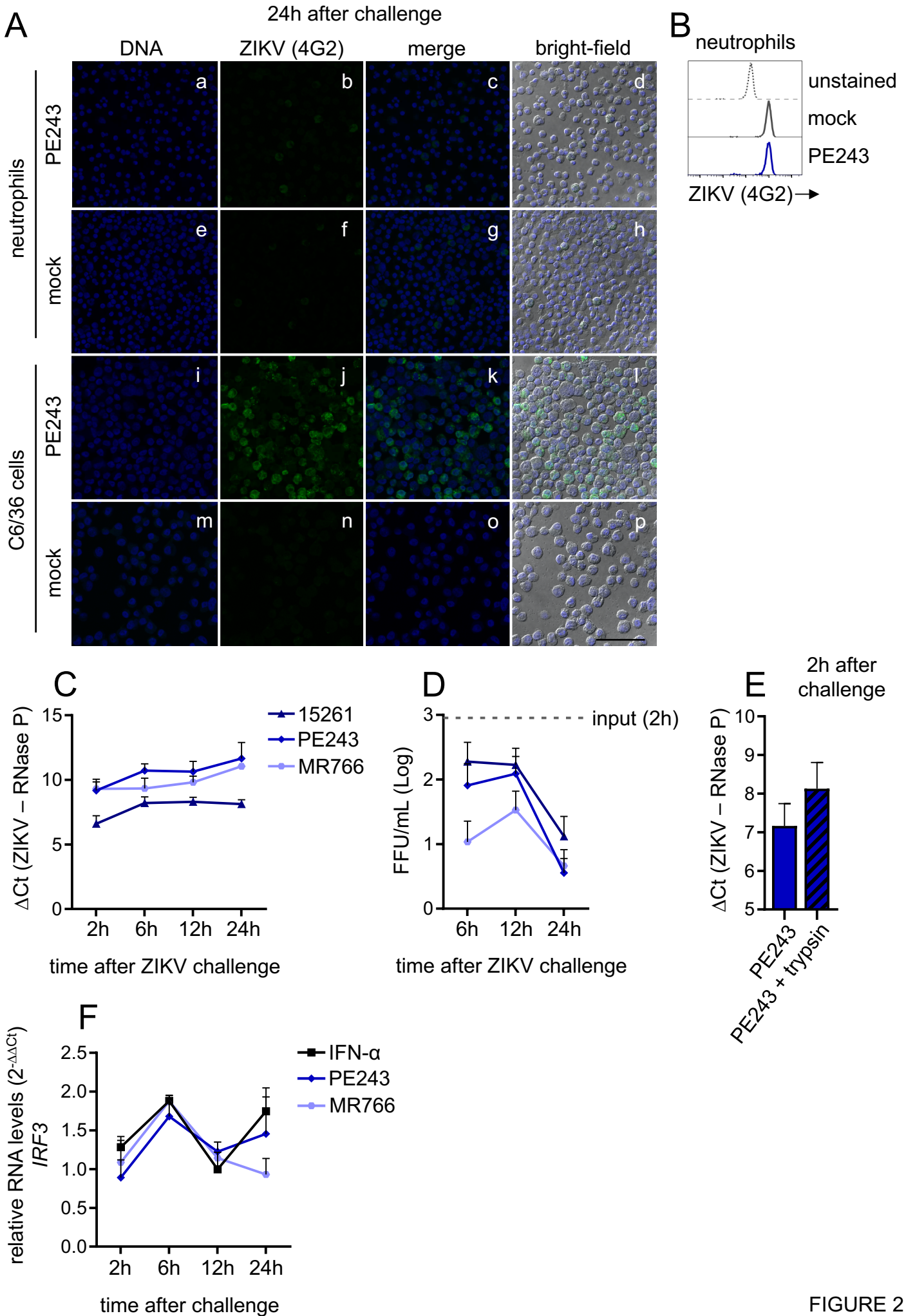


FIGURE 2

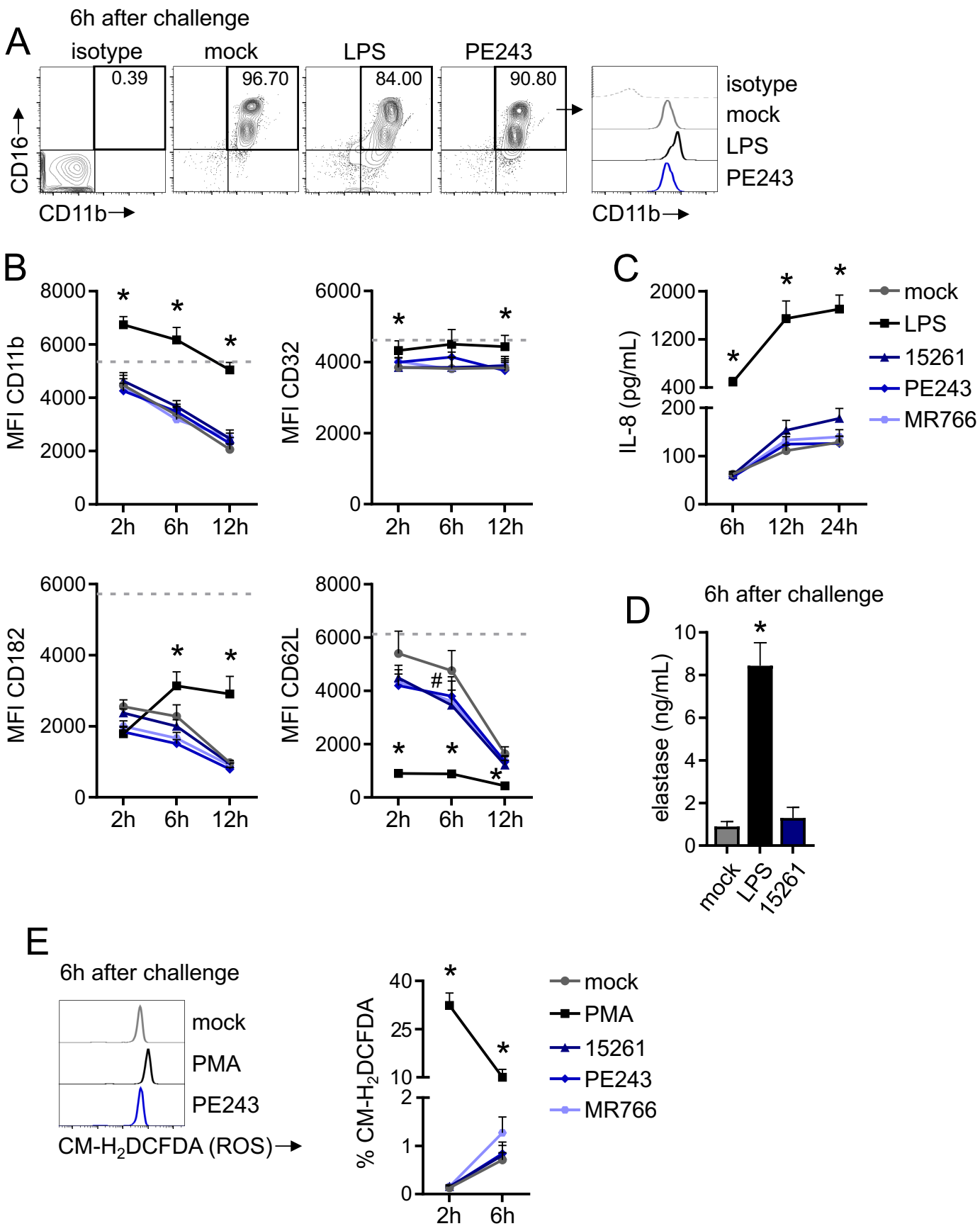


FIGURE 3

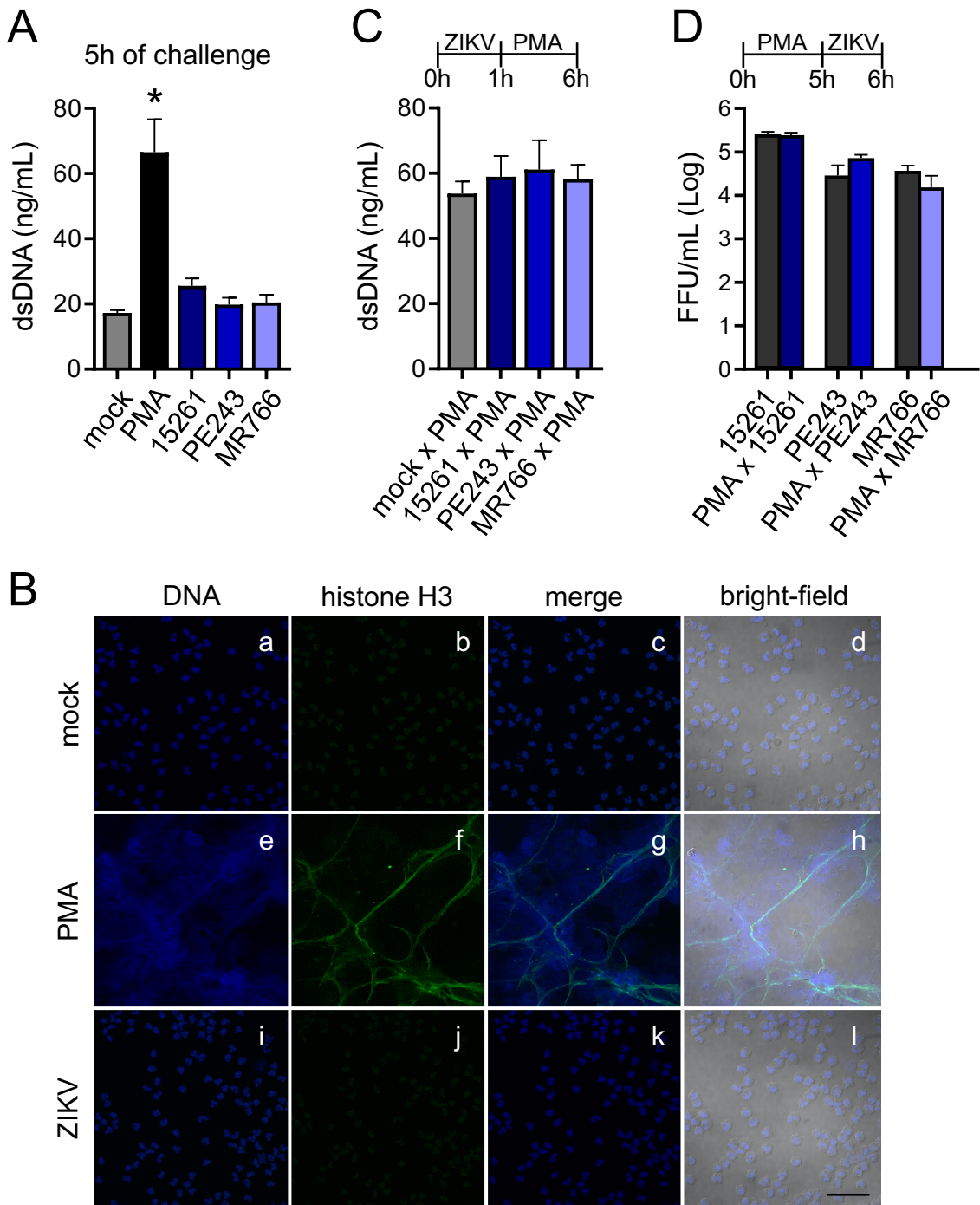


FIGURE 4

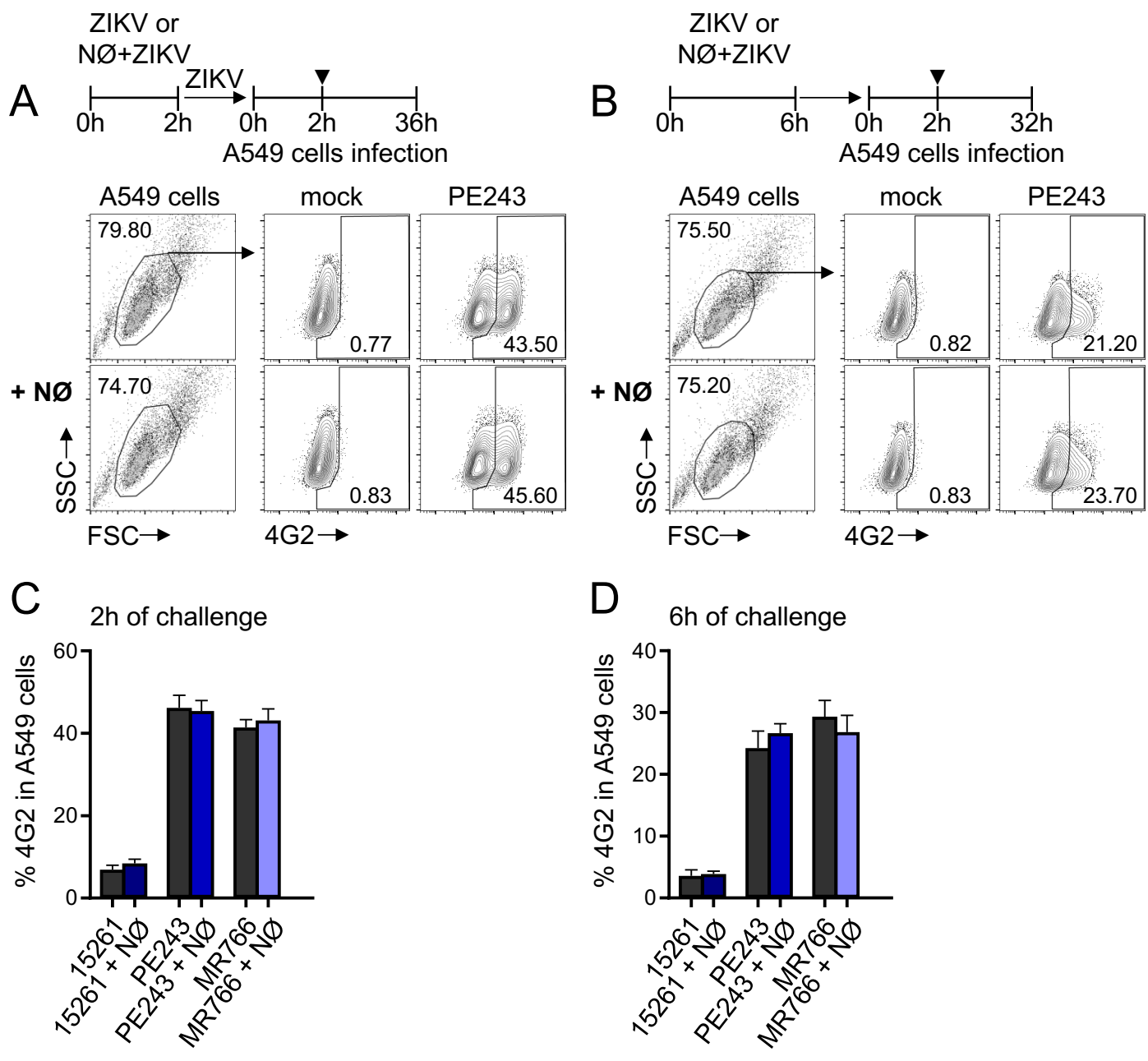


FIGURE 5

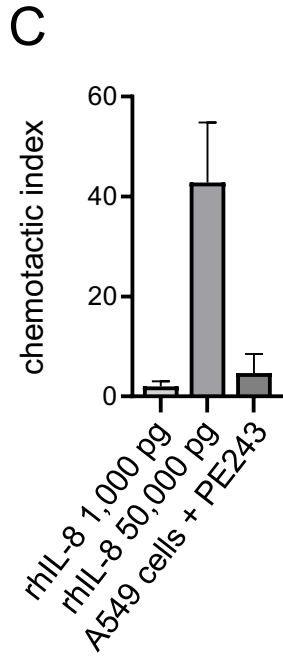
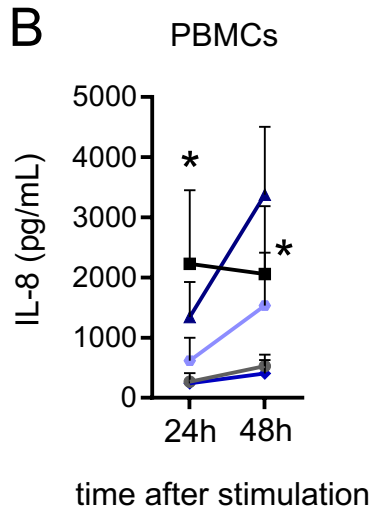
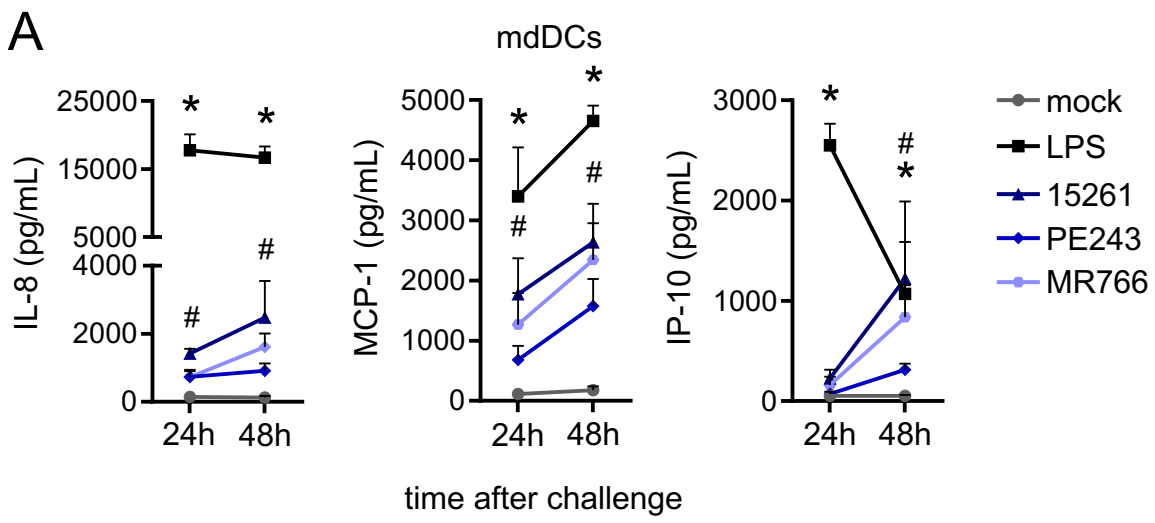
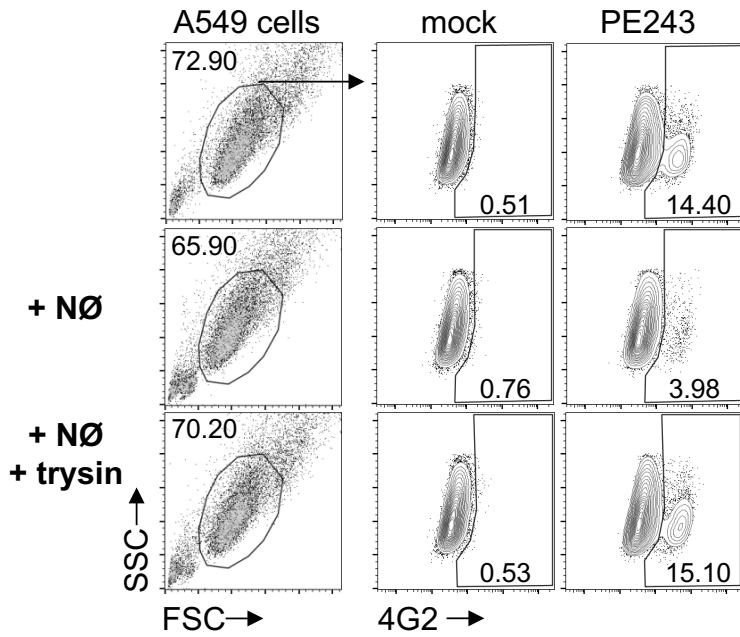


FIGURE 6

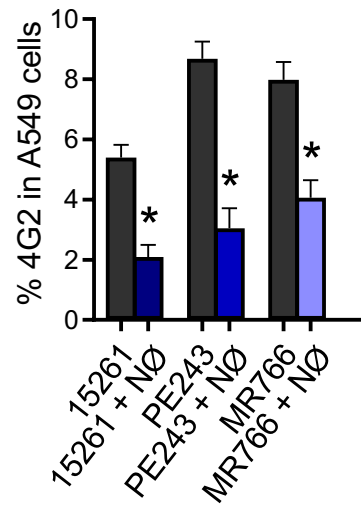
A neutrophil addition:
during ZIKV infection
in A549 cells

0h 2h 16h

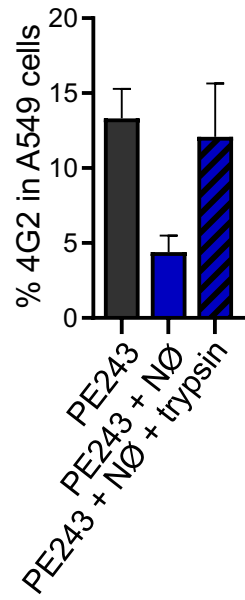
NØ+
ZIKV ▼



C



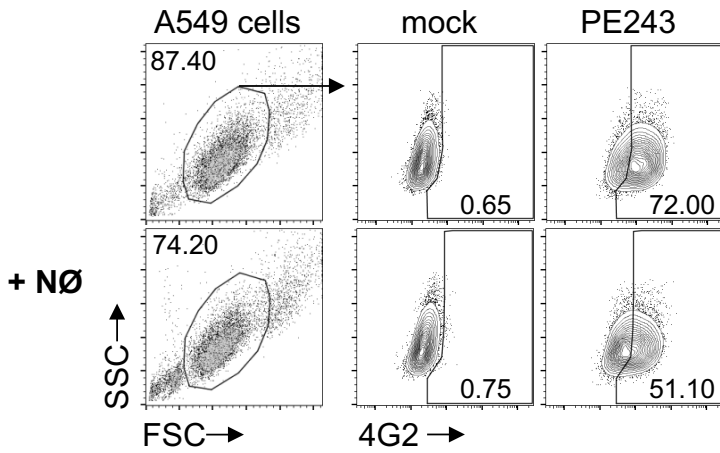
E



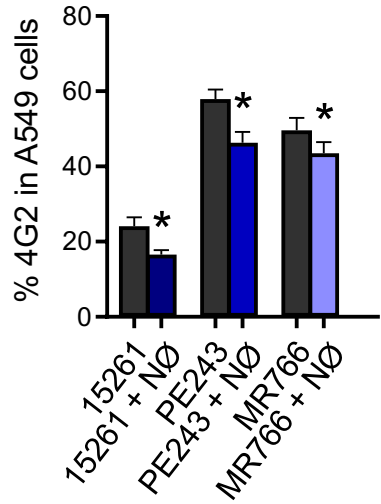
B 24h after ZIKV infection
in A549 cells

0h 2h 24h 40h

ZIKV ▼ NØ



D



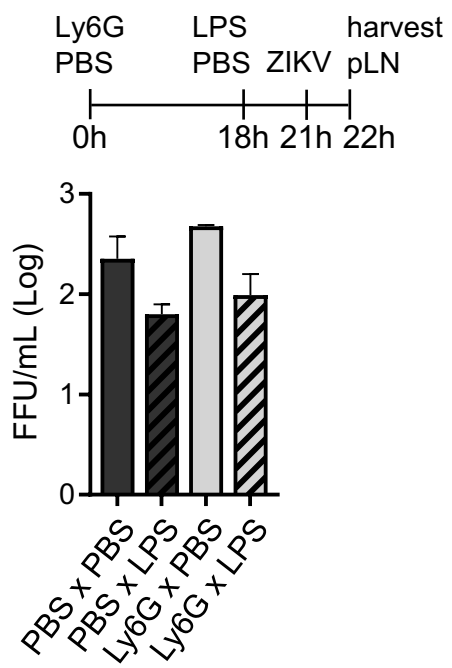
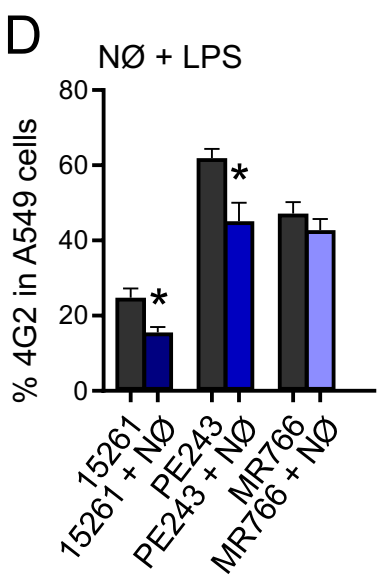
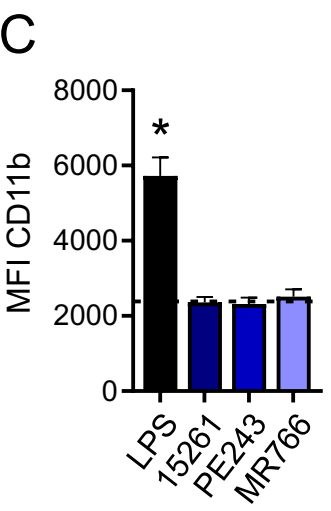
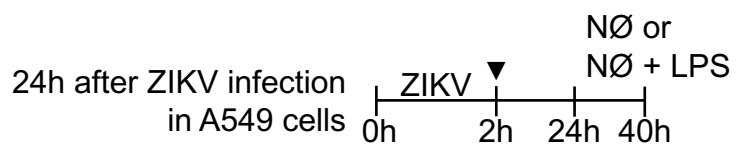
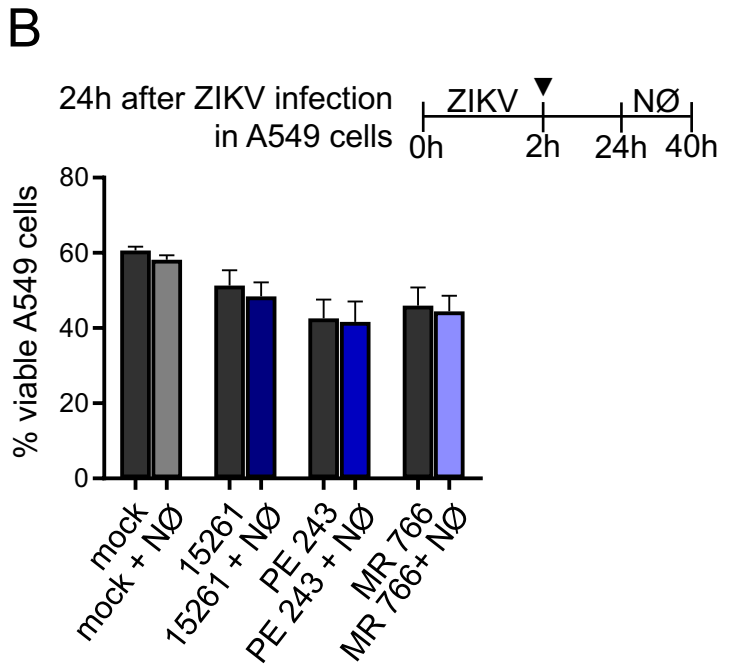
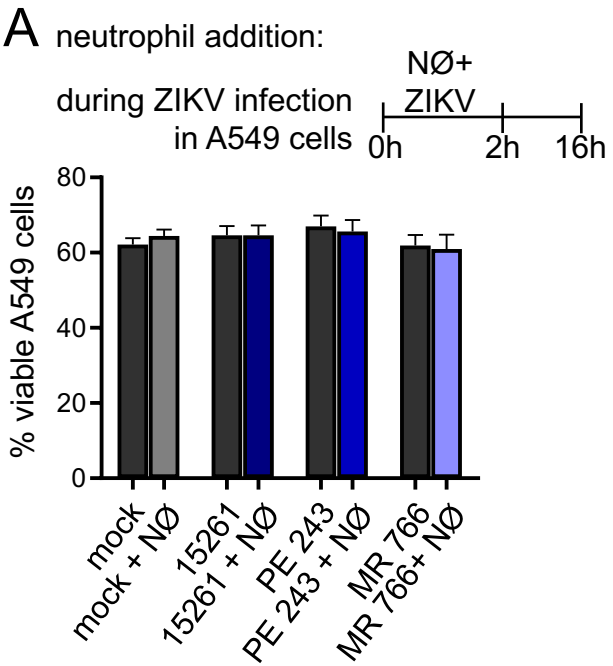
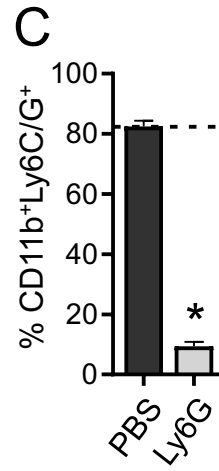
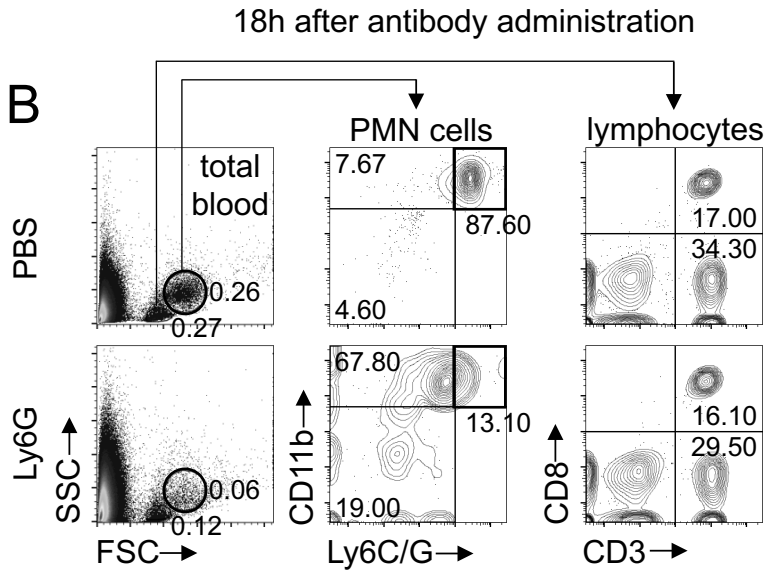
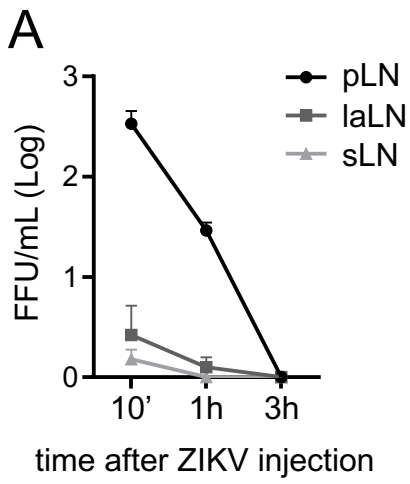
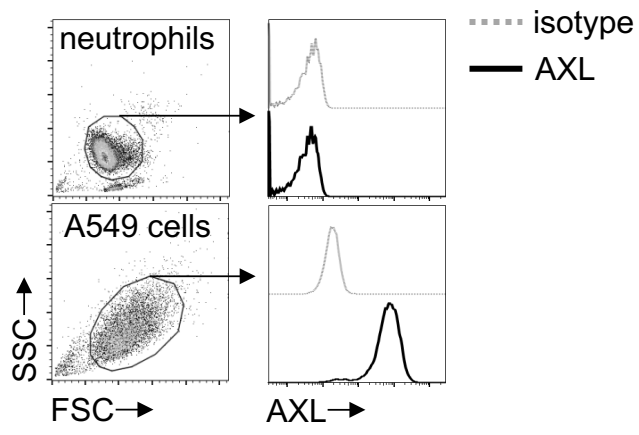
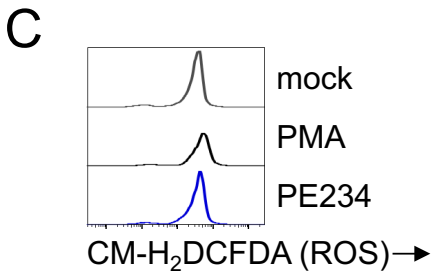
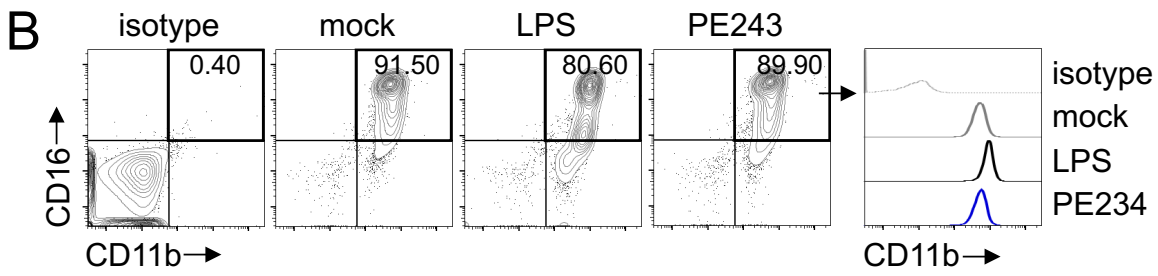
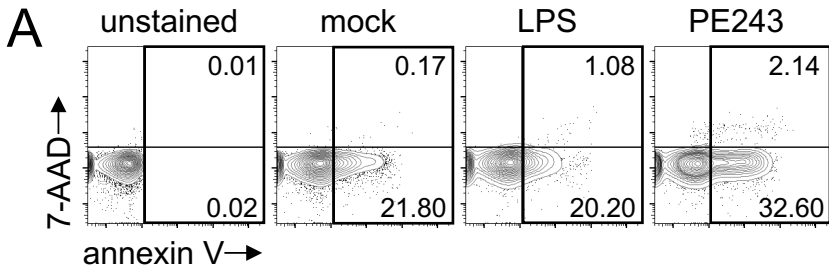
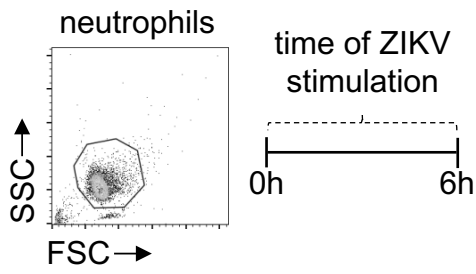


FIGURE 8









3.2 CHAPTER 2. Cellular migration to the draining lymph nodes in viral infection

3.2.1 Vaccinia virus infection inhibits skin dendritic cell migration to draining lymph nodes (paper)

The data from this section was published in The Journal of Immunology (impact factor: 4.886 (2019)/ Qualis: A1), on February of 2021: doi: [10.4049/jimmunol.2000928](https://doi.org/10.4049/jimmunol.2000928). Most of that paper results are available as a preprint article on Biorxiv platform since February of 2020, doi: [10.1101/2020.02.17.952374](https://doi.org/10.1101/2020.02.17.952374).

Title: Vaccinia Virus Infection Inhibits Skin Dendritic Cell Migration to the Draining Lymph Node

Authors: Juliana Bernardi Aggio, Veronika Krmeská, Brian J. Fergusin, Priscilla Fanini Wowk and Antonio Gigliotti Rothfuchs

Resumo: Há uma escassez de informação sobre a resposta de células dendríticas (DCs) para *vaccinia vírus* (VACV), incluindo a tráfego de DCs para o linfonodo drenante (dLN). Neste estudo, usando um modelo murino de infecção, nós estudamos a migração de DCs da pele em resposta a VACV e a comparamos com a vacina contra tuberculose *Mycobacterium bovis* bacilo Calmette-Guérin (BCG), outra vacina atenuada administrada pela pele. Em contraste com BCG, DCs da pele não se deslocaram para o dLN em resposta a VACV. A infecção com VACV inativada por UV ou *modified VACV Ankara* promoveram o movimento de DCs para o dLN, indicando que a interferência em DCs da pele requer VACV competente em replicação. Este efeito supressivo de VACV foi capaz de mitigar respostas para um segundo desafio com BCG na pele, abalando a migração de DCs, reduzindo o transporte de BCG, e retardando a ativação de linfócitos CD4 no dLN. A expressão de mediadores inflamatórios associados com a migração de DCs desencadeada por BCG estavam ausentes na pele infectada com o vírus, sugerindo que outra via de sinalização provoca o movimento de DCs em resposta a VACV deficientes para replicação. Apesar da forte supressão da migração de DCs, VACV foi detectada cedo no dLN e ativou linfócitos CD4 antígeno específicos. Eu resumo, VACV bloqueia a mobilização de DCs da pele do local de infecção, mas retém a habilidade de acessar o dLN e ativar linfócitos CD4.

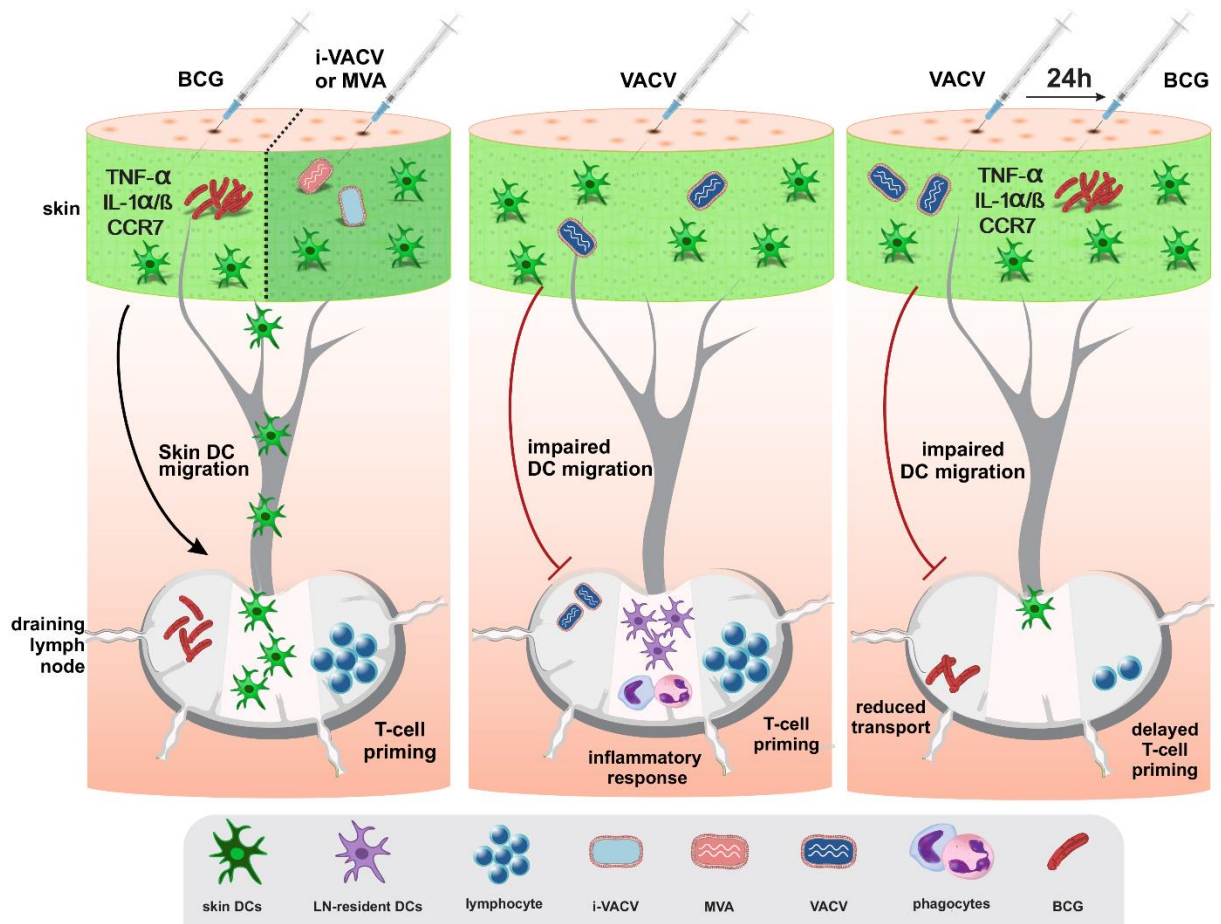


Figure 4. Graphical abstract of the publication *Vaccinia virus infection inhibits skin dendritic cell migration to draining lymph node.*

Vaccinia Virus Infection Inhibits Skin Dendritic Cell Migration to the Draining Lymph Node

Juliana Bernardi Aggio,^{*,†} Veronika Krmeská,^{*} Brian J. Ferguson,[‡] Priscilla Fanini Wowk,^{*,†} and Antonio Gigliotti Rothfuchs^{*}

There is a paucity of information on dendritic cell (DC) responses to vaccinia virus (VACV), including the traffic of DCs to the draining lymph node (dLN). In this study, using a mouse model of infection, we studied skin DC migration in response to VACV and compared it with the tuberculosis vaccine *Mycobacterium bovis* bacille Calmette–Guérin (BCG), another live attenuated vaccine administered via the skin. In stark contrast to BCG, skin DCs did not relocate to the dLN in response to VACV. Infection with UV-inactivated VACV or modified VACV Ankara promoted DC movement to the dLN, indicating that interference with skin DC migration requires replication-competent VACV. This suppressive effect of VACV was capable of mitigating responses to a secondary challenge with BCG in the skin, ablating DC migration, reducing BCG transport, and delaying CD4⁺ T cell priming in the dLN. Expression of inflammatory mediators associated with BCG-triggered DC migration were absent from virus-injected skin, suggesting that other pathways invoke DC movement in response to replication-deficient VACV. Despite adamant suppression of DC migration, VACV was still detected early in the dLN and primed Ag-specific CD4⁺ T cells. In summary, VACV blocks skin DC mobilization from the site of infection while retaining the ability to access the dLN to prime CD4⁺ T cells. *The Journal of Immunology*, 2021, 206: 000–000.

Dendritic cells (DCs) excel in their capacity to capture, transport, and present microbial Ag to prime naive T cells in secondary lymphoid organs (1). The lymph node (LN) is a major site for such Ag presentation, which is often preceded by the relocation of DCs from the site of infection in the periphery to the draining LN (dLN) (2). Despite a large body of data on immunizations with model Ags, DC migration remains incompletely understood during infection with pathogens and live attenuated bacterial or viral vaccines. Using an infection model in mice and a novel assay to track DC migration in vivo, we have previously identified a role for IL-1R signaling in mobilizing skin DCs to the dLN in response to *Mycobacterium bovis* bacille

Calmette–Guérin (BCG), the live attenuated tuberculosis vaccine (3). We found that the population of migratory EpCAM^{low} CD11b^{high} skin DCs were important for the transport of BCG from its inoculation site in the skin to the dLN and, in doing so, for priming mycobacteria-specific CD4⁺ T cells in the dLN (3).

Similar to BCG, the smallpox vaccine vaccinia virus (VACV) is a live attenuated microorganism administered via the skin. Despite many studies on the immune response to poxviruses and countless investigations on antiviral T cell priming, there is a knowledge gap on the initial immunological events that unfold in vivo in response to VACV. Because of its large genome and replication cycle features, VACV is readily used as an expression vector and live recombinant vaccine for infectious diseases and cancer (4–7). Because BCG efficacy is suboptimal, there is a standing need to improve tuberculosis vaccination. Recombinant BCG strains as well as novel vaccine candidates are considered or have been developed, some of which are currently undergoing clinical trials. These efforts include attenuated or recombinant VACV vectors and, in fact, modified VACV Ankara (MVA) expressing *Mycobacterium tuberculosis* Ag85A is an example of a clinically advanced vaccine candidate (8).

Following inoculation of VACV in the skin, infected cells, including DCs and macrophages, can be detected in the dLN within a few hours (9–12). It is not entirely clear if this rapid relocation of virus from skin to the dLN occurs through direct viral access to lymphatic vessels, as also observed after skin infection with Zika virus (12), or if it is supported by other mechanisms. In contrast, other studies indicate that VACV is largely restricted to its inoculation site in the skin, with limited or no relocation of virus to the dLN (13, 14). In this regard, VACV can interfere with fluid transport in lymphatic vessels and, as such, can curb its dissemination (15). In addition to data on viral traffic to the dLN, there is substantive literature on immune evasion and immunosuppression mediated by VACV in vitro and in models of infection (16). Using an established toolset and mouse model for investigating DC responses to mycobacteria we compared local BCG-triggered inflammatory responses in the skin and skin dLN with that of VACV

*Department of Microbiology, Tumor and Cell Biology, Karolinska Institutet, SE-171 77 Stockholm, Sweden; †Instituto Carlos Chagas, FIOCRUZ, Curitiba PR 81310-020, Brazil; and ‡Department of Pathology, University of Cambridge, Cambridge CB2 1QP, United Kingdom

ORCID: 0000-0001-8094-6266 (V.K.); 0000-0002-6873-1032 (B.J.F.); 0000-0002-8976-2647 (P.F.W.); 0000-0001-6001-7240 (A.G.R.).

Received for publication August 6, 2020. Accepted for publication December 8, 2020.

This work was supported by the Swedish Research Council and Karolinska Institutet, Sweden (both to A.G.R.), Instituto Carlos Chagas, FIOCRUZ, Brazil (to P.F.W.), Coordenação de Aperfeiçoamento de Pessoal de Nível Superior, Brazil (to J.B.A. and P.F.W.), and UK Research and Innovation, Biotechnology and Biological Sciences Research Council Grant RG94719 (to B.J.F.). The funders had no role in study design, data collection and interpretation, or the decision to submit the work for publication.

Address correspondence and reprint requests to Dr. Antonio Gigliotti Rothfuchs, Department of Microbiology, Tumor and Cell Biology, Karolinska Institutet, Biomedicum, Solnavägen 9, SE-171 77 Stockholm, Sweden. E-mail address: antonio.rothfuchs@ki.se

The online version of this article contains supplemental material.

Abbreviations used in this article: BCG, bacille Calmette–Guérin; DC, dendritic cell; dLN, draining LN; FFU, focus-forming unit; i-VACV, VACV inactivated with UV radiation; LN, lymph node; MVA, modified VACV Ankara; pLN, popliteal LN; rVACV-Ag85B, recombinant VACV expressing mycobacterial Ag85B; SCS, subcapsular sinus; Tg, transgenic; VACV, vaccinia virus; WR, Western Reserve.

This article is distributed under the terms of the [CC BY 4.0 Unported license](https://creativecommons.org/licenses/by/4.0/).

Copyright © 2021 The Authors

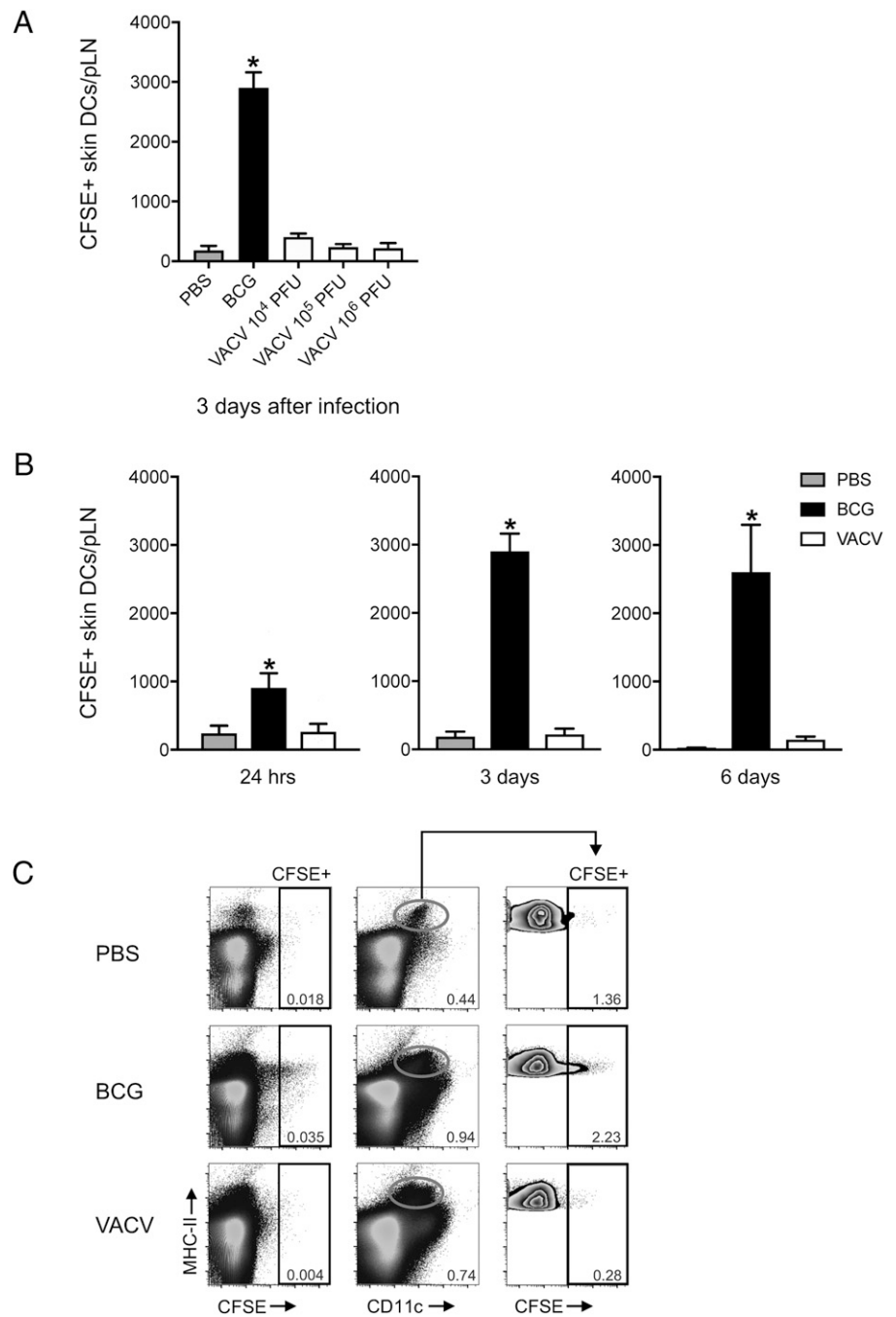


FIGURE 1. Skin DCs migrate to the dLN in response to BCG but not VACV. C57BL/6 mice were inoculated in the footpad skin with PBS, BCG, or VACV and subjected to the CFSE migration assay (3, 25). Single-cell suspensions were generated from the dLN and pLN and analyzed by flow cytometry. **(A)** Total number of CFSE-labeled skin DCs (MHC-II^{high} CD11c^{+/low}) in the pLN 3 d postinfection with 1×10^6 CFUs of BCG or given doses of VACV. **(B)** Total number CFSE-labeled skin DCs in the pLN at the given time points after footpad infection with BCG (1×10^6 CFUs) or VACV (1×10^6 PFUs). **(C)** Concatenated FACS plots showing CFSE-labeled cells from pLN 3 d after PBS, BCG (1×10^6 CFUs), or VACV (1×10^6 PFUs). Representation of CFSE-labeled cells relative to MHC-II (left plots). Skin DCs were gated (center plots), and CFSE-labeled cells are shown (right plots). Four to five animals per time point and group were used in each experiment. One of two independent experiments is shown. Bars indicate SEM. The asterisk (*) denotes statistical difference between PBS and BCG.

and focused on the ability of VACV to mobilize skin DCs to the dLN. Unlike the early reaction to BCG, we found that VACV actively inhibits skin DC migration to the dLN but retains the ability to enter the dLN in the absence of DC transport and prime CD4⁺ T cells therein.

Materials and Methods

Mice

C57BL/6NRj mice were purchased from JANVIER LABS (Le Genest-Saint-Isle, France) and used as wild-type controls. P25 TCR transgenic (Tg) RAG-1^{-/-} mice expressing EGFP (17) were kindly provided by Dr. R. Germain (National Institute of Allergy and Infectious Diseases, National Institutes of Health). Animals were maintained at the Department of Comparative Medicine, Karolinska Institutet. Both male and female mice between 8 and 12 wk old were used. Animals were housed and handled at the Department of Comparative Medicine according to the directives and

guidelines of the Swedish Board of Agriculture, the Swedish Animal Protection Agency, and Karolinska Institutet. Experiments were approved by the Stockholm North Animal Ethics Council.

Mycobacteria

M. bovis BCG strain Pasteur 1173P2 was expanded in Middlebrook 7H9 broth supplemented with ADC (BD Biosciences) as previously described (18). Quantification of mycobacterial CFUs for bacterial stocks and determination of bacterial load in LNs was performed by culture on 7H11 agar supplemented with OADC (BD Biosciences).

Vaccinia virus

VACV Western Reserve (WR) and deletion mutants Δ A49 (19), Δ B13 (20), and Δ B15 (21) (kindly provided by Prof. G. Smith, Cambridge University, Cambridge, U.K.) were expanded on BSC-1 cells. MVA was expanded in BHK-21. Viral stocks were purified by saccharose gradient ultracentrifugation. Quantification of PFUs from WR and focus-forming units (FFUs) from MVA was performed as previously described (22) with MVA stocks

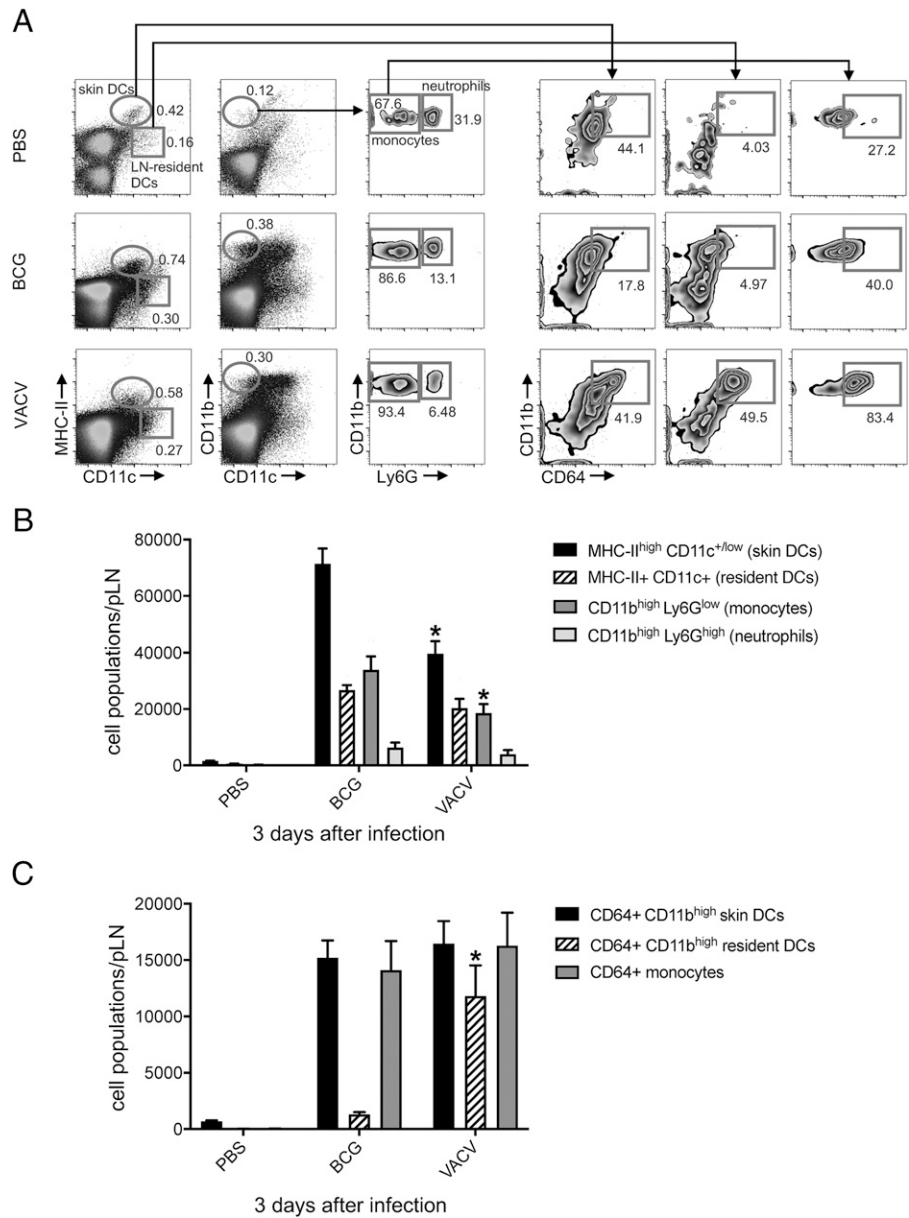


FIGURE 2. Expansion of phagocyte populations in the dLN after BCG and VACV infection in the skin. C57BL/6 mice were inoculated in the footpad skin with PBS, BCG (1×10^6 CFUs), or VACV (1×10^6 PFUs). Three days later, single-cell suspensions were obtained from the pLN and analyzed by flow cytometry. **(A)** Representative FACS plots showing frequency of different phagocyte populations in each group. **(B and C)** Graph showing total numbers for populations in **(A)**. Five animals per group were used in each experiment. Bars indicate SEM. The asterisk (*) denotes statistical significance between BCG and VACV groups **(B and C)**. BCG and VACV populations in **(B)** and **(C)** are statistically significant from PBS controls.

quantified in chicken embryo fibroblasts cells, and WR stocks or WR viral load in LNs were quantified on BSC-1. In some experiments, VACV was inactivated with UV radiation (i-VACV) by placing the virus for 2 min in a UV Stratalinker 2400 equipped with 365-nm long-wave UV bulbs (StrataGene). UV inactivation was confirmed by lack of cytopathic effect on BSC-1 cells infected with i-VACV for up to 3 d (data not shown).

Recombinant VACV expressing mycobacterial Ag85B (rVACV-Ag85B) was constructed using the transient dominant selection method (23, 24). Briefly, a cassette containing Ag85B from *M. tuberculosis* (BEI Resources, Manassas, VA) was cloned in a pUC13 plasmid containing the *Escherichia coli* guanylylphosphoribosyl transferase (Ecogtp) gene fused in-frame with the EGFP gene under the control of the VACV 7.5k promoter. The correct insertion was confirmed by restriction enzyme digestion and Sanger sequencing. CV-1 cells were infected with WR VACV at a multiplicity of infection of 0.1 PFUs and transfected with the constructed plasmid using TransIT-LT1 in a 2:1 ratio. Progeny virus was harvested after 72 h and used to infect BSC-1 cells in the presence of mycophenolic acid (25 μ g/ml), hypoxanthine (15 μ g/ml), and xanthine (250 μ g/ml). EGFP-positive plaques were selected and purified by three rounds of dilution-infection using BSC-1 cells in the presence of the drugs, as above. Intermediate virus was resolved in BSC-1 cells by three rounds of dilution-infection in the absence of the drugs. The genotype of resolved virus was confirmed to express Ag85B by Sanger sequencing and PCR following proteinase K treatment of infected BSC-1 cells using primers that anneal to the flanking

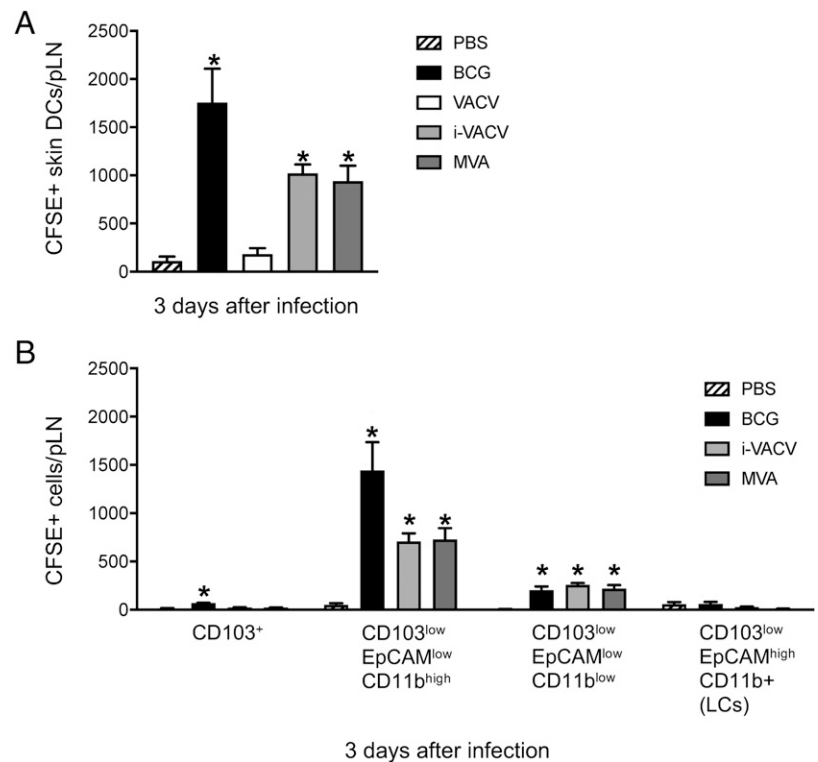
regions of the Ag85B fragment. rVACV-Ag85B was amplified, purified, and quantified in BSC-1, as described above.

Inoculation of mice

Animals were inoculated in the hind footpad with 30 μ l of PBS containing (unless otherwise stated) 1×10^6 CFUs of BCG, 1×10^6 PFUs of VACV, or 1×10^6 FFUs of MVA. i-VACV was used at an amount equivalent to 1×10^6 PFUs before UV-inactivation. Control animals received 30 μ l of PBS only. For footpad conditioning experiments, animals were injected in the footpad with PBS, VACV, or i-VACV 24 h before receiving BCG into the same footpad. For studying gene expression in the skin, mice were inoculated in the ear dermis with 5 μ l of PBS containing the same concentration of mycobacteria or virus as above. Control animals received 5 μ l of PBS.

Assessment of cell migration from the footpad skin to the dLN was done as previously described (3, 25). Briefly, animals previously injected with vaccine or PBS were injected 24 h before sacrifice in the same footpad with 30 μ l of 0.5 mM CFSE (Invitrogen). For assessing migration after 24 h, CFSE was injected 2 h after vaccine or PBS inoculation. In control experiments, migration was assessed in response to 1×10^5 PFUs of HSV-1 strain 17 or 100 μ g of zymosan (InvivoGen). For studying CD4⁺ Ag-specific T cell responses, 1×10^5 LN cells from naive P25 TCRTg RAG-1^{-/-} EGFP mice were injected i.v. in the tail vein of C57BL/6 recipients in a final volume of 200 μ l. Recipients were infected 24 h later in the footpad with 30 μ l of BCG or virus. Control animals received PBS. In footpad conditioning experiments, recipients received naive T cells as above and were injected in

FIGURE 3. Skin DCs migrate to dLN in response to i-VACV and MVA. C57BL/6 mice were inoculated in the footpad skin with PBS, BCG (1×10^6 CFUs), VACV (1×10^6 PFUs), i-VACV (equivalent to 1×10^6 PFUs before inactivation), or MVA (1×10^6 FFUs) and subjected to CFSE migration assay as in Fig. 1. dLN and pLNs were analyzed by flow cytometry 3 d postinfection. **(A)** Total number of CFSE-labeled skin DCs is shown. **(B)** CFSE expression within defined subsets of skin DCs based on previously published gating strategy (3, 25) are shown. Four to five animals per group were used in each experiment. One of two independent experiments is shown. Bars indicate SEM. The asterisk (*) denotes statistical significance between PBS- and vaccine-injected groups. LCs, Langerhans cells.



the footpad 2 h later with PBS, VACV, or i-VACV. BCG was given the next day, and animals were sacrificed 3 and 6 d after BCG, respectively.

Generation of single-cell suspensions from tissue

Popliteal LNs (pLNs) were aseptically removed, transferred to microcentrifuge tubes containing FACS buffer (5 mM EDTA and 2% FBS in PBS), and gently homogenized using a tissue grinder. The resulting single-cell suspension was counted by trypan blue exclusion. In certain experiments, an aliquot was taken and subjected to CFU or PFU determinations as described above. LN suspensions were otherwise washed in FACS buffer and stained for flow cytometry. Ears were excised, transferred into TRIzol reagent (Sigma-Aldrich), and homogenized in a TissueLyser (QIAGEN) for subsequent RNA extraction, as explained below.

Flow cytometric staining

Single-cell suspensions from pLN were incubated with various combinations of fluorochrome-conjugated rat anti-mouse mAbs specific for CD4 (L3T4), CD11b (M1/70), CD11c (HL3), MHC-II I-A/I-E (M5/114.15.2), Ly-6G (1A8), Vβ11 (RR3-15) (BD Biosciences), CD326/EpCAM (G8.8), CD103 (2E7) (BioLegend), CD64 (X54-5/7), and CD4 (RM4-5) (eBiosciences) for 45 min at 4°C in FACS buffer containing 0.5 mg/ml anti-mouse CD16/CD23 (2.4G2) (BD Biosciences). Flow cytometry was performed on an LSR II with BD FACSDiva software (BD Biosciences). The acquired data were analyzed on FlowJo software (BD Biosciences).

Real-time TaqMan PCR

RNA was extracted from ear homogenates and reverse transcribed into cDNA using M-MLV Reverse Transcriptase (Promega). Real-time PCR was performed on an Applied Biosystems PRISM 7500 Sequence Detection System (Applied Biosystems) using commercially available primer pairs and TaqMan probes for TNF-α, IL-1α, IL-1β, CCR7, and GAPDH (Thermo Fisher Scientific). The relative expression of the above factors was determined by the $2^{-\Delta\Delta C_t}$ method, in which samples were normalized to GAPDH and expressed as fold change over uninfected, PBS-injected controls.

Statistical analyses

The significance of differences in data group means was analyzed by Student *t* test or ANOVA where appropriate, using GraphPad Prism 8 (GraphPad Software) or JMP (SAS Institute), with a cutoff of $p < 0.05$. In some experiments, outliers were excluded from analysis following Grubbs test for outliers (GraphPad).

Results

Skin DCs migrate to dLN in response to BCG but not VACV

To investigate DC migration in response to VACV, we inoculated the virus in the footpad skin of C57BL/6 wild-type mice and used a CFSE fluorochrome-based migration assay to track the movement of skin DCs to the dLN and pLN (3, 25). We have used this setup in the past to study early responses to BCG, another live attenuated vaccine given via the skin and so included BCG in this study as a comparison with VACV. In line with our previous results (3), BCG footpad infection triggered migration of skin DCs to the dLN. However, in stark contrast to BCG, skin DCs did not relocate to the dLN in response to VACV (Fig. 1). The lack of DC movement in response to VACV was independent of viral inoculation dose (Fig. 1A) and the time point at which DC migration was investigated (Fig. 1B). Interestingly, the absence of CFSE labeling in skin DCs in the dLN of VACV-infected mice was not concurrent with CFSE labeling in other MHC class II (MHC-II)⁺ cells or even in MHC-II-negative populations, suggesting a generalized absence of cells moving from skin to the dLN in response to the virus (Fig. 1C).

Although migratory skin DCs did not readily relocate to the dLN in response to VACV, the infection did provoke a robust inflammatory response in the dLN, expanding several phagocyte populations (Fig. 2A, 2B). The lack of skin DC migration recorded in our CFSE assay was in line with a marked decrease in the overall number of skin DCs (MHC-II^{high} CD11c^{+/low} cells) found in VACV-infected LN, suggesting a major negative impact of virus infection on these cells (Fig. 2B). We also observed high surface expression of CD64 on monocytes and CD11b^{high} LN-resident DCs in the VACV-infected group (Fig. 2A), in which CD11b^{high} LN-resident DCs expressing CD64 were clearly expanded compared with BCG (Fig. 2A, 2C).

VACV actively inhibits skin DC migration to dLN

Because many of the known immunomodulatory molecules produced by VACV require viral replication, we investigated whether

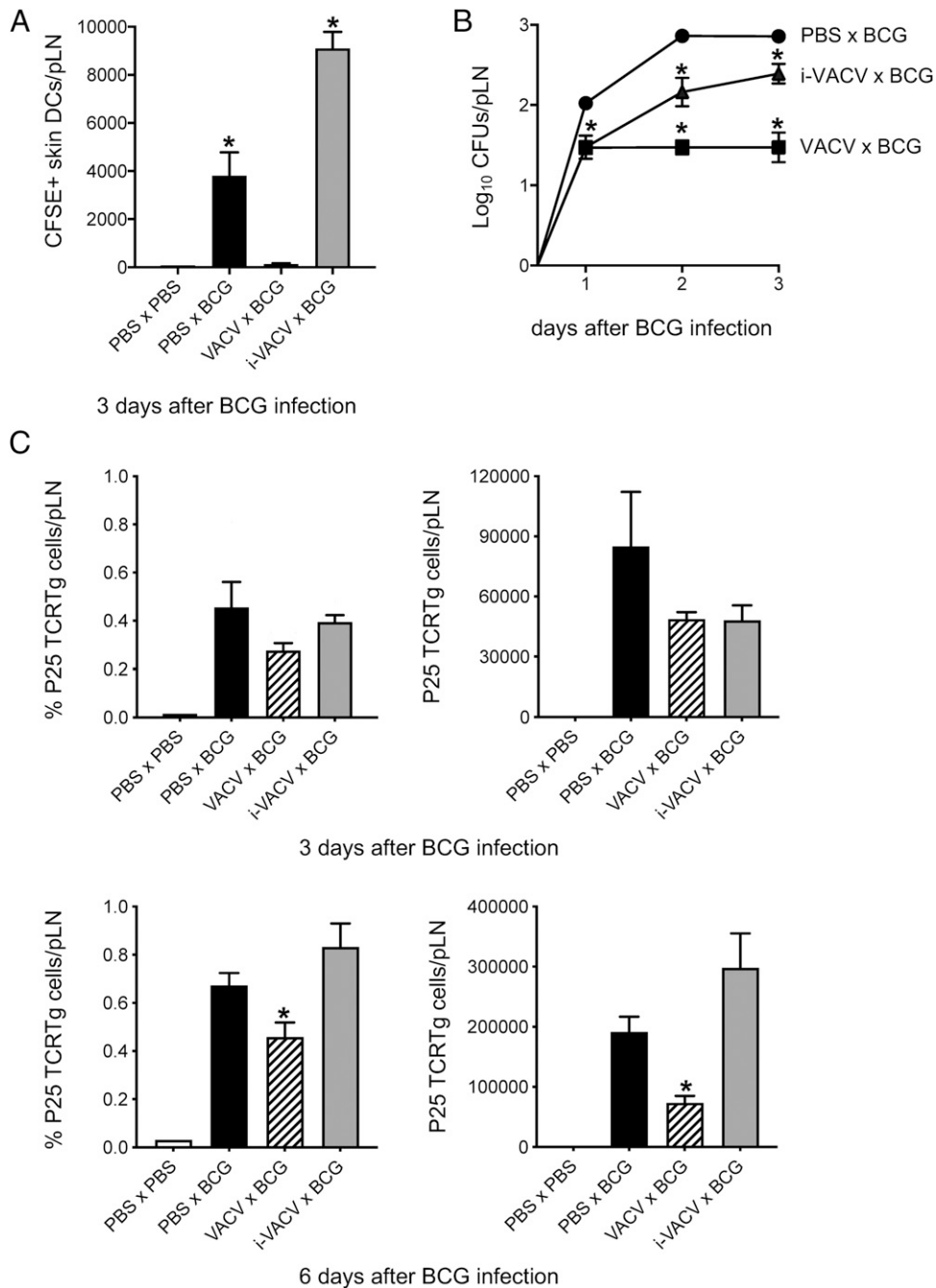


FIGURE 4. Conditioning the BCG injection site in the skin with VACV mutates DC responses to BCG. C57BL/6 mice were inoculated in the footpad skin with PBS, VACV (1×10^6 PFUs), or i-VACV (corresponding to a dose of 1×10^6 PFUs before inactivation). Twenty-four hours later, the same footpads were inoculated with BCG (1×10^6 CFUs), and the CFSE-based migration assay was performed. **(A)** Total number of CFSE-labeled skin DCs in the pLN 3 d after BCG. **(B)** Recovery of BCG CFUs from the pLN after conditioning with VACV. Before giving BCG, footpads were inoculated 24 h earlier with PBS (PBS \times BCG), VACV (VACV \times BCG) or i-VACV (i-VACV \times BCG). **(C)** Frequency and total number of P25 TCRTg cells in the pLN 3 and 6 d after BCG. Naive P25 TCRTg cells were given i.v. to C57BL/6 recipients, which were then conditioned as in (B). Three and 6 d after BCG, pLNs were processed, and P25 TCRTg cells (EGFP⁺ V β 11⁺ CD4⁺) were analyzed by flow cytometry. Five animals per group were used in each experiment. One of two independent experiments is shown. Bars indicate SEM. The asterisk (*) denotes statistical significance between PBS \times PBS controls and vaccine-injected groups (A); between PBS \times BCG and i-VACV \times BCG or VACV \times BCG groups (B); between PBS \times BCG and VACV \times BCG groups (C). Expansion of P25 TCRTg cells is statistically significant in conditioned groups relative to PBS \times PBS controls (C).

the absence of DC migration in response to VACV was coupled to productive infection. We thus exposed VACV to UV cross-linking at levels sufficient to ablate viral replication but without abolishing viral entry into cells (26). Interestingly, inoculation with i-VACV in the footpad promoted skin DC mobilization to the dLN (Fig. 3A). Similarly, skin infection with MVA, a highly attenuated VACV lacking numerous immunomodulators that infects but fails to assemble new

virions in mammalian cells (27), also triggered DC migration to the dLN (Fig. 3A). These results indicate that replication-competent VACV actively blocks skin DC migration. Similar to BCG (3, 28), EpCAM^{low} CD11b^{high} DCs were the main DC subpopulation migrating in response to i-VACV and MVA (Fig. 3B).

Consistent with a potent suppressive effect on skin DC migration, conditioning the footpad with VACV prior to injecting BCG in

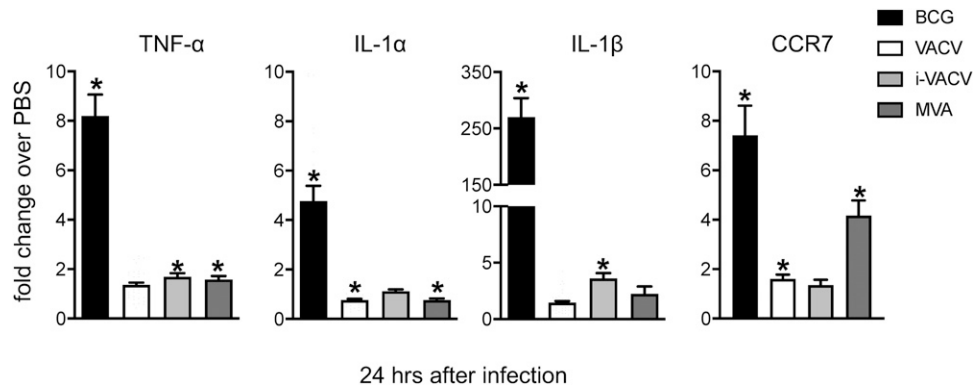


FIGURE 5. Enhanced mRNA expression of proinflammatory mediators associated with BCG-triggered DC migration are absent from virus-infected skin. C57BL/6 mice were inoculated intradermally in the ear with PBS, BCG (1×10^6 CFUs), VACV (1×10^6 PFUs), i-VACV (equivalent to 1×10^6 PFUs before inactivation), or MVA (1×10^6 FFUs). Ears were removed 24 h postinfection and subjected to RNA extraction and cDNA synthesis. The mRNA accumulation of TNF- α , IL-1 α , IL-1 β , and CCR7 relative to GAPDH was determined by real-time TaqMan PCR, and the fold change of infected animals over PBS controls was calculated. Data pooled from three independent experiments (including 15–38 samples per group) are shown. Bars indicate the SEM. The asterisk (*) denotes statistical significance between PBS- and vaccine-injected groups.

the same footpad completely blocked skin DC migration to BCG (Fig. 4A). As expected, the absence of skin DCs entering the dLN was associated with a massive reduction in BCG detected in the dLN (Fig. 4B). DC migration was not impaired when conditioning was done with i-VACV (Fig. 4A). Rather, the number of moving DCs was increased in the i-VACV-conditioned group (Fig. 4A), although BCG entry itself was slightly lower in this group compared with controls conditioned with PBS instead of virus (Fig. 4B). In line with muted DC responses and BCG transport to the dLN, VACV conditioning also delayed the priming of mycobacterial Ag85B-specific P25 TCRTg cells in the dLN (Fig. 4C). Overall, these experiments suggest a carry-over of the DC migration-dampening properties of VACV to a secondary challenge with BCG.

Enhanced mRNA expression of inflammatory mediators associated with BCG-triggered DC migration is absent from the skin of VACV-infected mice

Next, we compared local changes at the site of infection following inoculation with either vaccine. Transcription of the proinflammatory cytokines TNF- α , IL-1 α , and IL-1 β was clearly detected in the skin 24 h after BCG infection (Fig. 5), corroborating our previous data on a role for IL-1R signaling in regulating DC migration to BCG (3). On the contrary, enhanced expression of TNF- α and IL-1 was absent in response to VACV (Fig. 5). Interestingly, the same was also observed in response to i-VACV and MVA (Fig. 5). Furthermore, expression of the LN-homing chemokine receptor CCR7 was high in the skin postinfection with BCG and MVA but not VACV or i-VACV (Fig. 5), suggesting differences between i-VACV and MVA, although both trigger skin DC migration.

VACV is detected early in dLN postinfection in the skin and primes Ag-specific CD4⁺ T cells

Although DC migration was blocked in response to VACV, the virus was detected in the dLN as early as 10 min postinfection in the footpad skin, and levels remained steady over time (Fig. 6A). The kinetics of this response was different and notably faster than the entry of BCG into the dLN (Fig. 6B), which is reliant on DC transport (3). To compare priming of CD4⁺ T cells to VACV and BCG using the same tool, we engineered rVACV-Ag85B, and used P25 TCRTg cells to gauge T cell priming in the dLN after footpad infection. BCG and rVACV-Ag85B but not VACV expanded P25

TCRTg cells in the dLN (Fig. 6C, 6D). This reveals that the amount of VACV that relocates to the dLN in the absence of DC transport is clearly sufficient to expand Ag-specific CD4⁺ T cells in the dLN.

Discussion

VACV infects a variety of cell types in the skin, including keratinocytes and epidermal and dermal DCs (29). The virus is intriguing, given that it carries a diverse immunosuppressive arsenal but remains highly immunogenic. Concurrent with this complexity, the outcome of DC-VACV interactions remains incompletely understood. The fate of the virus and its transport to the dLN for Ag presentation are matters of interest, given that attenuated or recombinant VACV is often considered as a vaccine vector, oncolytic agent, and tool for Ag delivery. We report that VACV profoundly inhibits the ability of skin DCs to mobilize to the dLN. This inhibition is dependent on viral replication and capable of dampening DC migration to a subsequent challenge with BCG. VACV can nevertheless relocate to the dLN in the absence of DC mobilization and prime CD4⁺ T cells. Our study supports recent observations that LN conduits transport VACV to the dLN for T cell priming (12). We also add to a large body of data on the immunosuppressive properties of VACV (16) and extend these to include virus-mediated inhibition of skin DC migration.

VACV can infect DCs but undergoes abortive replication (30–33). That said, VACV infection is known to have many negative effects on DC function. For instance, the virus can inhibit expression of DC costimulatory molecules and cytokines (30, 32, 33). Splenic DCs isolated from VACV-infected mice express less MHC-II and have lower Ag presentation capacity (34). We find lower expression of MHC-II on migratory skin DCs from the dLN of both VACV- and BCG-infected mice (Supplemental Fig. 1A). VACV and MVA can induce apoptosis in DCs (34). Although we did not investigate virus-induced DC death in our studies, the frequency of migratory skin DCs in the dLN of VACV-infected mice was similar to that of PBS-injected controls (Fig. 2A, Supplemental Fig. 1B). This speaks against massive DC death in the skin, which would lower the availability of migratory DCs in the skin and consequently the frequency of these DCs in the dLN. Results from our migration assay point instead to an impediment of skin DC traffic to the dLN during VACV infection.

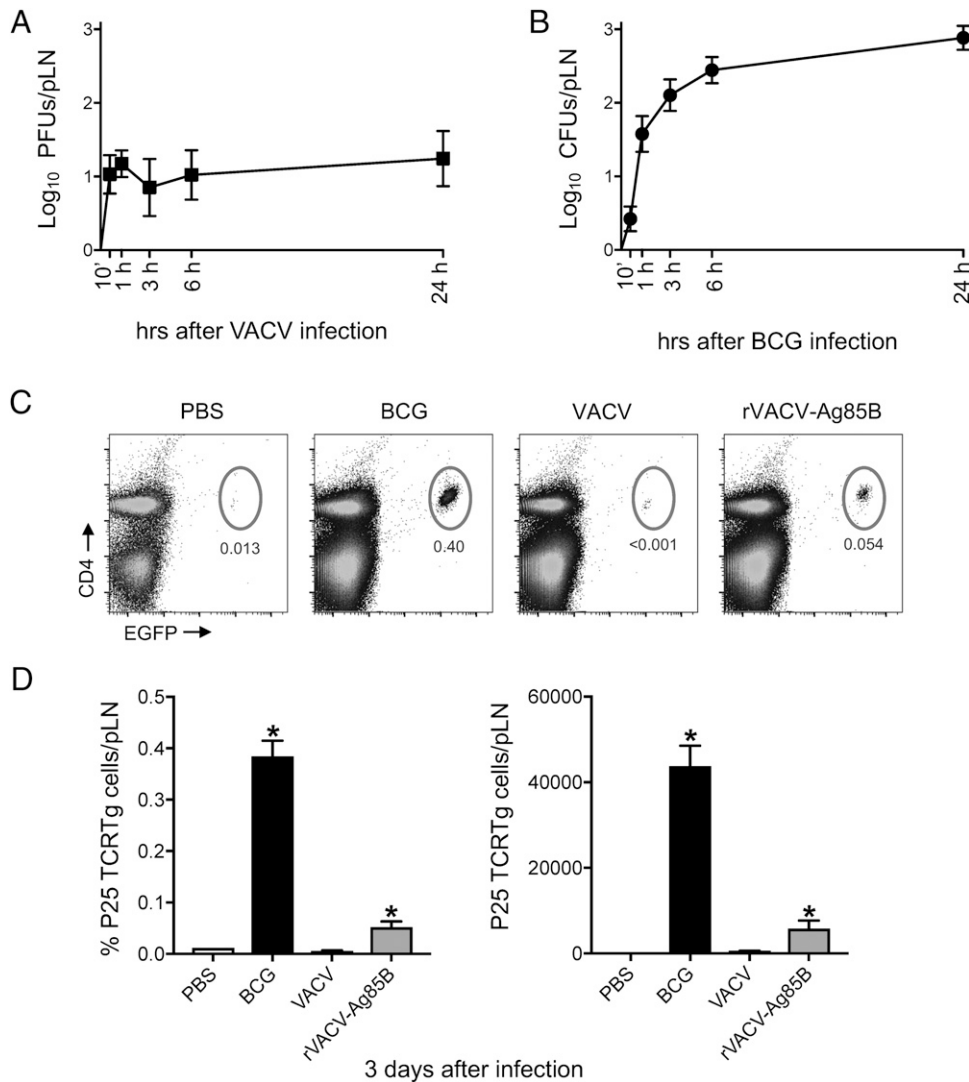


FIGURE 6. VACV is detected early in dLN postinfection in the skin and leads to priming of CD4⁺ T cells. (**A** and **B**) C57BL/6 mice were inoculated in the footpad skin with VACV (1×10^6 PFUs) or BCG (1×10^6 CFUs). Viral (**A**) and mycobacterial (**B**) loads in pLN were determined at different time points postinfection. (**C** and **D**) Frequency of P25 TCRTg cells in pLN after footpad infection with BCG or rVACV-Ag85B. Naive P25 TCRTg cells were given i.v. to C57BL/6 recipients, which were infected 24 h later in the footpad skin with PBS, BCG (1×10^6 CFUs), VACV (1×10^6 PFUs), or rVACV-Ag85B (1×10^6 PFUs). Three days postinfection, pLNs were processed, and P25 TCRTg cells (EGFP⁺ Vβ11⁺ CD4⁺) were analyzed by flow cytometry. Five animals per time point and group were used in each experiment. One of two independent experiments is shown. Bars indicate SEM. The asterisk (*) denotes statistical significance between PBS- and vaccine-injected cohorts.

Both VACV and MVA have previously been shown to inhibit migration of human monocyte-derived DCs toward CCL19 by interfering with CCR7 signaling rather than surface expression of the receptor (35). Although we did not formally investigate this in our model, inhibition of CCR7 signaling by VACV could be a possible explanation for impaired DC migration. Indeed, we observed muted influx of skin DCs and BCG into the dLN when the injection site in the footpad skin was preconditioned with VACV. Thus, the suppressive effect of VACV on DC migration was robust enough to interfere with DC movement triggered by a secondary stimulus (BCG). Interestingly, conditioning with i-VACV doubled the number of migratory skin DCs reaching the dLN without enhancing the entry of BCG. We speculate that migration elicited by inactivated virus depleted skin DC pools available for BCG transport, contributing, in turn, to the delayed priming of BCG-specific CD4⁺ T cells noted in this setting.

VACV also blocked skin DC migration in response to a subsequent challenge with zymosan (Supplemental Fig. 2A), suggesting that this VACV-inhibitory effect is a more general phenomenon of skin

infection with VACV. That said, this does not apply broadly to viral infections in the skin. There is a large body of data on the enveloped DNA viruses HSV-1 and HSV-2 showing that they trigger DC migration from skin (HSV-1) or the vaginal mucosa (HSV-2) to the dLN (36–39). Skin DC migration is also observed in response to the enveloped RNA viruses Semliki Forest virus and West Nile virus and the nonenveloped DNA virus adenovirus (40, 41). In these studies, DC migration was investigated mainly by FITC skin painting. We also confirm the ability of HSV-1 to trigger skin DC migration to the dLN in our footpad infection model that uses a CFSE injection-based migration assay (Supplemental Fig. 2B). VACV conditioning also blocked HSV-1-triggered DC migration (Supplemental Fig. 2B), in line with the VACV-inhibitory effect being a more general phenomenon.

Interestingly, respiratory infection with VACV has been shown to mobilize lung DCs to the dLN, and these lung-migratory DCs can also prime CD8⁺ T cells (42). Our study focused on DC migration in skin and, as such, did not investigate migration at other

sites. Similar observations of bona fide DC migration from lung to the dLN have nevertheless been made in response to influenza virus (42–47), respiratory syncytial virus (48), and Sendai virus (49), supporting lung DC migration during virus respiratory infections. Thus, we propose that the DC migration-blocking effect of VACV in our model is a general phenomenon of VACV infection targeted to the skin. This is an important consideration for the future use of VACV vectors in vaccines and Ag delivery applications.

Enhanced mRNA accumulation of TNF- α , IL-1, and CCR7 in the skin was accompanied by skin DC migration in response to BCG but not VACV. Infection with VACV deletion mutants Δ A49, Δ B13, and Δ B15, which lack molecules that inhibit NF- κ B, caspase-1, and IL-1, respectively, did to provoke DC migration (Supplemental Fig. 3), revealing, at least, that deletion of these specific molecules from VACV could not rescue the migration phenotype observed in our model. The contribution of IL-1R signaling to BCG-triggered migration is partial (3), so additional factors must regulate this process. During *M. tuberculosis* infection, IFN- α/β has been shown to block IL-1 production from myeloid cells (50). Whether the lack of IL-1 expression in VACV-infected skin or VACV inhibition of skin DC migration is coupled to IFN- α/β remains to be determined. Evaluating cytokine expression and DC migration in IFN- α/β R^{-/-} mice may help clarify this point.

Both i-VACV and MVA promoted migration of skin DC subsets that also relocate in response to BCG, but to our surprise, neither virus triggered the inflammatory transcription profile seen with BCG in the skin. It is possible that i-VACV and MVA trigger skin DC migration by different pathways. Indeed, enhanced CCR7 mRNA accumulation was observed with BCG and MVA but not with i-VACV. CCR7 expression is not an obligatory predictor of DC migration, and both CXCR4 and CXCR5 have been reported to guide DCs from the skin to the dLN (51, 52). Also, accumulation of migratory skin DCs in the dLN is not inhibited by footpad infection with the mouse-pathogenic poxvirus ectromelia (53), suggesting that blockade of DC migration by orthopoxviruses cannot be explained by virulence alone.

Although VACV did not induce transcription of proinflammatory cytokines in the skin, it did unleash a profound inflammatory infiltrate in the dLN. CD169⁺ subcapsular sinus (SCS) macrophages are directly exposed to afferent lymph-borne particulates and thus form a strategic line of defense in the dLN against free-flowing viruses, including VACV, preventing systemic viral spread (54). Previous studies confirm VACV infection of SCS macrophages (9, 55). In addition, MVA triggers inflammasome activation in SCS macrophages that leads to the recruitment of inflammatory cells into the LN (56). We observed an expansion of MHC-II⁺ CD11c^{high} CD11b^{high} cells expressing CD64 in VACV-infected dLN. Although MHC-II⁺ CD11c^{high} cells are generally recognized as LN-resident DCs, a network of macrophages with similar markers has recently been described in the LN paracortex during steady state (57). CD64⁺ DCs have also been observed in the dLN during *Listeria* infection, where they expand in response to IFN- α/β (58).

Migratory skin DCs are tasked with the transport of microbes and their Ags to the dLN and thus play a central role in priming T cells in the dLN postinfection or vaccination in the skin. In our study, VACV reached the dLN without mobilizing skin DCs, whose migration was blocked by the virus. Using a novel recombinant VACV, rVACV-Ag85B, we confirmed using P25 TCRTg cells that the virus is still clearly capable of priming Ag-specific CD4⁺ T cells in the dLN. This provides evidence for migratory skin DC-independent priming of CD4⁺ T cells during vaccination with a live attenuated vaccine. We speculate that DC-independent virus relocation occurs by VACV gaining direct access to lymphatic

vessels. Previous studies show that VACV appear in the dLN within a few minutes after injection in the skin (9–12). We also report the virus in the pLN just minutes after inoculation in the footpad. This rapid relocation of virus to the dLN is in favor of direct viral access to lymphatics after skin infection. The rVACV-Ag85B developed for our studies may be a useful tool for mechanistic dissection of CD4⁺ T cell responses to heterologous Ags in the context of VACV vaccination. Indeed, the fate of DC transport-independent VACV in the LN paracortex, its interactions with APCs at this site, and the quality of ensuing CD4⁺ T cell priming are topics that merit further investigation and are likely to contribute to the development of novel vaccine-based counter-measures against infection and cancer.

Acknowledgments

We thank Susanne Nylén (Karolinska Institutet, Stockholm, Sweden), for critical reading of this manuscript. We also thank Aubin Pitiot, Nuno Rufino de Sousa, Lei Shen, Sören Hartmann, Gabriel Rydholm, Benjamin Heller Sahlgren (Karolinska Institutet), Marisa Oliveira, Dayana Hristova (Cambridge University, U.K.), and Wagner Nagibde Souza (Instituto Carlos Chagas, FIOCRUZ-PR) for technical assistance. Flow cytometry was performed at the Biomedicum Flow Cytometry Core Facility, Department of Microbiology, Tumor and Cell Biology, Karolinska Institutet.

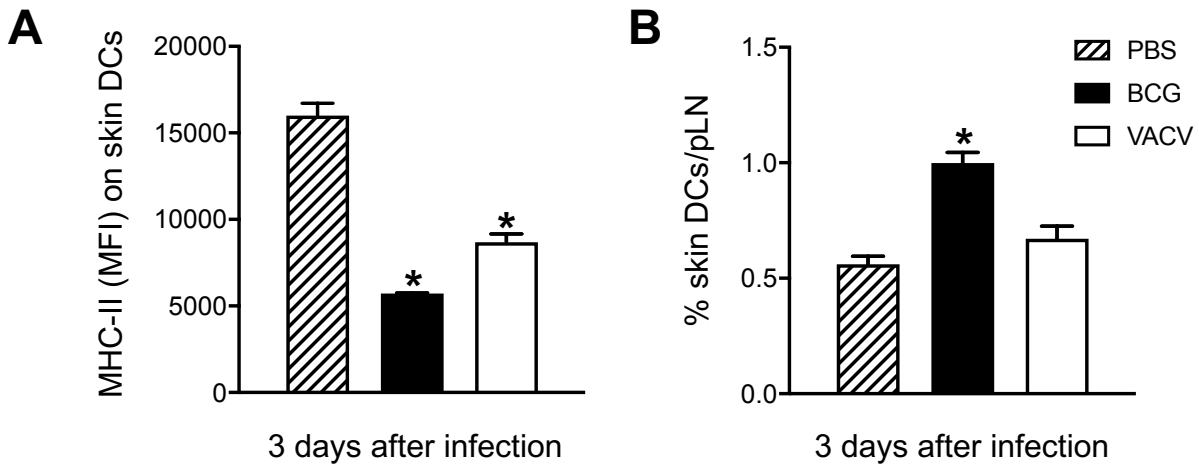
Disclosures

The authors have no financial conflicts of interest.

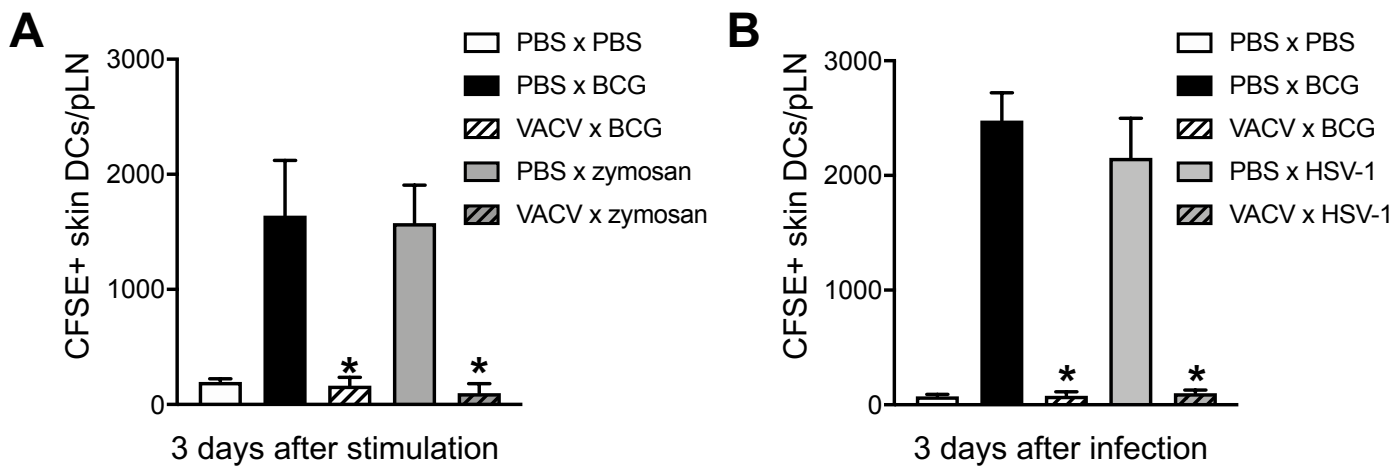
References

1. Worbs, T., S. I. Hammerschmidt, and R. Förster. 2017. Dendritic cell migration in health and disease. *Nat. Rev. Immunol.* 17: 30–48.
2. Randolph, G. J., V. Angeli, and M. A. Swartz. 2005. Dendritic-cell trafficking to lymph nodes through lymphatic vessels. *Nat. Rev. Immunol.* 5: 617–628.
3. Bollampalli, V. P., L. Harumi Yamashiro, X. Feng, D. Bierschenk, Y. Gao, H. Blom, B. Henriques-Normark, S. Nylén, and A. G. Rothfuchs. 2015. BCG skin infection triggers IL-1R-MyD88-dependent migration of EpCAMlow CD11bhigh skin dendritic cells to draining lymph node during CD4+ T-cell priming. *PLoS Pathog.* 11: e1005206.
4. Mackett, M., G. L. Smith, and B. Moss. 1982. Vaccinia virus: a selectable eukaryotic cloning and expression vector. *Proc. Natl. Acad. Sci. USA* 79: 7415–7419.
5. Panicali, D., and E. Paoletti. 1982. Construction of poxviruses as cloning vectors: insertion of the thymidine kinase gene from herpes simplex virus into the DNA of infectious vaccinia virus. *Proc. Natl. Acad. Sci. USA* 79: 4927–4931.
6. Perkus, M. E., A. Piccini, B. R. Lipinskas, and E. Paoletti. 1985. Recombinant vaccinia virus: immunization against multiple pathogens. *Science* 229: 981–984.
7. Moss, B. 1991. Vaccinia virus: a tool for research and vaccine development. *Science* 252: 1662–1667.
8. Ndiaye, B. P., F. Thienemann, M. Ota, B. S. Landry, M. Camara, S. Dièye, T. N. Dieye, H. Esmail, R. Goliath, K. Huygen, et al. MVA85A 030 trial investigators. 2015. Safety, immunogenicity, and efficacy of the candidate tuberculosis vaccine MVA85A in healthy adults infected with HIV-1: a randomised, placebo-controlled, phase 2 trial. *Lancet Respir. Med.* 3: 190–200.
9. Norbury, C. C., D. Malide, J. S. Gibbs, J. R. Bennink, and J. W. Yewdell. 2002. Visualizing priming of virus-specific CD8+ T cells by infected dendritic cells in vivo. *Nat. Immunol.* 3: 265–271.
10. Hickman, H. D., K. Takeda, C. N. Skon, F. R. Murray, S. E. Hensley, J. Loomis, G. N. Barber, J. R. Bennink, and J. W. Yewdell. 2008. Direct priming of antiviral CD8+ T cells in the peripheral interfollicular region of lymph nodes. *Nat. Immunol.* 9: 155–165.
11. Kastenmüller, W., P. Torabi-Parizi, N. Subramanian, T. Lämmermann, and R. N. Germain. 2012. A spatially-organized multicellular innate immune response in lymph nodes limits systemic pathogen spread. *Cell* 150: 1235–1248.
12. Reynoso, G. V., A. S. Weisberg, J. P. Shannon, D. T. McManus, L. Shores, J. L. Americo, R. V. Stan, J. W. Yewdell, and H. D. Hickman. 2019. Lymph node conduits transport virions for rapid T cell activation. *Nat. Immunol.* 20: 602–612.
13. Hickman, H. D., G. V. Reynoso, B. F. Ngudiankama, E. J. Rubin, J. G. Magadán, S. S. Cush, J. Gibbs, B. Molon, V. Bronte, J. R. Bennink, and J. W. Yewdell. 2013. Anatomically restricted synergistic antiviral activities of innate and adaptive immune cells in the skin. *Cell Host Microbe* 13: 155–168.
14. Khan, T. N., J. L. Mooster, A. M. Kilgore, J. F. Osborn, and J. C. Nolz. 2016. Local antigen in nonlymphoid tissue promotes resident memory CD8+ T cell formation during viral infection. *J. Exp. Med.* 213: 951–966.
15. Loo, C. P., N. A. Nelson, R. S. Lane, J. L. Booth, S. C. Loprinzi Hardin, A. Thomas, M. K. Slika, J. C. Nolz, and A. W. Lund. 2017. Lymphatic vessels balance viral dissemination and immune activation following cutaneous viral infection. *Cell Rep.* 20: 3176–3187.
16. Smith, G. L., C. T. O. Benfield, C. Maluquer de Motes, M. Mazzon, S. W. J. Ember, B. J. Ferguson, and R. P. Sumner. 2013. Vaccinia virus immune

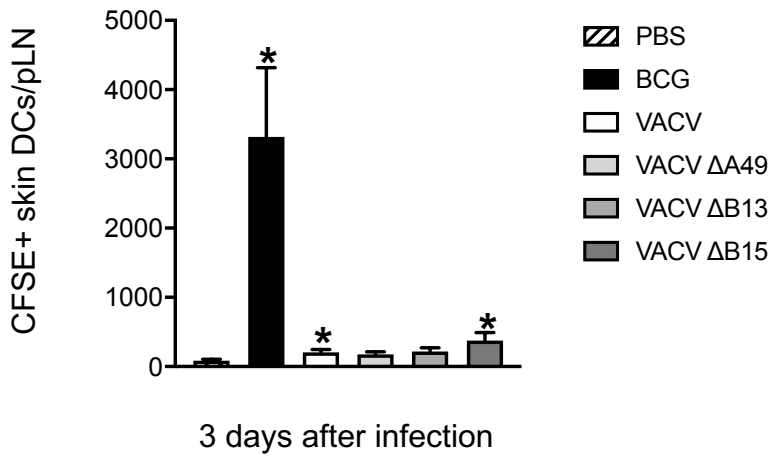
- evasion: mechanisms, virulence and immunogenicity. *J. Gen. Virol.* 94: 2367–2392.
17. Egen, J. G., A. G. Rothfuchs, C. G. Feng, M. A. Horwitz, A. Sher, and R. N. Germain. 2011. Intravital imaging reveals limited antigen presentation and T cell effector function in mycobacterial granulomas. *Immunity* 34: 807–819.
 18. Rothfuchs, A. G., J. G. Egen, C. G. Feng, L. R. Antonelli, A. Bafica, N. Winter, R. M. Locksley, and A. Sher. 2009. *In situ* IL-12/23p40 production during mycobacterial infection is sustained by CD11b^{high} dendritic cells localized in tissue sites distinct from those harboring bacilli. *J. Immunol.* 182: 6915–6925.
 19. Mansur, D. S., C. Maluquer de Motes, L. Unterholzner, R. P. Sumner, B. J. Ferguson, H. Ren, P. Strnadova, A. G. Bowie, and G. L. Smith. 2013. Poxvirus targeting of E3 ligase β -TrCP by molecular mimicry: a mechanism to inhibit NF- κ B activation and promote immune evasion and virulence. *PLoS Pathog.* 9: e1003183.
 20. Kettle, S., N. W. Blake, K. M. Law, and G. L. Smith. 1995. Vaccinia virus serpins B13R (SPI-2) and B22R (SPI-1) encode M(r) 38.5 and 40K, intracellular polypeptides that do not affect virus virulence in a murine intranasal model. *Virology* 206: 136–147.
 21. Alcamí, A., and G. L. Smith. 1992. A soluble receptor for interleukin-1 beta encoded by vaccinia virus: a novel mechanism of virus modulation of the host response to infection. *Cell* 71: 153–167.
 22. Cotter, C. A., P. L. Earl, L. S. Wyatt, and B. Moss. 2017. Preparation of cell cultures and vaccinia virus stocks. *Curr. Protoc. Protein Sci.* 89: 5.12.1–5.12.18.
 23. Falkner, F. G., and B. Moss. 1988. *Escherichia coli* gpt gene provides dominant selection for vaccinia virus open reading frame expression vectors. *J. Virol.* 62: 1849–1854.
 24. Falkner, F. G., and B. Moss. 1990. Transient dominant selection of recombinant vaccinia viruses. *J. Virol.* 64: 3108–3111.
 25. Bollampalli, V. P., S. Nylén, and A. G. Rothfuchs. 2016. A CFSE-based assay to study the migration of murine skin dendritic cells into draining lymph nodes during infection with *Mycobacterium bovis* Bacille Calmette-Guérin. *J. Vis. Exp.* 116: 54620.
 26. Tsung, K., J. H. Yim, W. Marti, R. M. Buller, and J. A. Norton. 1996. Gene expression and cytopathic effect of vaccinia virus inactivated by psoralen and long-wave UV light. *J. Virol.* 70: 165–171.
 27. Sancho, M. C., S. Schleich, G. Griffiths, and J. Krijnse-Locker. 2002. The block in assembly of modified vaccinia virus Ankara in HeLa cells reveals new insights into vaccinia virus morphogenesis. *J. Virol.* 76: 8318–8334.
 28. Obieglo, K., X. Feng, V. P. Bollampalli, I. Dellacasa-Lindberg, C. Classon, M. Österblad, H. Helmbj, J. P. Hewitson, R. M. Maizels, A. Gigliotti Rothfuchs, and S. Nylén. 2016. Chronic gastrointestinal nematode infection mutes immune responses to mycobacterial infection distal to the gut. *J. Immunol.* 196: 2262–2271.
 29. Sandgren, K. J., J. Wilkinson, M. Miranda-Saksena, G. M. McInerney, K. Byth-Wilson, P. J. Robinson, and A. L. Cunningham. 2010. A differential role for macrophocytosis in mediating entry of the two forms of vaccinia virus into dendritic cells. *PLoS Pathog.* 6: e1000866.
 30. Yates, N. L., and M. A. Alexander-Miller. 2007. Vaccinia virus infection of mature dendritic cells results in activation of virus-specific CD8⁺ T cells: a potential mechanism for direct presentation. *Virology* 359: 349–361.
 31. Chahroudi, A., D. A. Garber, P. Reeves, L. Liu, D. Kalman, and M. B. Feinberg. 2006. Differences and similarities in viral life cycle progression and host cell physiology after infection of human dendritic cells with modified vaccinia virus Ankara and vaccinia virus. *J. Virol.* 80: 8469–8481.
 32. Jenne, L., C. Hauser, J. F. Arrighi, J. H. Saurat, and A. W. Hügin. 2000. Poxvirus as a vector to transduce human dendritic cells for immunotherapy: abortive infection but reduced APC function. *Gene Ther.* 7: 1575–1583.
 33. Engelmayr, J., M. Larsson, M. Subklewe, A. Chahroudi, W. I. Cox, R. M. Steinman, and N. Bhardwaj. 1999. Vaccinia virus inhibits the maturation of human dendritic cells: a novel mechanism of immune evasion. *J. Immunol.* 163: 6762–6768.
 34. Yao, Y., P. Li, P. Singh, A. T. Thiele, D. S. Wilkes, G. J. Renukaradhya, R. R. Brutkiewicz, J. B. Travers, G. D. Luker, S. C. Hong, et al. 2007. Vaccinia virus infection induces dendritic cell maturation but inhibits antigen presentation by MHC class II. *Cell. Immunol.* 246: 92–102.
 35. Humrich, J. Y., P. Thumann, S. Greiner, J. H. Humrich, M. Averbeck, C. Schwank, E. Kämpgen, G. Schuler, and L. Jenne. 2007. Vaccinia virus impairs directional migration and chemokine receptor switch of human dendritic cells. *Eur. J. Immunol.* 37: 954–965.
 36. Bedoui, S., P. G. Whitney, J. Waithman, L. Eidsmo, L. Wakim, I. Caminschi, R. S. Allan, M. Wojtasiak, K. Shortman, F. R. Carbone, et al. 2009. Cross-presentation of viral and self antigens by skin-derived CD103⁺ dendritic cells. *Nat. Immunol.* 10: 488–495.
 37. Lee, H. K., M. Zamora, M. M. Linehan, N. Iijima, D. Gonzalez, A. Haberman, and A. Iwasaki. 2009. Differential roles of migratory and resident DCs in T cell priming after mucosal or skin HSV-1 infection. *J. Exp. Med.* 206: 359–370.
 38. Allan, R. S., J. Waithman, S. Bedoui, C. M. Jones, J. A. Villadangos, Y. Zhan, A. M. Lew, K. Shortman, W. R. Heath, and F. R. Carbone. 2006. Migratory dendritic cells transfer antigen to a lymph node-resident dendritic cell population for efficient CTL priming. *Immunity* 25: 153–162.
 39. Zhao, X., E. Deak, K. Soderberg, M. Linehan, D. Spezzano, J. Zhu, D. M. Knipe, and A. Iwasaki. 2003. Vaginal submucosal dendritic cells, but not Langerhans cells, induce protective Th1 responses to herpes simplex virus-2. *J. Exp. Med.* 197: 153–162.
 40. Bachy, V., C. Hervouet, P. D. Becker, L. Chorro, L. M. Carlin, S. Herath, T. Papagatsias, J. B. Barbaroux, S. J. Oh, A. Benlahrech, et al. 2013. Langerin negative dendritic cells promote potent CD8⁺ T-cell priming by skin delivery of live adenovirus vaccine microneedle arrays. *Proc. Natl. Acad. Sci. USA* 110: 3041–3046.
 41. Johnston, L. J., G. M. Halliday, and N. J. King. 2000. Langerhans cells migrate to local lymph nodes following cutaneous infection with an arbovirus. *J. Invest. Dermatol.* 114: 560–568.
 42. Beauchamp, N. M., R. Y. Busick, and M. A. Alexander-Miller. 2010. Functional divergence among CD103⁺ dendritic cell subpopulations following pulmonary poxvirus infection. *J. Virol.* 84: 10191–10199.
 43. Kandasamy, M., P. C. Ying, A. W. Ho, H. R. Sumatoh, A. Schlitzer, T. R. Hughes, D. M. Kemeny, B. P. Morgan, F. Ginhoux, and B. Sivasankar. 2013. Complement mediated signaling on pulmonary CD103⁺ dendritic cells is critical for their migratory function in response to influenza infection. *PLoS Pathog.* 9: e1003115.
 44. Ho, A. W., N. Prabhu, R. J. Betts, M. Q. Ge, X. Dai, P. E. Hutchinson, F. C. Lew, K. L. Wong, B. J. Hanson, P. A. Macary, and D. M. Kemeny. 2011. Lung CD103⁺ dendritic cells efficiently transport influenza virus to the lymph node and load viral antigen onto MHC class I for presentation to CD8 T cells. *J. Immunol.* 187: 6011–6021.
 45. Ballesteros-Tato, A., B. León, F. E. Lund, and T. D. Randall. 2010. Temporal changes in dendritic cell subsets, cross-priming and costimulation via CD70 control CD8⁺ T cell responses to influenza. *Nat. Immunol.* 11: 216–224.
 46. Belz, G. T., C. M. Smith, L. Kleinert, P. Reading, A. Brooks, K. Shortman, F. R. Carbone, and W. R. Heath. 2004. Distinct migratory and nonmigrating dendritic cell populations are involved in MHC class I-restricted antigen presentation after lung infection with virus. *Proc. Natl. Acad. Sci. USA* 101: 8670–8675.
 47. Legge, K. L., and T. J. Braciale. 2003. Accelerated migration of respiratory dendritic cells to the regional lymph nodes is limited to the early phase of pulmonary infection. *Immunity* 18: 265–277.
 48. Lukens, M. V., D. Kruijzen, F. E. Coenjaerts, J. L. Kimpen, and G. M. van Bleek. 2009. Respiratory syncytial virus-induced activation and migration of respiratory dendritic cells and subsequent antigen presentation in the lung-draining lymph node. *J. Virol.* 83: 7235–7243.
 49. Grayson, M. H., M. S. Ramos, M. M. Rohlfing, R. Kitchens, H. D. Wang, A. Gould, E. Agapov, and M. J. Holtzman. 2007. Controls for lung dendritic cell maturation and migration during respiratory viral infection. *J. Immunol.* 179: 1438–1448.
 50. Mayer-Barber, K. D., B. B. Andrade, D. L. Barber, S. Hieny, C. G. Feng, P. Caspar, S. Oland, S. Gordon, and A. Sher. 2011. Innate and adaptive interferons suppress IL-1 α and IL-1 β production by distinct pulmonary myeloid subsets during *Mycobacterium tuberculosis* infection. *Immunity* 35: 1023–1034.
 51. Kabashima, K., N. Shiraiishi, K. Sugita, T. Mori, A. Onoue, M. Kobayashi, J. Sakabe, R. Yoshiki, H. Tamamura, N. Fujii, et al. 2007. CXCL12-CXCR4 engagement is required for migration of cutaneous dendritic cells. *Am. J. Pathol.* 171: 1249–1257.
 52. Saeki, H., M. T. Wu, E. Olasz, and S. T. Hwang. 2000. A migratory population of skin-derived dendritic cells expresses CXCR5, responds to B lymphocyte chemoattractant *in vitro*, and co-localizes to B cell zones in lymph nodes *in vivo*. *Eur. J. Immunol.* 30: 2808–2814.
 53. Stotesbury, C., E. B. Wong, L. Tang, B. Montoya, C. J. Knudson, C. R. Melo-Silva, and L. J. Sigal. 2020. Defective early innate immune response to ectromelia virus in the draining lymph nodes of aged mice due to impaired dendritic cell accumulation. *Aging Cell* 19: e13170.
 54. Louie, D. A. P., and S. Liao. 2019. Lymph node subcapsular sinus macrophages as the frontline of lymphatic immune defense. *Front. Immunol.* 10: 347.
 55. Tian, T., M. Q. Jin, K. Dubin, S. L. King, W. Hoetzenecker, G. F. Murphy, C. A. Chen, T. S. Kupper, and R. C. Fuhlbrigge. 2017. IL-1R type 1-deficient mice demonstrate an impaired host immune response against cutaneous vaccinia virus infection. *J. Immunol.* 198: 4341–4351.
 56. Sagoo, P., Z. Garcia, B. Breart, F. Lemaître, D. Michonneau, M. L. Albert, Y. Levy, and P. Bousso. 2016. *In vivo* imaging of inflammasome activation reveals a subcapsular macrophage burst response that mobilizes innate and adaptive immunity. *Nat. Med.* 22: 64–71.
 57. Baratin, M., L. Simon, A. Jorquera, C. Ghigo, D. Demebele, J. Nowak, R. Gentek, S. Wienert, F. Klauschen, B. Malissen, et al. 2017. T cell zone resident macrophages silently dispose of apoptotic cells in the lymph node. *Immunity* 47: 349–362.e5.
 58. Min, J., D. Yang, M. Kim, K. Haam, A. Yoo, J.-H. Choi, B. U. Schraml, Y. S. Kim, D. Kim, and S.-J. Kang. 2018. Inflammation induces two types of inflammatory dendritic cells in inflamed lymph nodes. [Published erratum appears in 2018 *Exp. Mol. Med.* 50: 33.] *Exp. Mol. Med.* 50: e458.



SUPPLEMENTARY FIGURE 1. Expression of MHC-II and frequency of skin DCs in dLN of VACV- and BCG-infected mice. (A and B) C57BL/6 mice were inoculated in the footpad skin with PBS, BCG (10^6 CFUs) or VACV (10^6 PFUs). Three days later, pLNs were processed and analyzed by flow cytometry. (A) Mean fluorescence intensity (MFI) for MHC-II on skin DCs in pLN. (B) Frequency of skin DCs in pLN. Five animals per group used in each experiment. One of 3 independent experiment shown. Bars indicate standard error of the mean. * denotes statistically significant difference between PBS and infected groups (A) and PBS and BCG (B).



SUPPLEMENTARY FIGURE 2. Conditioning with VACV mutes subsequent DC migration in response to zymosan and HSV-1. C57BL/6 mice were inoculated in the footpad skin with PBS or VACV (10^6 PFUs). Twenty-four hours later the same footpads were inoculated with BCG (10^6 CFUs) (A and B), zymosan (100 μ g) (A) or HSV-1 (10^5 PFUs) (B) and the CFSE-based migration assay performed as in Fig. 1. Total number of CFSE-labeled skin DCs in the pLN 3 days after stimulation/infection are shown. Four to 5 animals per group were used. Bars indicate standard error of the mean. One of 3 independent experiments for zymosan. One of 2 independent experiments for HSV-1. * denotes statistical significance between PBS- and VACV-conditioned groups. PBS x BCG, PBS x zymosan and PBS x HSV-1 groups are statistically significant from PBS x PBS controls.



SUPPLEMENTARY FIGURE 3. Infection with VACV Δ A49, Δ B13 and Δ B15 does not trigger skin DC migration to dLN. C57BL/6 mice were inoculated in the footpad skin with PBS, BCG (10^6 CFUs), VACV (10^6 PFUs) or the VACV deletion mutants Δ A49, Δ B13 and Δ B15 (10^6 PFUs) and subjected to the CFSE migration assay as in Fig. 1. Total number of CFSE-labeled skin DCs in the pLN 3 days after infection are shown. Five animals per group were used. Bars indicate standard error of the mean. * denotes statistical significance between PBS- and vaccine-injected groups.

3.2.3 Cellular migration to the draining lymph nodes after Zika virus infection

3.2.3.1 Methodology

Mice

C57BL/6 mice were obtained from Instituto Carlos Chagas/FIOCRUZ-PR animal facility, maintained and handled according to the directives of the Guide for the Care and Use of Laboratory Animals of the Brazilian National Council of Animal Experimentation. The protocols were approved by the Committee on Ethics of Animal Experimentation from Fundação Oswaldo Cruz – CEUA/FIOCRUZ (license LW 03-19). Both, 8-12 week old male and female mice were used.

Virus and Mycobacteria

Viral stocks of the *Zika virus* (ZIKV) Asian strain PE243 (DONALD et al., 2016), and *Dengue virus* (DENV serotype 4 LRV13/422; GenBank KU513441) were prepared in C6/36 cells. Yellow fever virus (YFV) strain 17DD was obtained after two passages of the commercial vaccine (Biomanguinhos, Fiocruz, Brazil) (JORGE et al., 2017) in Vero-E6 cells (ATCC CRL-1586). To ZIKV and DENV-4, seven days post-infection the cell culture supernatant was collected, clarified by centrifugation and later titrated by foci-forming immunodetection assay in C6/36 cells (CATANEO et al., 2019). YFV 17DD was quantified by plaque assay after 5 days of infection in Vero-E6 cells. *M. bovis* BCG strain Moraeu was kindly provided by Dr. Andre Báfica (Universidade Federal de Santa Catarina).

Inoculation of mice

Animals were inoculated in the hind footpad with 30 μ L of PBS containing 5×10^5 CFUs of BCG, 5×10^5 FFUs of ZIKV PE243 and DENV LRV13/422, or 5×10^5 PFUs of YFV 17DD. Control animals received 30 μ L of PBS only. Assessment of cell migration from the footpad skin to the dLN was done as previously described (AGGIO et al., 2021; BOLLAMPALLI et al., 2015). Briefly, animals previously injected with vaccine, virus or PBS were injected 24 hours before euthanasia in the same footpad with 30 μ L of 0.5 mM of CFSE (Sigma) to track cell migration.

Flow cytometric staining

Popliteal LNs (pLNs) were aseptically removed, transferred to tubes containing FACS buffer (5 mM EDTA and 5% FBS in PBS), and gently homogenized using a tissue

grinder. The resulting single-cell suspension was filtered in 40 µm cell strainers and counted by trypan blue exclusion. The cells were washed in FACS buffer and stained for flow cytometry. Single-cell suspension from pLN were incubated with various different combinations of fluorochrome-conjugated rat anti-mouse mAbs specific for CD3 (145-2C11), CD4 (RM4-5), CD8 (53-6.7), CD19 (1D3), CD11b (M1/70), CD11c (HL3), CD64 (X54-517.1.1), CD103 (M290), CD326/EpCAM (G8.8), MHC-II I-A/I-E (M5/11.4.15.2), Ly-6G (1A8), Ly-6C/G (RB6-8C5) (BD Biosciences) for 45 minutes at 4°C in FACS buffer containing 0.5 mg/mL of anti-mouse CD16/CD23 (2.4G2) (BD Biosciences). Flow cytometry was performed on a FACS Canto II with BD FACSDiva software (BD Biosciences) and the acquired data analyzed on FlowJoV10 (BD Biosciences).

Statistical analyses

Analyses were performed using GraphPad Prism 6 (GraphPad Software, Inc., USA). one-way Anova with Tukey's multiple comparison test. A cut-off of $p < 0.05$ was considered significant.

3.2.3.2 Results

Three days after subcutaneous infection with ZIKV, DENV, and YFV, the animals pLN presented lymphadenopathy (Figure 5B and 6C) with expanded lymphocytes and phagocyte populations, such as CD64⁺ cells, neutrophils and monocytes (Figure 5). Among the virus, DENV resulted in the highest numbers in all assessed populations (Figure 5). However, monocytes/neutrophils Ly-6C/G^{high} seem not to be provenient from the infected skin, since no CFSE was detected in the pLN of virus infected mice in this time point (Figure 6B). CFSE detected in the pLN was mostly associated to skin DCs MHC-II^{high}CD11c^{+/low} (Figure 6A). As BCG, ZIKV and DENV induced migration of skin DCs (Figure 6A and 6D) and dowregulation of MHC-II in this population (Figure 6E), but to a lesser extent. Within the subset of skin DCs, CD103⁻CD11b^{high}EpCAM^{low} showed to be the predominant migratory population in response to BCG and virus (Figure 7).

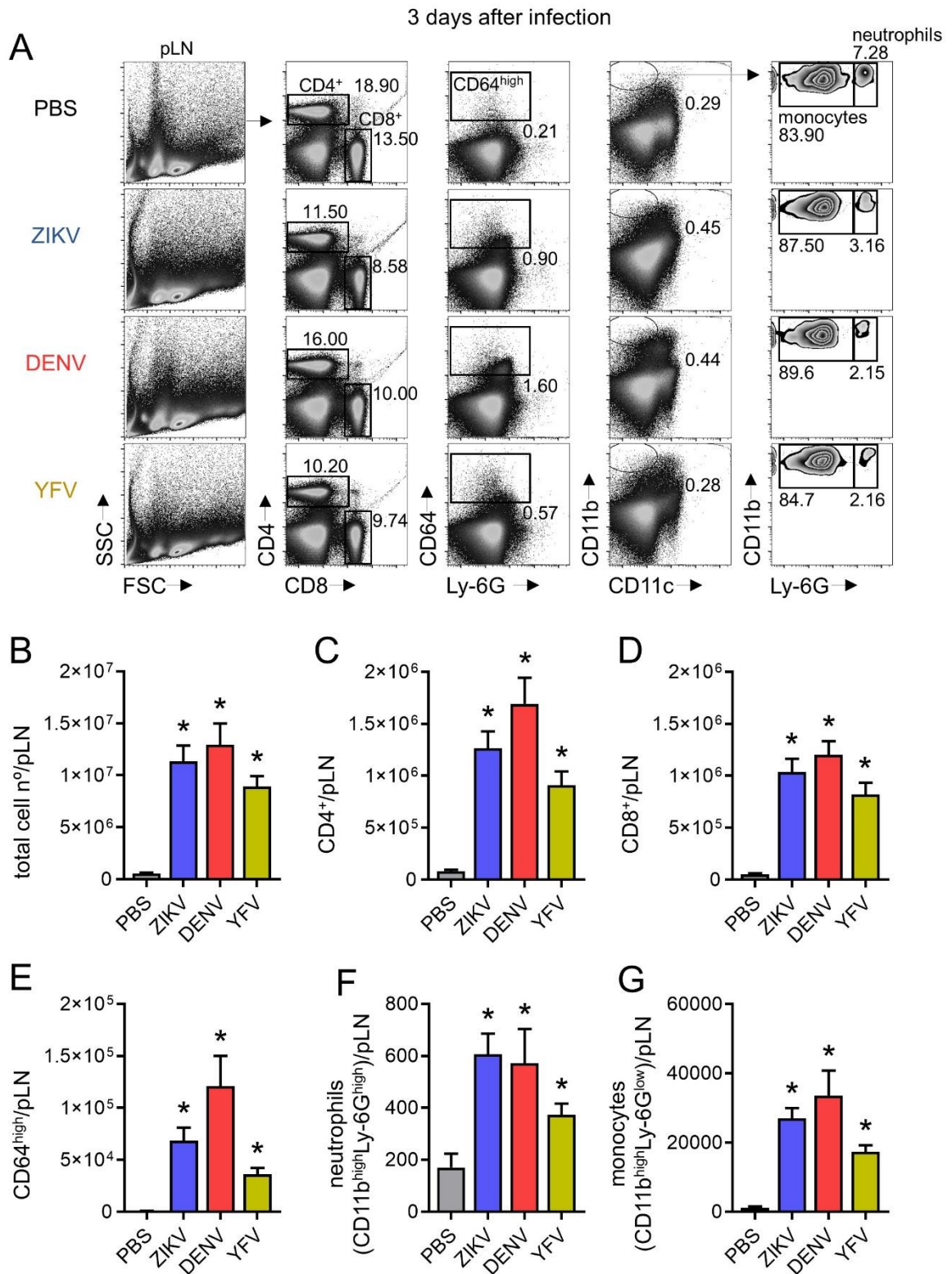


Figure 5. Populations expanded in the dLN after flavivirus infection. C57BL/6 mice were subcutaneously inoculated in the footpad with PBS, ZIKV PE243 (5×10^5 FFU), DENV LRV13/422 (5×10^5 FFU), or YFV 17DD (5×10^5 PFU). Three days later, single-cell suspensions were obtained from the pLN and analyzed by flow cytometry. **(A)** Representative FACS plots showing frequency of the different populations; **(B)** Total cell numbers into the pLN; **(C-G)** Total number of specific populations (CD4⁺ T cells, CD8⁺ T cells, CD64^{high} cells, neutrophils CD11b^{high}Ly-6G^{high}, and monocytes CD11b^{high}Ly-6G^{low}). Three-four mice per group were used. One independent experiment is shown. Bars indicated SEM. The asterisk (*) denotes statistical significance between PBS.

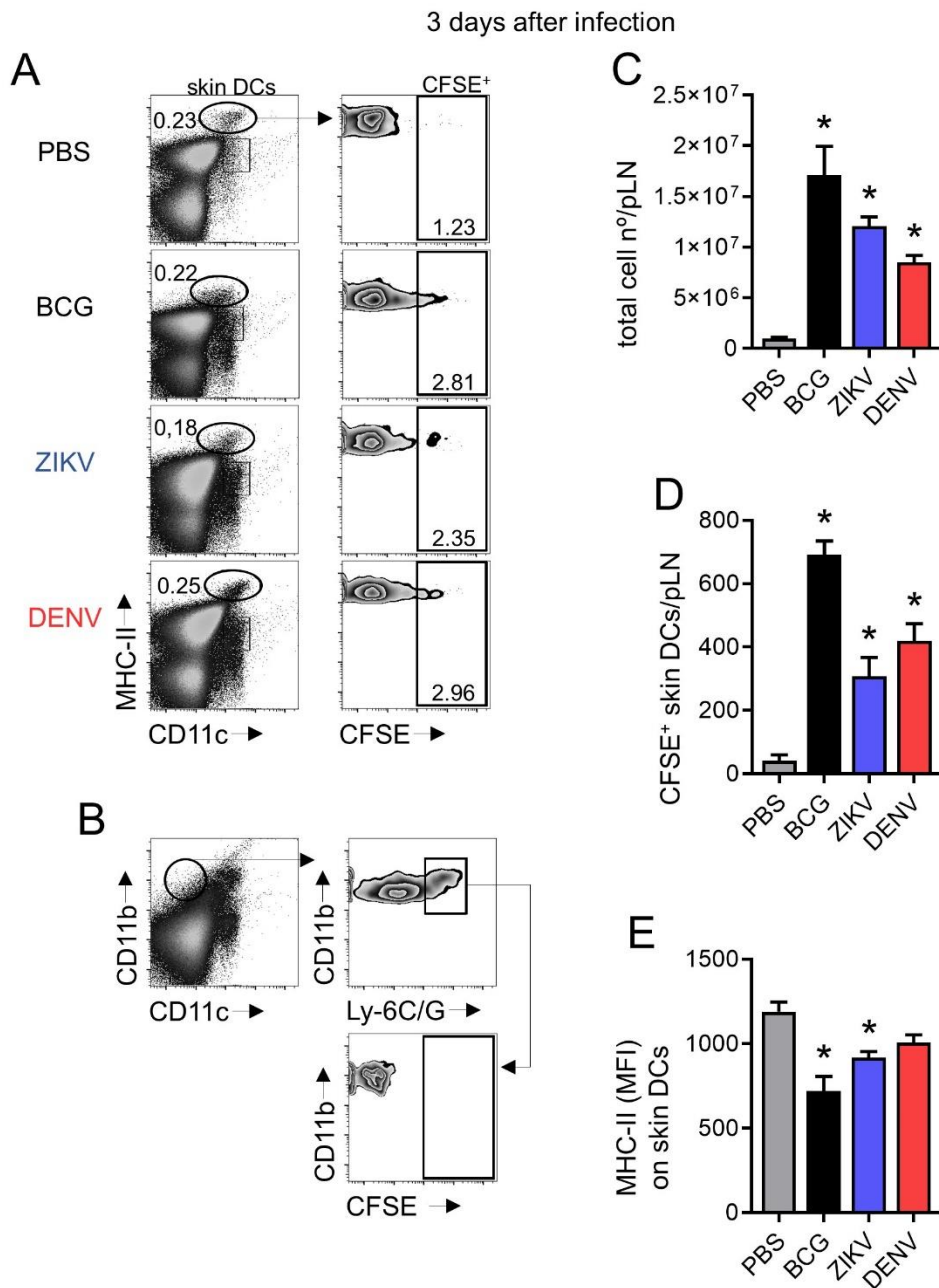


Figure 6. Skin DCs migrate to the dLN in response to ZIKV and DENV. C57BL/6 mice were inoculated in the footpad skin with PBS, BCG (5×10^5 CFU), ZIKV PE243 (5×10^5 FFU), or DENV LRV13/422 (5×10^5 FFU) and subjected to a 3 days CFSE migration assay. Single-cell suspensions were prepared from the pLN and analyzed by flow cytometry. **(A)** FACS plots showing CFSE⁺ cells from pLN; **(B)** FACS plots showing the absence of CFSE staining in the neutrophils/monocytes population (CD11b^{high}Ly-6C/G^{high}) in pLN; **(C)** Total cell numbers in the pLN; **(D)** Total number of CFSE-labeled skin DCs (MHC-II^{high}CD11c^{+/low}) in the pLN; **(E)** Mean fluorescence intensity (MFI) for MHC-II on skin DCs in pLN. One of two independent experiments is shown. Two-four mice per group were used. Bars indicated SEM. The asterisk (*) denotes statistical significance between PBS and the other groups.

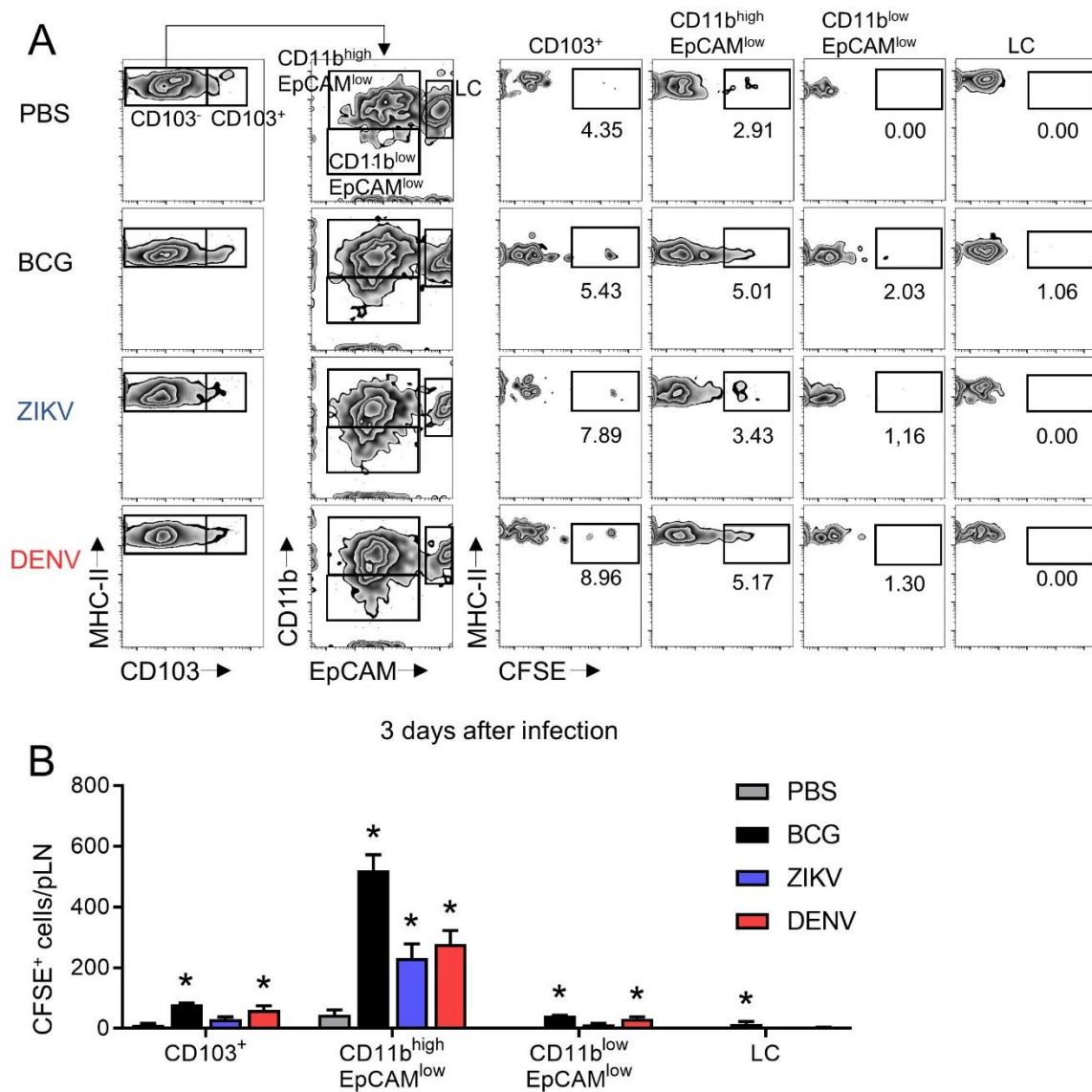


Figure 7. Skin DCs migratory subsets in response to ZIKV and DENV. Same set up of figure 6. **(A)** Representative FACS plots showing frequency of CFSE with defined subsets of skin DCs (AGGIO et al., 2021; BOLLAMPALLI et al., 2015) in PBS, BCG, or virus treated mice; **(B)** CFSE expression within these populations. One of two independent experiments is shown. Two-four mice per group were used. Bars indicated SEM. The asterisk (*) denotes statistical significance between PBS and the other groups.

4. DISCUSSION

The first chapter of this thesis comprises the results of the original topic of interest of this work: the human neutrophil interaction with *Zika virus* (ZIKV). The aim of this study was to assess *in vitro* classical neutrophil mechanisms of action during viral stimulation and differences in ZIKV infection in the presence or under depletion of neutrophils. The motivation of this study was mainly the ambiguous roles neutrophils seem to play during viral infection (MIDDLETON et al., 2020; SAITOH et al., 2012) and the possible neutrophil involvement in aspects of ZIKV pathology that remain unclear (e.g. ZIKV persistence in some organs, infection in immune-privileged sites, autoimmune disorders, sexual transmission and the exacerbated inflammatory response associated with severe ZIKV pathogenicity) (PIERSON; DIAMOND, 2018; TRIPATHI et al., 2017; WANG et al., 2018). Moreover, neutrophils showed relevant participation in other neurotropic arbovirus (*West Nile virus* and *Semliki forest virus*) infections (PAUL et al., 2017; PINGEN et al., 2016).

The manuscript unexpectedly reports an *in vitro* absence of human neutrophils action during interaction with ZIKV. These findings spoke against a beneficial role of neutrophils in viral clearance and suggested that neutrophils by themselves would not contribute to spreading the virus or increasing inflammation during ZIKV infection. Reports of such lack of action of neutrophils in viral infections, even when the cells reached the inflamed site are not unusual (CORTJENS et al., 2016b; KIRSEBOM et al., 2020; WOJTASIAK et al., 2010; XU et al., 2018). Even though our results did not show neutrophil migration in response to the levels of IL-8 produced by ZIKV infected cells, based in several reports of neutrophil infiltration in inflamed regions after ZIKV infection (ALIOTA et al., 2016; DOWALL et al., 2016; HAYASHIDA et al., 2019; LUM et al., 2019; MANANGEESWARAN; IRELAND; VERTHELYI, 2016; MCDONALD et al., 2018, 2020; NGUYEN et al., 2017; O'CONNOR et al., 2018; ZUKOR et al., 2018), we speculate that neutrophils migration require a specific milieu. The ideal conditions can be linked to the mosquito saliva (HASTINGS et al., 2019; PINGEN et al., 2016). That way, in an inflammation where neutrophils would not act directly on the virus, its presence could contribute negatively through cell overactivation in the milieu, damaging tissue or recruiting other susceptible cells to propagate the infection.

It is also important to consider the limitations of *in vitro* and animal models to flavivirus infection. This work is one of the first to focus on neutrophils and ZIKV interactions, adding to the discussion on the relevance of neutrophil during flavivirus infections, which is important to the assertive development of antiviral strategies. The

work also incentivizes a more often inclusion of neutrophils in scientific investigations.

Still seeking an understanding of the participation of neutrophils in ZIKV infection, aspects related to the draining lymph node (dLN) were next evaluated. A compelling feature of ZIKV is its ability to persist for long periods of time in immunocompetent hosts and during pregnancy, which may be linked to adverse infection outcome. One consistent site of viral persistence are lymphoid tissues. The LN is an early amplification site for pathogens, including *Dengue virus* (DENV) and *Yellow fever virus* (YFV) (FINK et al., 2009; LEE; LOBIGS, 2008; MEIER et al., 2009). It is known that free ZIKV reaches the dLN very fast post infection (up to 5 minutes) (REYNOSO et al., 2019). ZIKV could persist and replicate until up to 72 days in LNs (paracortical regions and germinal centers), cerebrospinal fluid, reproductive tissues of infected monkeys (rhesus, pigtail, and cynomolgus), notwithstanding acute viremia was rapidly controlled in peripheral blood (AID et al., 2017; COFFEY et al., 2017; HIRSCH et al., 2017; O'CONNOR et al., 2018; OSUNA et al., 2016).

The viral persistence in this regions correlated with upregulation of mTOR, proinflammatory, and anti-apoptotic pathways, which promote survival in infected cells, and downregulation of extracellular matrix pathways, that may be important for lymphocyte recruitment to sites of infection (AID et al., 2017). ZIKV RNA was also detected in mothers and fetal LNs during rhesus macaques and anti-IFNAR Ab-treated Rag1^{-/-} (AIR) mice pregnancy (NGUYEN et al., 2017; WINKLER et al., 2020). At 28 days post infection, ZIKV RNA was found in macrophages, non-classical monocytes and B cell subsets with reduced levels in DC subsets in LN follicles (HIRSCH et al., 2017; O'CONNOR et al., 2018). ZIKV RNA was also found in myeloperoxidase⁺ neutrophils into the LN 7 days after infection in cynomolgus macaques (OSUNA et al., 2016). Based in reports that showed neutrophils presence in LN after inflammation or evidence of roles in enhancing/containing pathogens spread, or yet in regulating adaptive responses (ABADIE et al., 2009; BEAUVILLAIN et al., 2011; CHTANOVA et al., 2008; HAMPTON et al., 2015; KAMENYEVA et al., 2015; KASTENMÜLLER et al., 2012; MANTOVANI et al., 2011; PIZZAGALLI et al., 2019; YANG et al., 2010), we interrogated whether neutrophils in dLN after 3 days of ZIKV subcutaneous infection (Figure 5) could be arriving from the site of infection. To achieve that goal we used a novel *in vivo* fluorochrome-based migration assay

proposed by Dr. Rothfuchs group (BOLLAMPALLI et al., 2015; BOLLAMPALLI; NYLÉN; ROTHFUCHS, 2016).

Dr. Rothfuchs group is interested in the early events that take place during *Mycobacterium bovis* bacillus Calmette-Guérin (BCG) skin infection/vaccination. The group has set up a mouse model to mimic intradermal BCG infection (footpad injection in C57BL/6 wild type mouse), a CFSE fluorochrome-based migration assay to track dendritic cells (DCs) migration in that model, and the study of priming of BCG specific CD4⁺ T cells using transgenic mice with mycobacteria antigen-specific P25 T-cell receptor. Using that approach, EpCAM^{low}CD11b^{high} migratory skin DCs were identified as the main DCs subset mobilized to the dLN in response to BCG, and responsible for the transport of alive BCG from its inoculation site to the dLN, priming CD4⁺ T cells. This process was showed to be dependent on the inflammatory cytokine IL-1 (IL-1 receptor, MyD88, TNFR-I and IL-12p40 signaling) (BOLLAMPALLI et al., 2015).

With the purpose of learning the methodology, the work presented in chapter 2.1 of this thesis was performed during an exchange (Sep/2017 - Dec/2017 and Nov/2018 - Dec/2019) in the Department of Microbiology, Tumor and Cell biology from the Karolinska Institutet under the supervision of the Dr. Antonio Rothfuchs and in collaboration with Dr. Brian Ferguson from the Department of Pathology from the University of Cambridge. As in Sweden ZIKV is considered a biosafety level 3 organism (whose handling implies a series of practical impediments), a parallel project was developed using *vaccinia virus* (VACV) as a model. Cellular migration in response to ZIKV was answered next.

VACV is a double-stranded DNA virus belonging to the *Orthopoxvirus* genus of unknown origin and natural host. VACV remains the only vaccine to have eradicated a human disease, smallpox. It randomly replaced cowpox or horsepox at some point between 1796 and 1939 due to the procedures used at the time for vaccine production and given the cross protection it confers. Despite the eradication of this disease by the 1970s, VACV is still greatly studied as a platform to develop novel vaccines against heterologous agents (the large genome allows the insertion and high level expression of large foreign genes), and its wide range of immunomodulatory proteins make it an excellent model for studying interactions between viruses and their host. Complications of smallpox vaccination led investigators to develop safer candidate vaccines for smallpox, like modified virus

Ankara (MVA) in Germany, LC16m8 in Japan, and NYVAC in USA (DAMASO, 2018; JACOBS et al., 2009; SMITH, 2008).

Following intradermal infection in mice, the virus causes a localized mild disease characterized by the formation of a lesion that heals in about 2 weeks. VACV immunomodulators are numerous and so are their targets. These VACV proteins function either by preventing soluble factors binding to receptors or preventing the establishment of chemokine concentration gradients: intracellular proteins (A49, A46, A52, K1, M2, and N1) inhibit signaling pathways (TLRs, ILs, TNF and IFN receptors), apoptosis (B13, F1, and N1), action of IFN-induced antiviral proteins (K3 and E3); additionally, extracellular proteins bind to complement factors, IFN types I and II, IL-1 β , IL-18, TNF- α , and CC chemokines (B15, VCP, B8, B18, B15, C12, CrmC, vCKBP, B7, and A41) (SMITH, 2008; SMITH et al., 2013). VACV infection induces a robust antibody and T-cell response, but the outcome of DC-VACV interactions remains incompletely understood.

The aim of the study was to investigate DCs migration to the dLN in response to VACV and to compare it to the live tuberculosis vaccine BCG, another live-attenuated vaccine given through the same route. Using the CFSE migration assay and a VACV engineered to express mycobacterial Ag85b, we show that interestingly, in stark contrast to BCG, VACV infection actively interferes with the mobilization of skin DCs to the dLN, but not with the priming of CD4⁺ T cells therein, and the virus freely reaches the dLN. Moreover, this inhibition is capable of impairing DCs migration upon secondary challenges. This work reports an unprecedented immunosuppressive mechanism in VACV infection.

One of the motivations to compare BCG and VACV is the different sizes of them. Although VACV is a large virus (300 nm), it is still considerably smaller than the bacteria and can easily access the lymphatics. BCG can access lymphatic vessels and reach the dLN in the absence of DC transport. Indeed, BCG arrives in the dLN even when cell migration from the skin has been impaired by Pertussis toxin (BOLLAMPALLI et al., 2015). The arrival of free pathogens to the LN without or before the mobilization of DCs may potentially affect the development of adaptive responses in ways not explored. Reynoso *et al.* (2019), showed that VACV that freely reached the dLN infected cells in the T cell zone which leads to a more rapid activation of CD8⁺ T cells in comparison with cells infected in nodal regions, conferring a temporal advantage to the host.

Other interesting comparison between the two vaccines is regarding the mechanisms that trigger DCs movement to bacterial or viral infection. The data pointed out that IL-1 is not involved in the skin environment that permits DCs migration in response to inactivated VACV or *modified VACV Ankara*, a modified VACV that was developed as a safer candidate vaccine for smallpox and lost a significant part of its genome responsible for encoding proteins responsible for the evasion of the immune system. The contribution of IL-1R signaling to BCG-triggered migration is partial, so additional unknown factors must regulate this process. It is possible that IFN- α/β , more present in viral infections, interfere with IL-1 signaling (MAYER-BARBER et al., 2011).

Our results on the regulation of skin DCs traffic in response to live attenuated vaccines/immunization with antigen models add to the understanding of particular means in which microorganisms initiate immune response *in vivo*, a subject weakly explored in viral infection. This work impacts vaccination understanding and may contribute in new developments or the improvement of current low efficient vaccines, e.g. BCG (DOHERTY; ANDERSEN, 2005). For example, a replication inducible VACV (vINDs) expressing ZIKV pre-membrane and envelope proteins was recently tested and showed anti-envelope IgG titers and protection in mice (JASPERSE et al., 2021).

At last, chapter 2.2 showed evidences that despite immunocompetent mice respond to ZIKV expanding leukocytes populations in the dLN three days post infection, even in the absence of viral particles at this time point (manuscript chapter 1, supplementary figure 2), neutrophils in the dLN were not recruited from the infected skin. The mobilization of skin DCs to the dLN during flavivirus infection reinforce the specific suppressive effect of VACV infection and the relevance of the development of adaptive responses to contain ZIKV infection. These first results urged a close look at the ZIKV infection site to understand the mechanism that contained ZIKV dispersion in immunocompetent mice in comparison with susceptibility models, as well as the stimuli that still drive skin DCs mobilization 3 days after the infection.

5. CONCLUSIONS

- *Zika virus* (ZIKV) does not establish a functional infection in human neutrophils;
- Human neutrophils are non responsive to ZIKV;
- ZIKV infection does not provide a favorable environment for human neutrophil migration;
- Neutrophil depletion does not alter ZIKV titers in the draining lymph node (dLN) from immunocompetent mice;
- Neutrophils are recruited to the dLN after 3 days of flavivirus subcutaneous infection in immunocompetent mice, as other inflammatory populations;
- Neutrophils identified in the dLN of ZIKV-infected mice 3 days after infection do not migrate from skin;
- ZIKV and DENV induced migration of CD103⁺CD11b^{high}EpCAM^{low} skin DCs and downregulation of MHC-II in general skin DCs;
- Replication-competent *vaccinia virus* (VACV) inhibits skin dendritic cells (DCs) migration to dLNs;
- The VACV-suppressive effect is a general phenomenon of VACV infection in the skin;
- VACV can dampen the skin DCs migration to secondary challenges;
- Skin localized inflammatory responses at the site of infection associated with BCG-triggered skin DCs migration are absent in response to VACV;
- Replication-deficient VACV trigger DCs migration by a different pathway than IL-1;
- VACV can access the LNs in the absence of DCs transport and prime CD4⁺ T cells.

Understanding how inflammation and T cell response are initiated during viral challenge can be the base for improving viral treatments or vaccines in a time of viral pandemics. Curiously in this work, two different viral models and infection models, questioned very classical statements of immunology: neutrophils are the first line of defense against infections and DCs migrate to LN to prime T cells.

5.1 PERSPECTIVES

Listed below are some ideas and questions that remain unexplored and that might be tackled in the future:

1. Compare ZIKV-neutrophil *in vivo* results with the cell response to other flavivirus infection (such as DENV, YFV and WNV);
2. To use the IFN receptor deficient mouse model to assess neutrophil responses during ZIKV infection (depletion assay, viral spreading, neutrophil migration to infection site);
3. Do murine neutrophils replicate flavivirus?
4. How does neutrophil behave in the presence of *A. aegypti* saliva?
5. Does ZIKV infection increase in neutrophils in the presence of immunocomplex with DENV immune sera?
6. Are there differences in neutrophil susceptibility to ZIKV in pregnant women?
7. Improvement of the co-culture model, e.g. extending it to other relevant cell lineages;
8. How is leukocytes migration and LNs cell population in shorter time points after flavivirus infection?
9. Does VACV act directly in skin DCs inhibiting their migration or is it an environmental response?
10. Does VACV infect skin or pLN cells?
11. Does i-VACV/MVA migrate in IFN α / β knockout mice?
12. Are skin DCs viable after VACV infection?
13. Do skin DCs express CD80 and CD86 after VACV infection?
14. What are the differences in the ensuing adaptive immunity between VACV (no skin DCs migration) and BCG (skin DCs mobilization)?

Provisional titles of manuscripts in preparation:

- IL-1 Regulates *Mycobacterium bovis* BCG-Triggered Skin Dendritic Cell Migration to Draining Lymph Node via Production of COX-Derived PGE₂;
- Trypanosomatid Microvesicles as Immunogenic Potential in Chagas disease.

6. REFERENCES

- ABADIE, V. et al. Neutrophils rapidly migrate via lymphatics after Mycobacterium bovis BCG intradermal vaccination and shuttle live bacilli to the draining lymph nodes. **Blood**, v. 106, n. 5, p. 1843–1850, 2005.
- ABADIE, V. et al. Original Encounter with Antigen Determines Antigen-Presenting Cell Imprinting of the Quality of the Immune Response in Mice. **PLoS ONE**, v. 4, n. 12, p. e8159, 2009.
- ABDALLAH, D. S. A. et al. Mouse neutrophils are professional antigen-presenting cells programmed to instruct Th1 and Th17 T-cell differentiation. **International Immunology**, v. 23, n. 5, p. 317–326, 2011.
- AGGIO, J. B. et al. Vaccinia Virus Infection Inhibits Skin Dendritic Cell Migration to the Draining Lymph Node. **The Journal of Immunology**, v. 206, n. 4, p. 776–784, 2021.
- AID, M. et al. Zika Virus Persistence in the Central Nervous System and Lymph Nodes of Rhesus Monkeys. **Cell**, v. 169, n. 4, p. 610–620, 2017.
- AKK, A.; SPRINGER, L. E.; PHAM, C. T. N. Neutrophil Extracellular Traps Enhance Early Inflammatory Response in Sendai Virus-Induced Asthma Phenotype. **Frontiers in Immunology**, v. 7, p. 325, 2016.
- ALFARO, C. et al. Dendritic Cells Take up and Present Antigens from Viable and Apoptotic Polymorphonuclear Leukocytes. **PLoS ONE**, v. 6, n. 12, p. e29300, 2011.
- ALIOTA, M. T. et al. Characterization of Lethal Zika Virus Infection in AG129 Mice. **PLoS Neglected Tropical Diseases**, v. 10, n. 4, p. e0004682, 2016.
- ASSIL, S. et al. Plasmacytoid Dendritic Cells and Infected Cells Form an Interferogenic Synapse Required for Antiviral Responses. **Cell Host and Microbe**, v. 25, n. 5, p. 730–745, 2019.
- AYALA-NUNEZ, N. V. et al. Zika virus enhances monocyte adhesion and transmigration favoring viral dissemination to neural cells. **Nature Communications**, v. 10, n. 1, p. 4430, 2019.
- BAI, F. et al. A Paradoxical Role for Neutrophils in the Pathogenesis of West Nile Virus. **The Journal of Infectious Diseases**, v. 202, n. 12, p. 1804–1812, 2010.
- BARNES, B. J. et al. Targeting potential drivers of COVID-19: Neutrophil extracellular traps. **Journal of Experimental Medicine**, v. 217, n. 6, p. e20200652, 2020.
- BAYER, A. et al. Type III Interferons Produced by Human Placental Trophoblasts Confer Protection against Zika Virus Infection. **Cell Host and Microbe**, v. 19, n. 5, p. 705–712, 2016.
- BEAUVILLAIN, C. et al. Neutrophils efficiently cross-prime naive T cells in vivo. **Blood**, v. 110, n. 8, p. 2965–2973, 2007.
- BEAUVILLAIN, C. et al. CCR7 is involved in the migration of neutrophils to lymph nodes. **Blood**, v. 117, n. 4, p. 1196–1204, 2011.
- BOLLAMPALLI, V. P. et al. BCG Skin Infection Triggers IL-1R-MyD88-Dependent Migration of EpCAM^{low} CD11b^{high} Skin Dendritic cells to Draining Lymph Node During CD4⁺ T-Cell Priming. **PLoS Pathogens**, v. 11, n. 10, p. e1005206, 2015.

- BOLLAMPALLI, V. P.; NYLÉN, S.; ROTHFUCHS, A. G. A CFSE-based Assay to Study the Migration of Murine Skin Dendritic Cells into Draining Lymph Nodes During Infection with *Mycobacterium bovis* Bacille Calmette-Guérin. **Journal of Visualized Experiments**, v. 2016, n. 116, p. e54620, 2016.
- BONNEAU, M. et al. Migratory monocytes and granulocytes are major lymphatic carriers of *Salmonella* from tissue to draining lymph node. **Journal of Leukocyte Biology**, v. 79, n. 2, p. 268–276, 2006.
- BOS, S. et al. Zika Virus Inhibits IFN- α Response by Human Plasmacytoid Dendritic Cells and Induces NS1-Dependent Triggering of CD303 (BDCA-2) Signaling. **Frontiers in Immunology**, v. 11, p. 582061, 2020.
- BOWEN, J. R. et al. Zika Virus Antagonizes Type I Interferon Responses during Infection of Human Dendritic Cells. **PLoS Pathogens**, v. 13, n. 2, p. e1006164, 2017.
- BRASIL, P. et al. Zika Virus Infection in Pregnant Women in Rio de Janeiro. **New England Journal of Medicine**, v. 375, n. 24, p. 2321–2334, 2016.
- BRINKMANN, V. et al. Neutrophil Extracellular Traps Kill Bacteria. **Science**, v. 303, n. 5663, p. 1532–1535, 2004.
- BUCKLEY, C. D. et al. Identification of a phenotypically and functionally distinct population of long-lived neutrophils in a model of reverse endothelial migration. **Journal of Leukocyte Biology**, v. 79, n. 2, p. 303–311, 2006.
- CAMP, J. V.; JONSSON, C. B. A Role for Neutrophils in Viral Respiratory Disease. **Frontiers in Immunology**, v. 8, p. 550, 2017.
- CAMPOS, G. S. et al. New Challenge for Zika Virus Infection: Human Reservoirs? **Viral Immunology**, v. 00, n. 00, p. 1–4, 2020.
- CAO-LORMEAU, V. M. et al. Guillain-Barré Syndrome outbreak associated with Zika virus infection in French Polynesia: a case-control study. **Lancet**, v. 387, n. 10027, p. 1531–1539, 2016.
- CASTAÑEDA-SÁNCHEZ, J. I. et al. Expression of Antimicrobial Peptides in Human Monocytic Cells and Neutrophils in Response to Dengue Virus Type 2. **Intervirology**, v. 59, n. 1, p. 8–19, 2016.
- CATANEO, A. H. D. et al. The citrus flavonoid naringenin impairs the in vitro infection of human cells by Zika virus. **Scientific Reports**, v. 9, p. 16348, 2019.
- CHAUDHARY, V. et al. Selective Activation of Type II Interferon Signaling by Zika Virus NS5 Protein. **Journal of Virology**, v. 91, n. 14, p. e00163-17, 2017.
- CHAZAL, M. et al. RIG-I Recognizes the 5' Region of Dengue and Zika Virus Genomes. **Cell Reports**, v. 24, n. 2, p. 320–328, 2018.
- CHEN, J. et al. AXL promotes Zika virus infection in astrocytes by antagonizing type I interferon signalling. **Nature Microbiology**, v. 3, n. 3, p. 302–309, 2018.
- CHTANOVA, T. et al. Dynamics of Neutrophil Migration in Lymph Nodes during Infection. **Immunity**, v. 29, n. 3, p. 487–496, 2008.
- CINATL, J. et al. Decreased Neutrophil Adhesion to Human Cytomegalovirus-Infected Retinal Pigment Epithelial Cells Is Mediated by Virus-Induced Up-Regulation of Fas Ligand

- Independent of Neutrophil Apoptosis. **The Journal of Immunology**, v. 165, n. 8, p. 4405–4413, 2000.
- COFFEY, L. L. et al. Zika Virus Tissue and Blood Compartmentalization in Acute Infection of Rhesus Macaques. **PLoS ONE**, v. 12, n. 1, p. e0171148, 2017.
- CORTJENS, B. et al. Neutrophil extracellular traps cause airway obstruction during respiratory syncytial virus disease. **Journal of Pathology**, v. 238, n. 3, p. 401–411, 2016a.
- CORTJENS, B. et al. Pneumovirus-Induced Lung Disease in Mice Is Independent of Neutrophil-Driven Inflammation. **PLoS ONE**, v. 11, n. 12, p. e0168779, 2016b.
- COSTANTINI, C. et al. Human neutrophils interact with both 6-sulfo LacNAc⁺ DC and NK cells to amplify NK-derived IFN γ : Role of CD18, ICAM-1, and ICAM-3. **Blood**, v. 117, n. 5, p. 1677–1686, 2011.
- COSTELLO, A. et al. Defining the syndrome associated with congenital Zika virus infection. **Bulletin of the World Health Organization**, v. 94, n. 6, p. 406- 406A, 2016.
- DA SILVA, M. H. M. et al. Innate immune response in patients with acute Zika virus infection. **Medical Microbiology and Immunology**, v. 208, n. 6, p. 703–714, 2019.
- DAMASO, C. R. Revisiting Jenner’s mysteries, the role of the Beaugency lymph in the evolutionary path of ancient smallpox vaccines. **The Lancet Infectious Diseases**, v. 18, n. 2, p. e55–e63, 2018.
- DANG, J. et al. Zika Virus Depletes Neural Progenitors in Human Cerebral Organoids through Activation of the Innate Immune Receptor TLR3. **Cell Stem Cell**, v. 19, n. 2, p. 258–265, 2016.
- DE NORONHA, L. et al. Zika virus damages the human placental barrier and presents marked fetal neurotropism. **Memorias do Instituto Oswaldo Cruz**, v. 111, n. 5, p. 287–293, 2016.
- DENG, Y. et al. Neutrophil-Airway Epithelial Interactions Result in Increased Epithelial Damage and Viral Clearance during Respiratory Syncytial Virus Infection. **Journal of Virology**, v. 94, n. 13, p. e02161-19, 2020.
- DEVIGNOT, S. et al. Genome-Wide Expression Profiling Deciphers Host Responses Altered during Dengue Shock Syndrome and Reveals the Role of Innate Immunity in Severe Dengue. **PLoS ONE**, v. 5, n. 7, p. e11671, 2010.
- DOHERTY, T. M.; ANDERSEN, P. Vaccines for Tuberculosis: Novel Concepts and Recent Progress. **Clinical Microbiology Reviews**, v. 18, n. 4, p. 687–702, 2005.
- DONALD, C. L. et al. Full Genome Sequence and sfRNA Interferon Antagonist Activity of Zika Virus from Recife, Brazil. **PLoS Neglected Tropical Diseases**, v. 10, n. 10, p. e0005048, 2016.
- DOWALL, S. D. et al. A Susceptible Mouse Model for Zika Virus Infection. **PLoS Neglected Tropical Diseases**, v. 10, n. 5, p. e0004658, 2016.
- DRESCHER, B.; BAI, F. Neutrophil in viral infections, Friend or foe? **Virus Research**, v. 171, n. 1, p. 1–7, 2013.
- DUDLEY, D. M. et al. A rhesus macaque model of Asian-lineage Zika virus infection. **Nature Communications**, v. 7, p. 12204, 2016.

- DUFFY, D. et al. Neutrophils Transport Antigen from the Dermis to the Bone Marrow, Initiating a Source of Memory CD8+ T Cells. **Immunity**, v. 37, n. 5, p. 917–929, 2012.
- ESSER-NOBIS, K. et al. Comparative Analysis of African and Asian Lineage-Derived Zika Virus Strains Reveals Differences in Activation of and Sensitivity to Antiviral Innate Immunity. **Journal of Virology**, v. 93, n. 13, p. e:00640-19, 2019.
- FARIA, N. R. et al. Zika virus in the Americas: Early epidemiological and genetic findings. **Science**, v. 352, n. 6283, p. 345–349, 2016.
- FEARS, J. R. The plague under Marcus Aurelius and the decline and fall of the Roman Empire. **Infectious Disease Clinics of North America**, v. 18, n. 1, p. 65–77, 2004.
- FILARDY, A. A. et al. Proinflammatory Clearance of Apoptotic Neutrophils Induces an IL-12low IL-10high Regulatory Phenotype in Macrophages. **The Journal of Immunology**, v. 185, n. 4, p. 2044–2050, 2010.
- FINK, K. et al. Depletion of macrophages in mice results in higher dengue virus titers and highlights the role of macrophages for virus control. **European Journal of Immunology**, v. 39, n. 10, p. 2809–2821, 2009.
- FISCHER, M. A. et al. CD11b+, Ly6G+ Cells Produce Type I Interferon and Exhibit Tissue Protective Properties Following Peripheral Virus Infection. **PLoS Pathogens**, v. 7, n. 11, p. e1002374, 2011.
- FOO, S.-S. et al. Asian Zika virus strains target CD14+ blood monocytes and induce M2-skewed immunosuppression during pregnancy. **Nature Microbiology**, v. 2, n. 11, p. 1558–1570, 2017.
- FUNCHAL, G. A. et al. Respiratory Syncytial Virus Fusion Protein promotes TLR-4-Dependent Neutrophil Extracellular Trap Formation by Human Neutrophils. **PLoS ONE**, v. 10, n. 4, p. e0124082, 2015.
- GALANI, I. E.; ANDREAKOS, E. Neutrophils in viral infections: Current concepts and caveats. **Journal of Leukocyte Biology**, v. 98, n. 4, p. 557–564, 2015.
- GARCÍA-NICOLÁS, O. et al. Monocyte-Derived Dendritic Cells as Model to Evaluate Species Tropism of Mosquito-Borne Flaviviruses. **Frontiers in Cellular and Infection Microbiology**, v. 9, p. 5, 2019.
- GIRALDO, D. M. et al. HIV-1–neutrophil interactions trigger neutrophil activation and Toll-like receptor expression. **Immunologic Research**, v. 64, n. 1, p. 93–103, 2016.
- GORLINO, C. V. et al. Neutrophils Exhibit Differential Requirements for Homing Molecules in Their Lymphatic and Blood Trafficking into Draining Lymph Nodes. **The Journal of Immunology**, v. 193, n. 4, p. 1966–1974, 2014.
- GOSSELIN, J. et al. Epstein-Barr virus primes human polymorphonuclear leucocytes for the biosynthesis of leukotriene B4. **Clinical and Experimental Immunology**, v. 126, n. 3, p. 494–502, 2001.
- GRUNDY, J. E. et al. Cytomegalovirus-infected endothelial cells recruit neutrophils by the secretion of C-X-C chemokines and transmit virus by direct neutrophil- endothelial cell contact and during neutrophil transendothelial migration. **Journal of Infectious Diseases**, v. 177, n. 6, p. 1465–1474, 1998.
- HADAD, N. et al. Direct Effect of Human Immunodeficiency Virus Protease Inhibitors on

- Neutrophil Function and Apoptosis via Calpain Inhibition. **Clinical and Vaccine Immunology**, v. 14, n. 11, p. 1515–1521, 2007.
- HAICK, A. K. et al. Neutrophils are needed for an effective immune response against pulmonary rat coronavirus infection, but also contribute to pathology. **Journal of General Virology**, v. 95, n. PART3, p. 578–590, 2014.
- HALFHIDE, C. P. et al. Respiratory Syncytial Virus Binds and Undergoes Transcription in Neutrophils From the Blood and Airways of Infants With Severe Bronchiolitis. **Journal of Infectious Diseases**, v. 204, n. 3, p. 451–458, 2011.
- HAMEL, R. et al. Biology of Zika Virus Infection in Human Skin Cells. **Journal of Virology**, v. 89, n. 17, p. 8880–8896, 2015.
- HAMPTON, H. R. et al. Microbe-dependent lymphatic migration of neutrophils modulates lymphocyte proliferation in lymph nodes. **Nature Communications**, v. 6, p. 7139, 2015.
- HAMPTON, H. R.; CHTANOVA, T. Lymphatic Migration of Immune Cells. **Frontiers in Immunology**, v. 10, p. 19–23, 2019.
- HASTINGS, A. K. et al. Aedes aegypti NeSt1 Protein Enhances Zika Virus Pathogenesis by Activating Neutrophils. **Journal of Virology**, v. 93, n. 13, p. e:00395-19, 2019.
- HAYASHIDA, E. et al. Zika virus encephalitis in immunocompetent mice is dominated by innate immune cells and does not require T or B cells. **Journal of Neuroinflammation**, v. 16, n. 1, p. 177, 2019.
- HEIT, B. et al. HIV and Other Lentiviral Infections Cause Defects in Neutrophil Chemotaxis, Recruitment, and Cell Structure: Immunorestorative Effects of Granulocyte-Macrophage Colony-Stimulating Factor. **The Journal of Immunology**, v. 177, n. 9, p. 6405–6414, 2006.
- HENRI, S. et al. Disentangling the complexity of the skin dendritic cell network. **Immunology and Cell Biology**, v. 88, n. 4, p. 366–375, 2010.
- HERBERT, J. A. et al. β 2-integrin LFA1 mediates airway damage following neutrophil trans-epithelial migration during respiratory syncytial virus infection. **European Respiratory Journal**, v. 56, n. 2, p. 1902216, 2020.
- HERTZOG, J. et al. Infection with a Brazilian isolate of Zika virus generates RIG-I stimulatory RNA and the viral NS5 protein blocks type I IFN induction and signaling. **European Journal of Immunology**, v. 48, n. 7, p. 1120–1136, 2018.
- HIROKI, C. H. et al. Neutrophil Extracellular Traps Effectively Control Acute Chikungunya Virus Infection. **Frontiers in Immunology**, v. 10, p. 3108, 2020.
- HIRSCH, A. J. et al. Zika Virus infection of rhesus macaques leads to viral persistence in multiple tissues. **PLoS Pathogens**, v. 13, n. 3, p. e1006219, 2017.
- HIRSCH, A. J. et al. Zika virus infection in pregnant rhesus macaques causes placental dysfunction and immunopathology. **Nature Communications**, v. 9, n. 1, p. 263, 2018.
- HOANG, L. T. et al. The Early Whole-Blood Transcriptional Signature of Dengue Virus and Features Associated with Progression to Dengue Shock Syndrome in Vietnamese Children and Young Adults. **Journal of Virology**, v. 84, n. 24, p. 12982–12994, 2010.
- HU, S. et al. Hepatitis B Virus Inhibits Neutrophil Extracellular Trap Release by Modulating Reactive Oxygen Species Production and Autophagy. **The Journal of Immunology**, v. 202,

n. 3, p. 805–815, 2019.

HUFFORD, M. M. et al. Influenza-Infected Neutrophils within the Infected Lungs Act as Antigen Presenting Cells for Anti-Viral CD8+ T Cells. **PLoS ONE**, v. 7, n. 10, p. e46581, 2012.

ISHIKAWA, H. et al. Influenza virus infection causes neutrophil dysfunction through reduced G-CSF production and an increased risk of secondary bacteria infection in the lung. **Virology**, v. 499, p. 23–29, 2016.

JACOBS, B. L. et al. Vaccinia virus vaccines: Past, present and future. **Antiviral Research**, v. 84, n. 1, p. 1–13, 2009.

JAEGER, B. N. et al. Neutrophil depletion impairs natural killer cell maturation, function, and homeostasis. **Journal of Experimental Medicine**, v. 209, n. 3, p. 565–580, 2012.

JAOVISIDHA, P. et al. Respiratory syncytial virus stimulates neutrophil degranulation and chemokine release. **Journal of immunology (Baltimore, Md. : 1950)**, v. 163, n. 5, p. 2816–20, 1999.

JASPERSE, B. et al. Single dose of a replication-defective vaccinia virus expressing Zika virus-like particles is protective in mice. **Scientific Reports**, v. 11, p. 6492, 2021.

JENNE, C. N. et al. Neutrophils Recruited to Sites of Infection Protect from Virus Challenge by Releasing Neutrophil Extracellular Traps. **Cell Host and Microbe**, v. 13, n. 2, p. 169–180, 2013.

JONES, J. F. Interactions between Human Neutrophils and Vaccinia Virus: Induction of Oxidative Metabolism and Virus Inactivation. **Pediatric Research**, v. 16, n. 7, p. 525–529, 1982.

JORGE, T. R. et al. Isolation and characterization of a Brazilian strain of yellow fever virus from an epizootic outbreak in 2009. **Acta Tropica**, v. 166, p. 114–120, 2017.

JUFFRIE, M. et al. Inflammatory Mediators in Dengue Virus Infection in Children: Interleukin-8 and Its Relationship to Neutrophil Degranulation. **Infection and Immunity**, v. 68, n. 2, p. 702–707, 2000.

JURADO, K. A. et al. Zika virus productively infects primary human placenta-specific macrophages. **JCI Insight**, v. 1, n. 13, p. e:88461, 2016.

KAM, Y.-W. et al. Specific Biomarkers Associated With Neurological Complications and Congenital Central Nervous System Abnormalities From Zika Virus-Infected Patients in Brazil. **The Journal of Infectious Diseases**, v. 216, n. 2, p. 172–181, 2017.

KAMENYEVA, O. et al. Neutrophil Recruitment to Lymph Nodes Limits Local Humoral Response to Staphylococcus aureus. **PLoS Pathogens**, v. 11, n. 4, p. e1004827, 2015.

KASTENMÜLLER, W. et al. A Spatially-Organized Multicellular Innate Immune Response in Lymph Nodes Limits Systemic Pathogen Spread. **Cell**, v. 150, n. 6, p. 1235–1248, 2012.

KENNY, E. F. et al. Diverse stimuli engage different neutrophil extracellular trap pathways. **eLife**, v. 6, p. e24437, 2017.

KHAIBOULLINA, S. F. et al. ZIKV infection regulates inflammasomes pathway for replication in monocytes. **Scientific Reports**, v. 7, p. 16050, 2017.

- KHAIBOULLINA, S. F. et al. Host immune Response to ZIKV in an Immunocompetent Embryonic Mouse Model of Intravaginal Infection. **Viruses**, v. 11, n. 6, p. 558, 2019.
- KIRSEBOM, F. et al. Neutrophils do not impact viral load or the peak of disease severity during RSV infection. **Scientific Reports**, v. 10, p. 1110, 2020.
- KOLACZKOWSKA, E.; KUBES, P. Neutrophil recruitment and function in health and inflammation. **Nature Reviews Immunology**, v. 13, n. 3, p. 159–175, 2013.
- KRUGER, P. et al. Neutrophils: Between Host Defence, Immune Modulation, and Tissue Injury. **PLoS Pathogens**, v. 11, n. 3, p. e1004651, 2015.
- KUBES, P. et al. In Vivo Impairment of Neutrophil Recruitment during Lentivirus Infection. **The Journal of Immunology**, v. 171, n. 9, p. 4801–4808, 2003.
- KUMAR, A. et al. Zika virus inhibits type-I interferon production and downstream signaling. **EMBO reports**, v. 17, n. 12, p. 1766–1775, 2016.
- KUSHWAH, R.; HU, J. Complexity of dendritic cell subsets and their function in the host immune system. **Immunology**, v. 133, n. 4, p. 409–419, 2011.
- LAROCHELLE, B. et al. Epstein-Barr Virus Infects and Induces Apoptosis in Human Neutrophils. **Blood**, v. 92, n. 1, p. 291–299, 1998.
- LAZEAR, H. M. et al. A Mouse Model of Zika Virus Pathogenesis. **Cell Host and Microbe**, v. 19, n. 5, p. 720–730, 2016.
- LAZEAR, H. M.; DIAMOND, M. S. Zika Virus: New Clinical Syndromes and Its Emergence in the Western Hemisphere. **Journal of Virology**, v. 90, n. 10, p. 4864–4875, 2016.
- LEE, E.; LOBIGS, M. E Protein Domain III Determinants of Yellow Fever Virus 17D Vaccine Strain Enhance Binding to Glycosaminoglycans, Impede Virus Spread, and Attenuate Virulence. **Journal of Virology**, v. 82, n. 12, p. 6024–6033, 2008.
- LEPPKES, M. et al. Vascular occlusion by neutrophil extracellular traps in COVID-19. **EBioMedicine**, v. 58, p. 102925, 2020.
- LI, M. et al. Dengue immune sera enhance Zika virus infection in human peripheral blood monocytes through Fc gamma receptors. **PLoS ONE**, v. 13, n. 7, p. e:0200478, 2018.
- LIU, K. T. et al. Serum neutrophil gelatinase-associated lipocalin and resistin are associated with dengue infection in adults. **BMC Infectious Diseases**, v. 16, p. 441, 2016.
- LIU, L. et al. Protection of ZIKV infection-induced neuropathy by abrogation of acute antiviral response in human neural progenitors. **Cell Death and Differentiation**, v. 26, n. 12, p. 2607–2621, 2019.
- LIU, Z. Y.; SHI, W. F.; QIN, C. F. The evolution of Zika virus from Asia to the Americas. **Nature Reviews Microbiology**, v. 17, n. 3, p. 131–139, 2019.
- LUCAS, C. G. O. et al. Critical role of CD4+ T cells and IFN γ signaling in antibody-mediated resistance to Zika virus infection. **Nature Communications**, v. 9, n. 1, p. 3136, 2018.
- LUM, F. et al. Zika Virus Infection Preferentially Counterbalances Human Peripheral Monocyte and/or NK Cell Activity. **mSphere**, v. 3, n. 2, p. e00120-18, 2018a.
- LUM, F. M. et al. Longitudinal Study of Cellular and Systemic Cytokine Signatures to Define

the Dynamics of a Balanced Immune Environment During Disease Manifestation in Zika Virus–Infected Patients. **The Journal of Infectious Diseases**, v. 218, n. 5, p. 814–824, 2018b.

LUM, F. M. et al. Immunological observations and transcriptomic analysis of trimester-specific full-term placentas from three Zika virus-infected women. **Clinical and Translational Immunology**, v. 8, n. 11, p. e1082, 2019.

LUO, H. et al. Zika, dengue and yellow fever viruses induce differential anti-viral immune responses in human monocytic and first trimester trophoblast cells. **Antiviral Research**, v. 151, p. 55–62, 2018.

MALEKSHAHI, Z. et al. Interference of the Zika Virus E-Protein With the Membrane Attack Complex of the Complement System. **Frontiers in Immunology**, v. 11, p. 569449, 2020.

MANANGEESWARAN, M.; IRELAND, D. D. C.; VERTHELYI, D. Zika (PRVABC59) Infection Is Associated with T cell Infiltration and Neurodegeneration in CNS of Immunocompetent Neonatal C57Bl/6 Mice. **PLoS Pathogens**, v. 12, n. 11, p. e1006004, 2016.

MANTOVANI, A. et al. Neutrophils in the activation and regulation of innate and adaptive immunity. **Nature Reviews Immunology**, v. 11, n. 8, p. 519–531, 2011.

MAYADAS, T. N.; CULLERE, X.; LOWELL, C. A. The Multifaceted Functions of Neutrophils. **Annual Review of Pathology: Mechanisms of Disease**, v. 9, p. 181–218, 2014.

MAYER-BARBER, K. D. et al. Innate and Adaptive Interferons Suppress IL-1 α and IL-1 β Production by Distinct Pulmonary Myeloid Subsets during Mycobacterium tuberculosis Infection. **Immunity**, v. 35, n. 6, p. 1023–1034, 2011.

MCDONALD, E. M. et al. Infection of epididymal epithelial cells and leukocytes drives seminal shedding of Zika virus in a mouse model. **PLoS Neglected Tropical Diseases**, v. 12, n. 8, p. e0006691, 2018.

MCDONALD, E. M. et al. Zika virus replication in myeloid cells during acute infection is vital to viral dissemination and pathogenesis in a mouse model. **Journal of Virology**, v. 94, n. 21, p. e00838-20, 2020.

MEIER, K. C. et al. A mouse model for Studying Viscerotropic Disease Caused by Yellow Fever Virus Infection. **PLoS Pathogens**, v. 5, n. 10, p. e1000614, 2009.

MICHLMAYR, D. et al. CD14+CD16+ monocytes are the main target of Zika virus infection in peripheral blood mononuclear cells in a paediatric study in Nicaragua. **Nature Microbiology**, v. 2, n. 11, p. 1462–1470, 2017.

MIDDLETON, E. A. et al. Neutrophil Extracellular Traps (NETs) Contribute to Immunothrombosis in COVID-19 Acute Respiratory Distress Syndrome. **Blood**, v. 136, n. 10, p. 1169–1179, 2020.

MINISTÉRIO DA SAÚDE. Monitoramento dos casos de dengue, febre de chikungunya e febre pelo vírus Zika até a Semana Epidemiológica 52, 2015. **Boletim Epidemiológico Arboviroses**, v. 47, n. 3, p. 1–10, 2016.

MINISTÉRIO DA SAÚDE. Monitoramento dos casos de dengue, febre de chikungunya e febre pelo vírus Zika até a Semana Epidemiológica 52, 2016. **Boletim Epidemiológico Arboviroses**, v. 48, n. 3, p. 1–11, 2017.

MINISTÉRIO DA SAÚDE. Monitoramento dos casos de dengue, febre de chikungunya e

- febre pelo vírus Zika até a Semana Epidemiológica 52, 2017. **Boletim Epidemiológico Arboviroses**, v. 49, n. 2, p. 1–13, 2018.
- MINISTÉRIO DA SAÚDE. Síndrome congênita pelo vírus Zika associada à infecção - situação epidemiológica, ações desenvolvidas e desafios de 2015 a 2019. **Boletim Epidemiológico Arboviroses**, 2019a.
- MINISTÉRIO DA SAÚDE. Monitoramento dos casos de dengue, febre de chikungunya e doença aguda pelo vírus Zika até a Semana Epidemiológica 52, 2018. **Boletim Epidemiológico Arboviroses**, v. 50, n. 4, p. 1–14, 2019b.
- MINISTÉRIO DA SAÚDE. Monitoramento dos casos de arboviroses urbanas transmitidas pelo Aedes (dengue, chikungunya e Zika), Semanas Epidemiológicas 01 a 52, 2019. **Boletim Epidemiológico Arboviroses**, v. 51, n. 2, p. 1–16, 2020.
- MINISTÉRIO DA SAÚDE. Monitoramento dos casos de arboviroses urbanas causados por vírus transmitidos por Aedes (dengue, chikungunya e zika), semanas epidemiológicas 1 a 53, 2020. **Boletim Epidemiológico Arboviroses**, v. 52, n. 03, p. 1–31, 2021a.
- MINISTÉRIO DA SAÚDE. Monitoramento dos casos de arboviroses urbanas causados por vírus transmitidos pelo mosquito Aedes (dengue, chikungunya e zika), semanas epidemiológicas 1 a 14, 2021. **Boletim Epidemiológico Arboviroses**, v. 52, n. 18, p. 1–24, 2021b.
- MURARO, S. P. et al. Respiratory Syncytial Virus induces the classical ROS-dependent NETosis through PAD-4 and necroptosis pathways activation. **Scientific Reports**, v. 8, n. 1, p. 14166, 2018.
- NARASARAJU, T. et al. Excessive Neutrophils and Neutrophil Extracellular Traps Contribute to Acute Lung Injury of Influenza Pneumonitis. **American Journal of Pathology**, v. 179, n. 1, p. 199–210, 2011.
- NEUFELDT, C. J. et al. Rewiring cellular networks by members of the Flaviviridae family. **Nature Reviews Microbiology**, v. 16, n. 3, p. 125–142, 2018.
- NGONO, A. E.; SHRESTA, S. Immune Response to Dengue and Zika. **Annual Review of Immunology**, v. 36, p. 279–308, 2018.
- NGUYEN, S. M. et al. Highly efficient maternal-fetal Zika virus transmission in pregnant rhesus macaques. **PLoS Pathogens**, v. 13, n. 5, p. e1006378, 2017.
- NOVKOVIC, M. et al. Topological Structure and Robustness of the Lymph Node Conduit System. **Cell Reports**, v. 30, n. 3, p. 893- 904.e6, 2020.
- O'CONNOR, M. A. et al. Early cellular innate immune responses drive Zika viral persistence and tissue tropism in pigtail macaques. **Nature Communications**, v. 9, p. 3371, 2018.
- OPASAWATCHAI, A. et al. Neutrophil Activation and Early Features of NET Formation Are Associated With Dengue Virus Infection in Human. **Frontiers in Immunology**, v. 10, p. 3007, 2019.
- ÖSTERLUND, P. et al. Asian and African lineage Zika viruses show differential replication and innate immune responses in human dendritic cells and macrophages. **Scientific Reports**, v. 9, p. 15710, 2019.
- OSUNA, C. E. et al. Zika viral dynamics and shedding in rhesus and cynomolgus macaques. **Nature Medicine**, v. 22, n. 12, p. 1448–1455, 2016.

- PALHA, N. et al. Real-Time Whole-Body Visualization of Chikungunya Virus Infection and Host Interferon Response in Zebrafish. **PLoS Pathogens**, v. 9, n. 9, p. e1003619, 2013.
- PANTOJA, P. et al. Zika virus pathogenesis in rhesus macaques is unaffected by pre-existing immunity to dengue virus. **Nature Communications**, v. 8, p. 15674, 2017.
- PAPAYANNOPOULOS, V. Neutrophil extracellular traps in immunity and disease. **Nature Reviews Immunology**, v. 18, n. 2, p. 134–147, 2018.
- PAUL, A. M. et al. Osteopontin facilitates West Nile virus neuroinvasion via neutrophil “Trojan horse” transport. **Scientific Reports**, v. 7, p. 4722, 2017.
- PEI, X. et al. Inhibition of innate immune response ameliorates Zika virus-induced neurogenesis deficit in human neural stem cells. **PLoS Neglected Tropical Diseases**, v. 15, n. 3, p. e0009183, 2021.
- PHUMEE, A. et al. Vertical transmission of Zika virus in *Culex quinquefasciatus* Say and *Aedes aegypti* (L.) mosquitoes. **Scientific Reports**, v. 9, p. 5257, 2019.
- PIERSON, T. C.; DIAMOND, M. S. The emergence of Zika virus and its new clinical syndromes. **Nature**, v. 560, n. 7720, p. 573–581, 2018.
- PIERSON, T. C.; DIAMOND, M. S. The continued threat of emerging flaviviruses. **Nature Microbiology**, v. 5, n. 6, p. 796–812, 2020.
- PINGEN, M. et al. Host Inflammatory Response to Mosquito Bites Enhances the Severity of Arbovirus Infection. **Immunity**, v. 44, n. 6, p. 1455–1469, 2016.
- PIRET, J.; BOIVIN, G. Pandemics Throughout History. **Frontiers in Microbiology**, v. 11, p. 631736, 2021.
- PIZZAGALLI, D. U. et al. Characterization of the Dynamic Behavior of Neutrophils Following Influenza Vaccination. **Frontiers in Immunology**, v. 10, p. 2621, 2019.
- PLATT, A. M.; RANDOLPH, G. J. Dendritic Cell Migration Through the Lymphatic Vasculature to Lymph Nodes. **Advances in Immunology**, v. 120, p. 51–68, 2013.
- PLEKHOVA, N. G. et al. Neutrophil Apoptosis Induction by Tick-Borne Encephalitis Virus. **Bulletin of Experimental Biology and Medicine**, v. 153, n. 1, p. 105–108, 2012.
- PRICE, P. J. R. et al. Complement Component C5 Recruits Neutrophils in the Absence of C3 during Respiratory Infection with Modified Vaccinia Virus Ankara. **The Journal of Immunology**, v. 194, n. 3, p. 1164–1168, 2015.
- PUGA, I. et al. B cell-helper neutrophils stimulate the diversification and production of immunoglobulin in the marginal zone of the spleen. **Nature Immunology**, v. 13, n. 2, p. 170–180, 2012.
- QUICKE, K. M. et al. Zika Virus Infects Human Placental Macrophages. **Cell Host and Microbe**, v. 20, n. 1, p. 83–90, 2016.
- RABELO, K. et al. Placental Inflammation and Fetal Injury in a Rare Zika Case Associated With Guillain-Barré Syndrome and Abortion. **Frontiers in Microbiology**, v. 9, p. 1018, 2018.
- RABELO, K. et al. Zika Virus Infects Human Placental Mast Cells and the HMC-1 Cell Line, and Triggers Degranulation, Cytokine Release and Ultrastructural Changes. **Cells**, v. 9, n. 4, p. 975, 2020.

- RAFTERY, M. J. et al. B2 integrin mediates hantavirus-induced release of neutrophil extracellular traps. **Journal of Experimental Medicine**, v. 211, n. 7, p. 1485–1497, 2014.
- RAJASAGI, N. K. et al. Controlling Herpes Simplex Virus-Induced Ocular Inflammatory Lesions with the Lipid-Derived Mediator Resolvin E1. **The Journal of Immunology**, v. 186, n. 3, p. 1735–1746, 2011.
- RANDOLPH, G. J.; ANGELI, V.; SWARTZ, M. A. Dendritic-Cell Trafficking to Lymph Nodes Through Lymphatic Vessels. **Nature Reviews Immunology**, v. 5, n. 8, p. 617–628, 2005.
- REYNOSO, G. V. et al. Lymph node conduits transport virions for rapid T cell activation. **Nature Immunology**, v. 20, n. 5, p. 602–612, 2019.
- RIGBY, D. A. et al. Neutrophils rapidly transit inflamed lymphatic vessel endothelium via integrin-dependent proteolysis and lipoxin-induced junctional retraction. **Journal of Leukocyte Biology**, v. 98, n. 6, p. 897–912, 2015.
- ROOZENDAAL, R.; MEBIUS, R. E.; KRAAL, G. The conduit system of the lymph node. **International Immunology**, v. 20, n. 12, p. 1483–1487, 2008.
- ROSSI, S. L. et al. Characterization of a Novel Murine Model to Study Zika Virus. **American Journal of Tropical Medicine and Hygiene**, v. 94, n. 6, p. 1362–1369, 2016.
- SAITOH, T. et al. Neutrophil Extracellular Traps Mediate a Host Defense Response to Human Immunodeficiency Virus-1. **Cell host & microbe**, v. 12, n. 1, p. 109–116, 2012.
- SCHIELA, B. et al. Active Human Complement Reduces the Zika Virus Load Via Formation of the Membrane-Attack Complex. **Frontiers in Immunology**, v. 9, p. 2177, 2018.
- SCHOUEST, B. et al. Immune outcomes of Zika virus infection in nonhuman primates. **Scientific Reports**, v. 10, p. 13069, 2020.
- SILVEIRA, E. L. V. et al. Immune Cell Dynamics in Rhesus Macaques Infected with a Brazilian Strain of Zika Virus. **The Journal of Immunology**, v. 199, n. 3, p. 1003–1011, 2017.
- SKENDROS, P. et al. Complement and tissue factor-enriched neutrophil extracellular traps are key drivers in COVID-19 immunothrombosis. **Journal of Clinical Investigation**, v. 130, n. 11, p. 6151–6157, 2020.
- SMITH, G. L. Vaccinia Virus. **Encyclopedia of Virology**, p. 243–250, 2008.
- SMITH, G. L. et al. Vaccinia virus immune evasion: mechanisms, virulence and immunogenicity. **Journal of General Virology**, v. 94, p. 2367–2392, 2013.
- SOUZA, P. S. S. et al. Neutrophil extracellular traps possess anti-human respiratory syncytial virus activity: Possible interaction with the viral F protein. **Virus Research**, v. 251, p. 68–77, 2018.
- SPÖRRI, R. et al. A Novel Role for Neutrophils As Critical Activators of NK Cells. **The Journal of Immunology**, v. 181, n. 10, p. 7121–7130, 2008.
- SRIVASTAVA, M. et al. Chemical proteomics tracks virus entry and uncovers NCAM1 as Zika virus receptor. **Nature Communications**, v. 11, p. 3896, 2016.
- SRIVASTAVA, S. et al. Degradation of Japanese encephalitis virus by neutrophils. **International Journal of Experimental Pathology**, v. 80, n. 1, p. 17–24, 1999.

- STRANDIN, T. et al. Neutrophil Activation in Acute Hemorrhagic Fever With Renal Syndrome Is Mediated by Hantavirus-Infected Microvascular Endothelial Cells. **Frontiers in Immunology**, v. 9, p. 2098, 2018.
- SUN, X. et al. Transcriptional Changes during Naturally Acquired Zika Virus Infection Render Dendritic Cells Highly Conducive to Viral Replication. **Cell Reports**, v. 21, n. 12, p. 3471–3482, 2017.
- SUN, X. et al. Immune-profiling of ZIKV-infected patients identifies a distinct function of plasmacytoid dendritic cells for immune cross-regulation. **Nature Communications**, v. 11, p. 2421, 2020.
- TABATA, T. et al. Zika Virus Targets Different Primary Human Placental Cells, Suggesting Two Routes for Vertical Transmission. **Cell Host and Microbe**, v. 20, n. 2, p. 155–166, 2016.
- TAKEUCHI, O.; AKIRA, S. Pattern Recognition Receptors and Inflammation. **Cell**, v. 140, n. 6, p. 805–820, 2010.
- TAPPE, D. et al. Cytokine kinetics of Zika virus-infected patients from acute to convalescent phase. **Medical Microbiology and Immunology**, v. 205, n. 3, p. 269–273, 2016.
- TATE, M. D. et al. Neutrophils Ameliorate Lung Injury and the Development of Severe Disease during Influenza Infection. **The Journal of Immunology**, v. 183, n. 11, p. 7441–7450, 2009.
- TATE, M. D. et al. The Role of Neutrophils during Mild and Severe Influenza Virus Infections of Mice. **PLoS ONE**, v. 6, n. 3, p. e17618, 2011.
- TECLE, T. et al. Human Neutrophil Defensins Increase Neutrophil Uptake of Influenza A Virus and Bacteria and Modify Virus-Induced Respiratory Burst Responses. **The Journal of Immunology**, v. 178, n. 12, p. 8046–8052, 2007.
- THEIN, T. L. et al. Short report: Severe Neutropenia in Dengue Patients: Prevalence and Significance. **American Journal of Tropical Medicine and Hygiene**, v. 90, n. 6, p. 984–987, 2014.
- TRIPATHI, S. et al. LL-37 modulates human neutrophil responses to influenza A virus. **Journal of Leukocyte Biology**, v. 96, n. 5, p. 931–938, 2014.
- TRIPATHI, S. et al. A novel Zika virus mouse model reveals strain specific differences in virus pathogenesis and host inflammatory immune responses. **PLoS Pathogens**, v. 13, n. 3, p. e1006258, 2017.
- TUMPEY, T. M. et al. Neutrophil-Mediated Suppression of Virus Replication after Herpes Simplex Virus Type 1 Infection of the Murine Cornea. **Journal of virology**, v. 70, n. 2, p. 898–904, 1996.
- TUMPEY, T. M. et al. Pathogenicity of Influenza Viruses with Genes from the 1918 Pandemic Virus: Functional Roles of Alveolar Macrophages and Neutrophils in Limiting Virus Replication and Mortality in Mice. **Journal of Virology**, v. 79, n. 23, p. 14933–14944, 2005.
- VAN DER LINDEN, M.; MEYAARD, L. Fine-tuning neutrophil activation: Strategies and consequences. **Immunology Letters**, v. 178, p. 3–9, 2016.
- VERAS, F. P. et al. SARS-CoV-2 triggered neutrophil extracellular traps (NETs) mediate

- COVID-19 pathology. **Journal of Experimental Medicine**, v. 217, n. 12, p. e20201129, 2020.
- VIELLE, N. J. et al. Silent infection of human dendritic cells by African and Asian strains of Zika virus. **Scientific Reports**, v. 8, p. 5440, 2018.
- WANG, J. P. et al. Toll-like receptor-mediated activation of neutrophils by influenza A virus. **Blood**, v. 112, n. 5, p. 2028–2034, 2008.
- WANG, W. et al. Zika virus infection induces host inflammatory responses by facilitating NLRP3 inflammasome assembly and interleukin-1 β secretion. **Nature Communications**, v. 9, p. 106, 2018.
- WEST, B. C. et al. Neutrophil Uptake of Vaccinia Virus in Vitro. **Journal of Infectious Diseases**, v. 156, n. 4, p. 597–606, 1987.
- WILDER-SMITH, A.; OSMAN, S. Public health emergencies of international concern: a historic overview. **Journal of Travel Medicine**, v. 27, n. 8, p. 1–13, 2020.
- WINKLER, C. W. et al. Placental Myeloid Cells Protect against Zika Virus Vertical Transmission in a Rag1-Deficient Mouse Model. **The Journal of Immunology**, v. 205, n. 1, p. 143–152, 2020.
- WOJTASIAK, M. et al. Depletion of Gr-1+, but not Ly6G+, immune cells exacerbates virus replication and disease in an intranasal model of herpes simplex virus type 1 infection. **Journal of General Virology**, v. 91, n. 9, p. 2158–2166, 2010.
- WORBS, T.; HAMMERSCHMIDT, S. I.; FÖRSTER, R. Dendritic cell migration in health and disease. **Nature Reviews Immunology**, v. 17, n. 1, p. 30–48, 2017.
- WU, Y. et al. Zika virus evades interferon-mediated antiviral response through the co-operation of multiple nonstructural proteins in vitro. **Cell Discovery**, v. 3, p. 17006, 2017.
- XU, D. et al. Gr-1+ Cells Other Than Ly6G+ Neutrophils Limit Virus Replication and Promote Myocardial Inflammation and Fibrosis Following Coxsackievirus B3 Infection of Mice. **Frontiers in Cellular and Infection Microbiology**, v. 8, p. 157, 2018.
- YANG, C.-W. et al. Neutrophils Influence the Level of Antigen Presentation during the Immune Response to Protein Antigens in Adjuvants. **The Journal of Immunology**, v. 185, n. 5, p. 2927–2934, 2010.
- YANG, W. et al. S100A4+ macrophages facilitate zika virus invasion and persistence in the seminiferous tubules via interferon-gamma mediation. **PLoS Pathogens**, v. 16, n. 12, p. e1009019, 2020.
- YOSHIKAWA, F. S. Y. et al. Zika Virus Infects Newborn Monocytes Without Triggering a Substantial Cytokine Response. **Journal of Infectious Diseases**, v. 220, n. 1, p. 32–40, 2019.
- ZANLUCA, C. et al. First report of autochthonous transmission of Zika virus in Brazil. **Memorias do Instituto Oswaldo Cruz**, v. 110, n. 4, p. 569–572, 2015.
- ZHAO, Y. et al. Neutrophils May Be a Vehicle for Viral Replication and Dissemination in Human H5N1 Avian Influenza. **Clinical Infectious Diseases**, v. 47, n. 12, p. 1575–1578, 2008.
- ZUKOR, K. et al. Zika virus-induced acute myelitis and motor deficits in adult interferon $\alpha\beta/\gamma$

receptor knockout mice. **Journal of NeuroVirology**, v. 24, n. 3, p. 273–290, 2018.

ZUO, Y. et al. Neutrophil Extracellular Traps in COVID-19. **JCI insights**, v. 5, n. 11, p. e138999, 2020.